Field Indicators for the Prediction of Appalachian Soil and Bedrock Geochemistry

Daniel Keith Johnson

Dissertation submitted to the faculty of the
Virginia Polytechnic Institute and State University
in partial fulfillment of the requirements for the degree of

DOCTOR OF PHILOSOPHY

In

CROP AND SOIL ENVIRONMENTAL SCIENCES

W. Lee Daniels, chair
Kenneth A. Eriksson
John M. Galbraith
Stephen H. Schoenholtz
Carl E. Zipper

29 June 2016
Blacksburg, VA

Keywords: total dissolved solids, specific conductance, mine reclamation

Field Indicators for the Prediction of Appalachian Soil and Bedrock Geochemistry

Daniel Keith Johnson

Abstract

Surface mining for coal in the Central Appalachians contributes total dissolved solids (TDS) to headwater streams, especially below larger mines and associated valley fills. My objective was to characterize the geochemical properties of a range of surface soils and associated geologic strata from the Central Appalachian coalfields and to relate those properties to simple field indicators, such as color or rock type. I hypothesized that these indicators can accurately predict certain geochemical properties. Thirty-three vertical weathering sequences were sampled from eight surface mines throughout the Central Appalachian coalfields, for a total of 204 individual samples. No differences were found among sites in overall saturated paste specific conductance (SC; used as a proxy for TDS) levels, but significant geochemical differences existed among samples. Sulfate release dominated SC levels, followed closely by Ca and Mg. Surficial soils and sandstones were yellowish-brown in color, high in citrate dithionite (CD) - extractable Al, Fe, and Mn, and low in SC, compared to underlying sandstones, shales, and mudstones, which were grayish to black, low in CD-extractable Al, Fe, and Mn, and significantly higher in SC. Saturated paste As and P were higher in A horizons, whereas Se was significantly higher in unweathered bedrock than in soil or weathered bedrock. Samples generating exothermic reactions with 30% H_2O_2 produced higher SC levels, sulfate, Mg, and Se. In conclusion, the mine spoils studied varied widely in geochemical properties. The simple field indicators presented here, such as color, weathering status, rock type, and H_2O_2 reaction can provide valuable guidance for identifying TDS risk which would greatly improve operator's ability to actively minimize TDS release. I recommend using soil and weathered, yellowish-brown sandstone layers as a source of

low TDS spoil material whenever possible. The H_2O_2 field test is useful for identification of TDS and Se risk. Underlying unweathered bedrock layers should be treated as "potentially high TDS spoils". Particularly high risk spoils include gray to black mudstones and shales, coals, and coal associated shales, mudstones, and clays directly associated with coal seams. I recommend hydrologically isolating these spoils using techniques similar to those used historically for acid-forming materials.

Dedication

I pondered much of this research while wondering along a shady stream or sitting high on a mountaintop in the Appalachians. Those old foggy hills have a special significance to me, since I was raised "up in the holler" there and my family has lived there for generations. Often, a trip up into the mountains was all I needed for a reset for when this project started to overwhelm me. Of course, my four-legged friend, Roxy, was also there with me for nearly all five years of this research – by far more than any person. She listened to me practice countless presentations and to my endless ramblings about the research. Most importantly, during the long hours of writing, she reminded me (sometimes quite forcefully) to get up, stretch, and go outside to play. Roxy was literally sitting on the keyboard at times; she even typed a few keystrokes. So, I must caution, even though you are likely reading this dissertation in electronic copy, you may still find a few stray dog hairs. Since Roxy and those mountain escapes helped me through it all, I found it fitting to dedicate this research to the preservation of the Appalachian Mountains and to my faithful Dalmatian, Roxy "Spotty" McSpotster. Thanks, Roxy.

Acknowledgements

I would like to thank the Powell River Project and Director Carl Zipper for funding much of the research presented here. Thanks also to the Office of Surface Mining Reclamation and Enforcement, who also contributed to a portion of the research. I would like to thank all of the mining companies and personnel who assisted with finding sample locations and getting site access. The staff and students of the marginal soils research group at Virginia Tech provided an enormous amount of technical support. There are too many of you to list here, but thank all of you so much. Special thanks to Julia Burger, who managed the majority of the data analysis for the samples. Thank you Julia for always helping keep me organized and letting me clutter up the lab with samples for five years. My family and friends have provided unwavering praise and encouragement through it all. I love you all and could not have done this without you.

I owe a very special thanks to my committee members. You all dedicated many hours to reading and editing my work. All of you provided very thoughtful, helpful feedback and for that I am deeply grateful. I really enjoyed all of our conversations about this research and I thank you all very much for your respective contributions. I would like to especially thank the chair of my committee, Dr. W. Lee Daniels and also Dr. John Galbraith. Lee, you dedicated countless hours offering advice, coaching me on teaching, and editing this work. You and the CSES department provided me with the opportunity to have a funded GTA position and to teach in the department, an opportunity I deeply appreciate. Dr. G., you provided more advice than I could ever give you credit for. You introduced me to my love and passion for soils. My travels with you and the soil judging team have certainly been one of the highlights of my life. I hope to see you out in the soil pits again one day!

TABLE OF CONTENTS

Chapter 1. Introduction

Background

The coal reserves of the Central Appalachian region are a valuable economic resource, both nationally and regionally (EIA, 2012). This resource is valued at billions of US dollars and generates large amounts of revenue for private companies while government agencies and localities also receive revenues through taxes paid, permitting fees, and regulatory penalty fees (BP, 2010). However, as commonly seen around the world in countries with abundant natural resources, these massive coal reserves have historically plagued the Appalachian region with "the resource curse", otherwise known as the "paradox of plenty" (Betz et al., 2015). Data from the Betz et al. (2015) study indicate this phenomenon may be diminishing in Appalachia in the post-2000 era, but this paradox explains how, historically, outside investors depleted the region's rich natural resources, funneling most of the wealth outside of the region, meanwhile causing severe environmental and socioeconomic impacts. Thus, it is important to develop sustainable coal mining practices using reclamation strategies that will provide enhanced socioeconomic benefits over the next century.

While the Central Appalachian region sits over one of the richest coal reserves in country, the region has historically been disadvantaged socioeconomically and Central Appalachian counties continue to be the poorest counties in the entire nation (EIA, 2012; Halverson and Bischak, 2007; Wood, 2005). In a study on poverty from 1960-2000, Wood (2005) stated "over time, Central Appalachia has remained one of the most distressed areas of the U.S., in comparison to the rest of the nation, and in comparison to the rest of Appalachia as well." This fact is ironic in that the public perception in the region is that mining brings wealth to the local inhabitants, so the local public stance is generally overwhelmingly pro-mining. In truth, some studies show the majority of wealth is funneled out of the region and doesn't end up in the hands of the common worker (Betz et al., 2015), but mining continues regardless. Since the Central Appalachian region is economically disadvantaged, it is especially important to monitor both the environmental and social impacts of coal mining, implement new policies and regulations where needed, and continue advancements in viable reclamation and impact mitigation practices.

Coal production is on the decline due to diminishing reserves, competition from natural gas, and pressure from environmental advocates, but will likely continue into the foreseeable future. A study from the National Bureau of Economic Research (Knittel, 2015) revealed natural gas to be a major competitor with the coal market. Burning natural gas is "cleaner" than burning coal in that it releases less greenhouse gases and other pollutants; meanwhile the price of natural gas fell almost 70% from 2008 to 2012. The study does note that the while the Appalachian and Western coal regions are driving an overall decline in US coal production, coal exports have increased during this period and those exports have historically been filled with high BTU and low S Appalachian coals. In 2014, Reaver and Khare published a model predicting US coal production to peak between 2009 and 2023 and decline afterwards, due to diminishing reserves, but noted US coal production will continue long after that peak as the remaining reserves are sought out. Thus, regardless of the drastic impacts mining has on the region, coal mining will likely continue in Appalachia until the last economically recoverable coal reserves are gone.

Historically (before the 1970s), surface mining companies bought or leased Appalachian properties, mined out whatever coal was easy to access, and often abandoned the property with little effort or investment put into reclamation (USEPA, 2005). Increasing environmental awareness from the public, however, led to a number of environmental laws regulating surface mining throughout the last half of the 20th century [e.g. the Clean Water Act (CWA) and the Surface Mining Control and Reclamation Act (SMCRA); USEPA, 2011]. The power struggle between those profiting from coal and environmental activists is apparent in surface mining regulation and implementation; regulations and policies change frequently and are constantly evolving. Lack of approximate original contour (AOC) restoration and acid mine drainage were historically major concerns, but advancements in reclamation have largely addressed these issues (Skousen et al., 2002) for active mine operations. While mining companies are now required by law to "reclaim" mined areas and those lands are not "abandoned" as they were in the past, the impacts caused by current mining methods, such as elevated levels of total dissolved solids (TDS; commonly estimated via specific conductance - SC) in receiving streams, can persist for decades after mining has ceased (Evans et al., 2014; Pond et al. 2014). Thus, over the past decade, TDS impacts have emerged as a leading concern for the surface mining industry in Appalachia.

Both long-term chronic and short-term acute elevated TDS levels cause negative impacts to stream aquatic life. A number of studies document the negative effects on aquatic life due to elevated stream TDS levels (Chapman et al., 2000; Cormier et al., 2013; Kennedy et al., 2005; Mount et al., 1997; Pond et al., 2008, 2014; Pond, 2010; Timpano et al., 2015). These studies use benthic macroinvertebrates or other aquatic life as proxies for overall stream biological condition and generally conclude that negative impacts to stream aquatic life increase as overall concentrations in TDS levels increase. Furthermore, the specific ionic concentrations making up overall TDS and seasonal spikes in TDS have additionally been shown to impact stream aquatic life (Mount et al., 1997, Timpano et al., 2015). Thus, scientific evidence indicates that chronic and acute elevated in-stream TDS levels generated by surface coal mines negatively impact the Appalachian region by degrading biological conditions in streams.

Contemporary coal-mine water treatment practices do not remove TDS from surface mine effluent effectively and TDS-specific treatment technologies are expensive; prevention is key. By definition, TDS (APHA, 1999) is the sum of the mass of all inorganic and organic filtrate components that will pass through a 2 µm or smaller filter. Traditional water treatment methods generally use precipitation methods to remove soluble metals, but many TDS components are soluble at very high concentrations (Na_2SO_4 saturation = 110,000 mg L^{-1}; NaCl saturation = 350,000 mg L^{-1}; $CaSO_4 \cdot 2H_2O$ = 1500 mg L^{-1}) and across a range of pH values. Some treatment technologies such as reverse osmosis do exist for specifically removing TDS from coal mine effluents, but are generally expensive (Geldenhuys et al., 2003; Pinto et al., 2016; Tolonen et al., 2015; Ziemkiewicz et al., 2003). Thus, while technologies do exist for reducing overall surface mine effluent TDS, prevention (where possible) would be a better option for mining companies than actual discharge water treatment for TDS.

Problem Summary and Need for Research

Since TDS is a relatively new concern for the mining industry, little science exists on TDS prediction and prevention. Past strategies of identifying acid-forming strata and isolating them from surface and near-surface water flow have been effective at limiting acid mine drainage (Skousen et al., 2002). A similar pre-mining approach to identifying high TDS mine spoils for special handling and isolation may also be effective, but few studies have been published to date on TDS prediction techniques; and no published studies describe TDS prediction techniques that can be used by mine operators and their consultants in the field. Thus, this lack of field TDS prediction methods led to the current study which investigates the geologic sources and geochemical characteristics of TDS in Central Appalachia. Our primary goal was to develop a set of simple field indicators usable by the mining industry, consultants and regulatory authorities to predict TDS potentials of a wide range of regional mine spoils.

My overall hypothesis for this study was that simple field indicators can predict certain geochemical properties of Appalachian soil and bedrock. I predicted ionic concentration would vary significantly among low, medium, and high TDS potential samples. Based on previous studies, I suggested low chroma, gray spoils would produce higher SC values than high chroma, brown spoils. Further, I predicted that weathered spoils would produce lower SC values than unweathered spoils. In addition, I postulated that fine-grained rocks generally produce higher SC values than coarse-grained rocks and that exothermic reaction to H_2O_2 could indicate high SC. In summary, I originally proposed that a combination of color, rock type, weathering status, and peroxide reaction could predict overall saturated paste SC conductance levels that would be directly reflective of mine spoil leachate loadings to local headwater streams.

Overall Research Objectives

This study addressed several different aspects of TDS generation and prediction. The overall research objectives were as follows:

1. Collect a range of materials originating from surface coal mines in Central Appalachia and analyze the following geochemical properties:
    a. Saturated paste SC, pH, and ionic composition

b. Microwave assisted acid digestion and total sulfur (total-S)

c. Citrate-dithionite (CD) - extractable Al, Fe, and Mn

d. Hydrogen peroxide (H_2O_2) pH and SC

e. Virginia Tech Soil Testing Lab dilute double acid extractable ions

2. Develop a set of simple field indicators for predicting TDS production risk by statistically relating the geochemical properties described above to the following properties:

   a. Munsell® color, hue, value, and chroma

   b. Rock type

   c. Horizon Type

   d. Degree of weathering

   e. Hydrochloric acid (HCl) reaction

   f. H_2O_2 reaction

3. Investigate the nature of the stratigraphic boundary between high and low TDS strata to determine if:

   a. An abrupt boundary exists at some confining layer, such as a shale or mudstone layer; or

   b. The boundary is more diffuse, being more related to the distance from the earth's surface.

References

APHA (American Public Health Association). 1999. Standard Methods for the Examination of Water and Wastewater, 20th ed. American Public Health Assoc Press, Washington DC.

Betz, M. R., M. D. Patridge, M. Farren, and L. Lobao. 2015. Coal mining, economic development, and the natural resources curse. Energy Econ.. 50:105-116.

British Petroleum. 2010. BP statistical review of world energy. Available at http://www.bp.com/liveassets/bp_internet/globalbp/globalbp_uk_english/reports_and_publications/statistical_energy_review_2011/STAGING/local_assets/spreadsheets/statistical_review_of_world_energy_full_report_2012.xlsx

Chapman, P.M., H. Bailey, and E. Canaria. 2000. Toxicity of total dissolved solids associated with two mine effluents to chironomid larvae and early life stages of rainbow trout. Env. Toxicol. Chem. 19:210-214.

Clean Water Act (CWA). 33 U.S.C. §1252.

Cormier, S.M., G.W. Suter and L. Zheng, 2013. Derivation of a benchmark for freshwater ionic strength. Env. Toxicol. Chem. 32:263-271.

EIA. 2012. Recoverable reserves at producing mines, estimated recoverable reserves, and demonstrated reserve base by mining method. U.S. Energy Information Administration. Available at http://www.eia.gov/coal/annual/xls/table15.xls.

Evans, D. M., C. E. Zipper, P. F. Donovan, and W. L. Daniels. 2014. Long Term trends of specific conductance in waters discharged by coal mine valley fills in Central Appalachia, USA. J. Am. Water Res. Assoc. 50 (6): 1449-60.

Geldenhuys, A.J., J.P. Maree, M. De Beer, P. Hlabela. 2003. An integrated limestone/lime process for partial sulphate removal J. S Afr. Inst. Min. Metall., 103: 345-354.

Halverson, J.A. and G. Bischak. 2007. Underlying Socioeconomic Factors Influencing Health Disparities in the Appalachian Region: report to the Appalachian Regional Commission. Morgantown (WV): Department of Community Medicine, West Virginia University.

Kennedy, A.J., D.S. Cherry, and C.E. Zipper. 2005. Evaluation of ionic contribution to the toxicity of a coal-mine effluent using *Ceriodaphnia dubia*. Arch. Environ. Contam. Toxicol. 49:155−162.

Knittel, C. R. 2015. Natural gas prices and coal displacement: Evidence from electricity markets. National Bureau of Economic Research. DOI 10.3386/w21627.

Mount, D. R., J. M. Gulley, J. R. Hockett, T. D. Garrison, and J. M. Evans. 1997. Statistical models to predict the toxicity of major ions to *Ceriodaphniadubia*, *Daphnia magna*, and fathead minnows (*Pimephalespromelas)*. Environ. Toxicol. Chem. 16:2009-2019.

Pinto, P. X., S. R. Al-Abed, D. A. Balz, B. A. Butler, R. B. Landy, and S. J. Smith. 2016. Bench-scale and pilot-scale treatment technologies for the removal of total dissolved solids from coal mine water: A review. Mine Water and the Environ. 35 (1): 94-112.

Pond, G.J. 2010. Patterns of Ephemeroptera taxa loss in Appalachian headwater streams (Kentucky, USA). Hydrobiologia 641:185–201.

Pond, G. J., M. E. Passmore, F. A. Borsuk, L. Reynolds, and C. J. Rose. 2008. Downstream effects of mountaintop coal mining: comparing biological conditions using family- and genus-level macroinvertebrate bioassessment tools. J. North Am. Benthol. Soc. 27:717–737.

Pond, G.J., M. E. Passmore, N.D. Pointon, J.K. Felbinger, C.A Walker, K.J. Krock, J.B. Fulton, W.L. Nash. 2014. Long-term impacts on macroinvertebrates downstream of reclaimed mountaintop mining valley fills in Central Appalachia. Environ. Manag. DOI 10.1007/s00267-014-0319-6.

Reaver, N. G., and S. V. Khare. 2014. Imminence of peak in US coal production and overestimation of reserves. Int. J. of Coal Geol. 131: 90-105.

Skousen, J., J. Simmons, L.M. McDonald and P. Ziemkiewicz. 2002. Acid-base accounting to predict post-mining drainage quality on surface mines. J. Env. Qual. 31:2034 - 2044.

SMCRA (Surface Mining Control and Reclamation Act). 1977. P.L. 95-87. Revision 2006. 25 U.S.C. § 1201.

Timpano, A. J., S. H. Schoenholtz, D. J. Soucek, and C. E. Zipper. 2015. Salinity as a limiting factor for biological condition in mining influenced Central Appalachian headwater streams. J. of the Am. Water Res. Assoc. 51 (1): 240-50.

Tolonen, E., J. Rämö, and U. Lassi. 2015. The effect of magnesium on partial sulphate removal from mine water as gypsum. J. Environ. Manage. 159: 143-6.

USEPA (U.S. Environmental Protection Agency). 2005. Mountaintop mining/valley fills in Appalachia. Final programmatic environmental impact statement. U.S. Environmental Protection Agency, Region 3, Philadelphia, PA. Available at https://www3.epa.gov/region03/mtntop/eis2005.htm.

USEPA (U.S. Environmental Protection Agency). 2011. The effects of mountaintop mines and valley fills on aquatic ecosystems of the Central Appalachian coalfields (2011 final). U.S. Environmental Protection Agency, Washington, DC. Available at http://cfpub.epa.gov/ncea/cfm/recordisplay.cfm?deid=225743

Wood, L.E. 2005. Trends in National and Regional Economic Distress: 1960–2000. Washington: Appalachian Regional Commission. Available at http://www.arc.gov/assets/research_reports/trendsinnationalandregionaleconomicdistress1960to2000.pdf.

Ziemkiewicz, P.F., J.G. Skousen, J. Simmons. 2003. Long-term performance of passive acid mine drainage treatment systems. Mine Water Environ. 22(3):118–129.

Chapter 2. Literature Review

Surface Mining Regulatory History

The United States sits on the world's largest coal reserves at 244 billion metric tons, more than one quarter of the entire Earth's coal reserves and nearly double that of Russia, the country with the next largest reserve (BP, 2010). The Central Appalachians contain a significant portion of the economic coal reserves in the continental United States, so the region is a globally significant source of coal (EIA, 2012). The Central Appalachian coalfields cover roughly 48,000 km^2 throughout eastern KY, southwestern VA, eastern TN, and WV (Fig. 2.1), but related coal reserves are also found in PA, OH, and AL. Central Appalachia has long been a source of U.S. coal, but extensive surface mining only began in the 1940’s (USEPA, 2005). A production prediction model by Reaver and Khare (2014) showed that overall US coal production will peak between 2009 and 2023 and decline afterwards, due to diminishing reserves, with 2010 being the most likely peak production year. However, the study also notes US coal production will continue into the foreseeable future. Thus, US coal mines are a regionally and globally important source of coal.

Originally, little was known about the effect large scale mining would have on the environment and aesthetics tended to be the dominant concern (USEPA, 2005). As environmental awareness increased throughout the mid-1900s, some individual states, such as WV, passed regulations governing surface mining operations. Sections 301, 402, and 404 of the Clean Water Act (CWA) passed in 1972 provided the USEPA, the US Army Corps of Engineers and individual states (via federal program delegation) the authority to regulate activities which could potentially degrade water quality. The CWA forbids any person to discharge regulated pollutants into waters of the US, except by the appropriate permit.

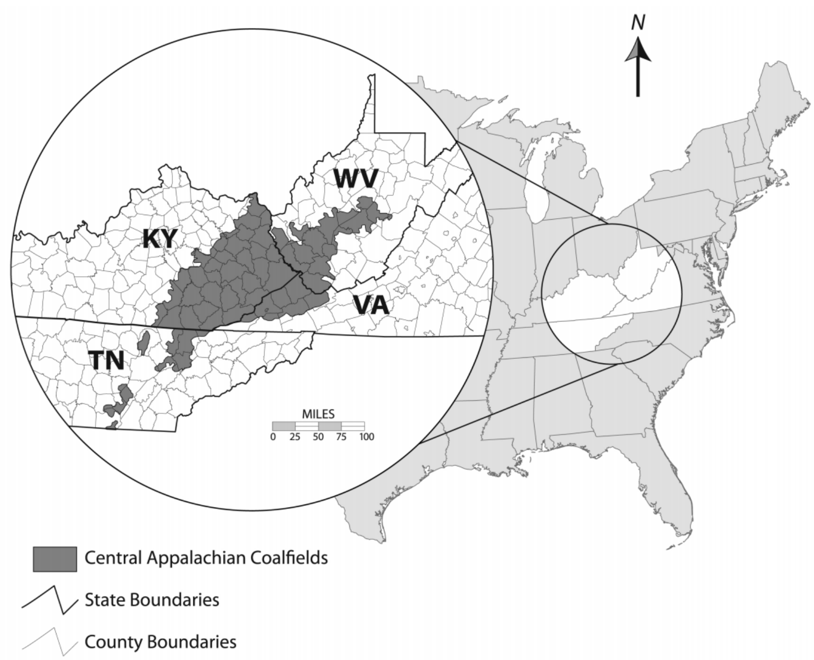

Figure 2.1. The Central Appalachian coalfields. Modified from USEPA, 2011.

The federal Surface Mine Control and Reclamation Act (SMCRA) of 1977 was passed in an effort to prevent further land and water degradation from surface coal mining, tying many federal regulations together under a government authority via establishment of uniform performance standards and criteria. Individual states were then allowed to develop similarly restrictive regulations and obtain primacy to regulate coal mining following approval by the federal Office of Surface Mining Reclamation and Enforcement (OSMRE). Alternatively, states can choose to let the OSMRE regulate mining. SMCRA requires mined lands to be returned to "equal or better" conditions, based on the intended post-mining land use and dictates that areas must be returned to the “approximate original contour” unless a specific permit waiver is granted. Thus, the CWA and SMCRA are the two key pieces of federal legislation regulating surface mining operations in Appalachia.

More recently in 2011, USEPA exercised its CWA authority under section 404 (c) to regulate the filling of materials into U.S. waters and revoked a West Virginia mining permit when it handed down a final determination on the Spruce No. 1 Mine in Logan County (USEPA, 2012). This was an important benchmark; since the USEPA had only made 12 other final 404 (c) determinations since 1972. The USEPA determined that the Spruce No. 1 Mine would have an adverse effect on stream chemistry by creating valley fills, leading to negative impacts on native faunal and floral communities. The final determination was later set aside in 2012 by the federal district court in Washington, D.C. (US Court of Appeals, 2013), but other current legal actions are underway, including a petition to force the EPA to set numerical standards on TDS in discharge waters from coal mining activities (USEPA, 2013). TDS is laborious and expensive to measure, so specific conductance (SC) is generally used as a proxy measurement (Timpano et al., 2015). Daniels et al. (2016) found that TDS was directly and linearly related to TDS.

Surface mining in the region commonly leads to stream SC values > 1000 $\mu S\ cm^{-1}$ during active mining and directly after (Evans et al., 2014; Pond et al., 2014); stream SC can also stay elevated for decades after mining has ceased. In 2000, Chapman et al. found that aquatic survival rates for Chironomids were significantly affected at TDS levels of >1750 $mg\ L^{-1}$ in mine effluents, even at moderate pH values. More recently, Pond and co-workers have produced a number of publications (Pond et al., 2008 and 2014; Pond, 2010) that report significant negative effects of increased ion concentrations on benthic macroinvertebrates at specific conductance levels of > 500 µS cm^{-1}. Other recent studies have suggested aquatic life is impacted at levels as low as 300 to 500 µS cm^{-1} (Cormier et al., 2013; Timpano et al., 2015). Daniels et al. (2014) concluded from a review of relevant studies that stream aquatic life begins to be affected between 200 to 700 µS cm^{-1}. In 2011, Timpano measured six reference sites and 22 test sites in SW Virginia for the effect of elevated TDS levels on aquatic health and found that "family-level biological effects, as defined by Virginia Stream Condition Index scores indicating stressed or severely stressed conditions, were observed with increasing probability from 0% at TDS ≤ 190 mg L^{-1} to 100 % at TDS ≥ 1,108 mg L^{-1}, with 50% probability of effects observed at TDS = 422 mg L^{-1}." In, 1997 Mount et al. found the relative ion toxicity to *Ceriodaphnia dubia*, *Daphnia mana*, and fathead minnows (*Pimephales promelas*) to be K > HCO_3^- ~ Mg > Cl > sulfate and Kennedy et al. (2005) found that both the acute and chronic toxicity to *Ceriodaphnia dubia* increased with increasing TDS. Similar ion toxicities were shown by the American Petroleum Institute (1998). These studies collectively indicate that the ionic composition of TDS is just as or more important than overall TDS concentration as a determinant of toxicity. While some debate remains around the exact toxicity mechanisms and relative effect levels, it is clear that elevated TDS concentrations in headwater streams have a negative effect on native species, particularly benthic macroinvertebrates.

Furthermore, the Timpano et al. (2015) study showed that seasonal variations in TDS occur. Reproductive periods for aquatic life are generally more sensitive to TDS, so spikes in TDS concentrations during spawning or mating periods can cause significant stresses on the biotic condition of the streams. Generally, ionic toxicities increase as overall stream TDS increases, but seasonal fluctuations in TDS and individual ion toxicities are also significant, making it challenging to place a regulatory benchmark at a single specific in-stream TDS value.

The Central Appalachian Surface Mining Process

Soil and rock materials above the coal seams being mined (termed "overburden") must be removed to access the coal beneath. Blasting the hard rock material increases void space and causes a considerable increase in volume (~ 20 – 30%), generating "excess spoils", which are first backfilled into the mined out pits before the excess must be filled into nearby valleys (USEPA, 2005). SMCRA calls for topsoil return during reclamation, but an important provision allows for the use of pre-designated overburden strata as a "topsoil substitute" material when both: (i) native topsoils (A+E horizons) are less than 15 cm (6 in.) thick; and (ii) the substitute material can be shown via pre-mine testing to support the post-mining land use. Using overburden strata to construct valley fills and as topsoil substitutes exposes previously isolated geologic materials to a more intensive weathering environment (increased oxidation, hydration, hydrolysis, etc.). Weathering products are quickly transported into streams via surface and shallow groundwater flow (Rose and Cravotta, 1998).

Historically, identification and avoidance of acid-forming spoils were of primary concern in Appalachian coal mine planning. Water percolating through mine pit and highwall backfills and head of valley excess spoil fills containing acid-forming spoils generated acid mine drainage in areas with sensitive headwater streams (Brady et al., 2000). Advancements in acid-base accounting (Skousen et al., 2002) and other similar predictive techniques largely resolved this problem by allowing miners to identify and isolate strongly acid-forming materials or to offset acid drainage production by mixing net alkaline and acid strata together, which allows neutralization reactions to occur, producing a presumably circumneutral effluent (USEPA, 2011).

As detailed above, recent research has shown that while these non acid-forming materials may support the post-mining land use and generate circumneutral effluents, there are still potentially negative water quality implications associated with these practices. Acid neutralization reactions by carbonates and other alkaline surfaces in rock spoils produce various dissolved ions as end products (EPA, 2011). These various dissolved ions are collectively termed TDS when expressed on a mass (mg L^{-1}) basis.

TDS Generation

Several processes generate increased TDS loads from coal surface mines to adjacent waterways. USEPA (2011) found the concentration of major ions to be increased tenfold in mined streams compared to unmined reference streams in Appalachia. Alkaline chemical reagents added to neutralize acid mine drainage can be a direct source of TDS where active water treatment is present. Mixing of net alkaline and net acid strata can also cause a similar effect, but strongly acid-forming strata are now identified and isolated from drainage waters whenever possible (Skousen et al., 2002). Acid neutralization reactions are not the only source of TDS. Freshly exposed geologic materials can also contribute significant loads via other weathering reactions such as hydrolysis and dissolution reactions (Brady et al., 2000). TDS-producing potential varies widely from material to material, as shown by previous studies (e.g. Daniels et al., 2016; Orndorff et al., 2015). In particular, oxidized and weathered surficial materials usually produce much lower TDS than unweathered spoils from the same strata. Howard (1979) showed that mine spoils generated from hard rock in the Wise Formation (southwestern VA) contained 20-40% soil sized materials (< 2 mm) along with a wide range of sizes of rock fragments. Howard also identified common complex metal-carbonates occurring as secondary rock cements and siderite at appreciable (> 2 %) levels. These "fresh" minerals in materials newly exposed to the surface rapidly weather, releasing a range of constituent ions (Brady et al., 2000). Thus, TDS does not have one specific source, rather it is the result of a conglomeration of reactions occurring across the mine site.

Reactions from the carbonate materials with the percolating waters commonly lead to net alkaline discharge waters. Metals, such as cadmium (Cd), chromium (Cr), copper (Cu), lead (Pb), and zinc (Zn) form insoluble precipitates or coprecipitates with Fe at moderate pH values and several studies have shown low concentrations in discharge waters (Lee et al., 2002). Nickel (Ni) and Mn are exceptions and may remain somewhat soluble at moderate pH (Larsen and Mann, 2005) for more extended periods of time. Daniels et al. (2009) examined chemical properties of 15 mine spoils from Virginia and Kentucky in a kinetic leaching test and found As, beryllium (Be), chromium (Cr), Cu, molybdenum (Mo), Ni, and Zn to be at or below detection limits (<0.010 mg L^{-1}). As such, certain ions are not generally considered to be problematic in Appalachian coal mine discharge.

A number of other common elements (e.g. Potassium – K, Mg, sulfate, etc.) are quite soluble at circumneutral pH values, however, and are found at elevated concentrations in recently mined land effluents. The current study focuses on elements which are soluble at moderate pH and have been demonstrated to be problem ions for water quality considerations in Central Appalachian streams. USEPA (2011) found sulfate, Ca, Mg, hardness, TDS, Mn, and bicarbonate (HCO_3^-) to be among the elevated parameters in streams associated with valley fills compared to unmined or reference stream areas (see Table 2.1). Sulfate was present in the highest mass concentrations, followed by HCO_3^-, Ca, and Mg, respectively. In the kinetic test (leaching column) study by Daniels et al. (2009) "six elements, Ca, K, Mg, sodium (Na), S (as sulfate) and C (as HCO_3^-) were found to be either quantitatively and/or functionally the major components of the leachate solutions." Variations were noted in elemental release depending on; a) the geologic weathering of the material, and b) the parent material of the spoil. Orndorff et al. (2015) found column leachates from mine spoils with higher Total-S to release higher TDS across a range of pH values. Skousen et al. (2000) also reported Ca, K, Mg, Na, sulfate, and HCO_3^- to be the dominant ions at circumneutral pH values, but noted increased levels of Al, Fe, and Mn at lower pH values. Although HCO_3^-, K, and Na have been shown to occur at elevated levels, they generally only compose a small fraction of TDS released from fresh mine spoils compared to Ca, Mg, and sulfate. Palmer et al. (2009) found 7 out of 11 stream mitigation projects reported levels of Se above the presumed in-stream threshold (5 µg L^{-1}) for impacts to aquatic life. Thus, several constituent ions of TDS are reported to be problematic in fresh mine spoil leachates throughout the literature, in particular combined loads of Ca, Mg, and sulfate at higher concentrations and Se at much lower levels.

Table 2.1. From USEPA's Report on The Effects of Mountaintop Mines and Valley Fills on Aquatic Ecosystems of the Central Appalachian Coalfields (2011). "Variables are by ordered ratio of their median concentration in unmined streams to those with valley fills. An asterisk (*) next to the variable name indicates that the mean concentration in streams below valley fills was statistically significantly greater than that in unmined streams at $p = 0.05$." Units are in ppm (mg L^{-1}).

Variable	Unmined			Filled			Detection limit
	Median	Mean	Range	Median	Mean	Range	
SO_4^{2-}*	12.6	16.0	11.0–21.6	523	696	155–1,520	5.0
Ca, total*	4.88	7.50	2.70–12.0	104	138	38.0–269	0.10
Mg, total*	4.10	4.30	2.30–7.00	86.7	122	28.0–248	0.50
Hardness*	29.1	42.0	17.0–72.0	617	801	225–1,620	3.3
TDS*	50.5	---	---	847	---	---	5.0
Mn, total	<0.005	0.034	<0.005– 0.083	0.044	0.14	0.009–9.0	0.010
Conductivity (µS/cm)*	66.4	62.0	34.0–133	585	1,020	159–2,540	---
HCO_3^-*	---	25.5	7.44–42.7	---	223	13.1–612	NA
Se, total*	<0.0015	<0.0015	<0.0015	0.012	0.011	<0.0015–0.037	0.003
Alkalinity	20.0	---	---	150	---	---	5.0
K, total*	1.58	1.60	1.30–2.00	8.07	9.90	3.00–19.0	0.75
Na, total*	1.43	2.40	0.70–5.50	4.46	12.6	2.60–39.0	0.50
Mn, dissolved	<0.005	0.021	<0.005–0.055	0.044	0.11	0.0065–0.85	0.01
Cl*	<2.5	2.8	<2.5–4.0	4.5	4.6	<2.5–11	5.0
Acidity	2.5	---	---	4.2	---	---	2.0
Ni, total	---	<0.010	<0.010	---	0.014	<0.010–0.059	0.02
NO_3^-/NO_2^-*	0.81	0.40	<0.10–0.90	0.95	3.4	0.80–17	0.10
pH (standard)*	6.8	7.1	6.1–8.3	7.8	7.9	6.3–8.9	---
Acidity, hot	<2.5	---	---	<2.5	---	---	5.0
Al, dissolved	<0.050	0.093	<0.050–0.19	<0.050	0.096	<0.050–0.27	0.10
Sb, total	<0.0025	---	---	<0.0025	---	---	0.005
As, total	<0.001	---	---	<0.001	---	---	0.002
Be, total	<0.0005	---	---	<0.0005	---	---	0.001

Weathering Mechanisms

Percolating rainwater and oxidizing conditions drive most of the mine spoil weathering reactions that generate TDS. Rain dissolves carbon dioxide (CO_2) as it passes through the atmosphere, forming carbonic acid and falls to the ground with a median pH of 5.6. Human activity can further acidify rainwater and many parts of the US experience rainfall with much lower pH; rainwater pH levels in Central Appalachian region are on the rise, but average levels still range from 4.8 to 5.0 (NADP, 2012; USGS, 1997). Rain also dissolves oxygen as it passes through the atmosphere and increased CO_2 partial pressures below ground further acidify groundwater as it passes through soil and rock layers (Wunsch, 1993). Thus, mineral weathering reactions are accelerated near the surface as water with increased oxygen and acidity is regularly refreshed by percolating rainwater.

As minerals undergo weathering reactions, some or all of the constituent ions are released to solution. Powell and Larson (1985) found K in weathering solutions to originate from "K-feldspar, Mg from chlorite, and Si from K-feldspar and chlorite. Silica is precipitated as chalcedony and kaolinite, and Al is precipitated as kaolinite." Iron also precipitates as ferric hydroxide in the presence of oxygen. Percolating waters react with plagioclase, chlorite, calcite, pyrite, and siderite releasing Ca, Mg, Na, sulfate, HCO_3^-, and Fe. Brady et al. (2000) attributed sulfate release to pyrite, Ca to plagioclase and calcite, Na to plagioclase, and Mg to chlorite weathering, but some Mg is likely attributable to Mg-carbonates and Mg-sulfates. In short, during weathering, ions are released from minerals according to the ionic concentrations present in the minerals and the susceptibility of those minerals to the various weathering mechanisms described below.

Silicate Mineral Hydrolysis

Quartz is assumed to be inert, but when silicate minerals, such as chlorite or oligoclase are exposed to carbonic acid in groundwater, hydrolysis occurs. The end products can include clays, dissolved silicic acid, Ca, Mg, Na, K, and HCO_3^- ions, depending on the exact chemical composition of the mineral. Hydrogen ions are consumed in the reaction, causing a short-term net increase in pH in local solutions, but reaction rates at neutral pH are slow (Powell and Larson, 1985). Below is an example of silicate hydrolysis (note that ions are released as the reaction moves to the right):

$$\underset{\text{Oligioclase}}{Na_{0.7}Ca_{0.3}Al_{1.3}Si_{2.7}O_8} + 1.3CO_2 + 1.95H_2O \rightarrow \underset{\text{Kaolinite}}{0.65Al_2Si_2O_5(OH)_4} + 0.7Na^+ + 0.3Ca^{2+} + 1.4SiO_2 + 1.3\,HCO_3^-$$

Carbonate Dissolution

Dissolution of carbonate minerals (commonly calcite, dolomite, siderite, or other complexed metal carbonates) by carbonation weathering can release a range of constituent ions forming the minerals.

Calcite: $CaCO_3 + H_2O + CO_2 \rightarrow Ca^{2+} + 2HCO_3^-$

Dolomite: $CaMg(CO_3)_2 + H_2O + 2CO_2 \rightarrow Ca^{2+} + Mg^{2+} + 4HCO_3^-$

Siderite: $FeCO_3 + H_2CO_3 \rightarrow Fe^{2+} + 2HCO_3^-$

Calcium, Mg, Fe, and HCO_3^- are released during these reactions. Dissolution of calcite and dolomite are associated with an increase in solution pH. Ferrous iron released by the dissolution of siderite oxidizes and hydrolyzes to produce acidity, resulting in a net neutral reaction (Powell and Larson, 1985). These reactions are promoted by low pH and high partial pressures of CO_2 in groundwater and soil/pore air. Groundwater chemistry varies considerably from mine to mine, depending on a number of factors, such as geology, flow regime, etc. and this also affects the rate of carbonate weathering (Kleinmann, 2000).

Sulfide Oxidation

Ferrous sulfide (pyrite) is a common mineral found in coal-related geologic material. The sulfides remain reduced in situ, deep beneath the surface, but when exposed to surface conditions (water and oxygen) by mining activities they quickly begin to oxidize. The net result of a complex series of reactions is summarized as:

$$Fe^{(2+)}S_2 + 3.75\ O_2 + 3.5\ H_20 \rightarrow Fe^{(3+)}(OH)_{3(s)} + 2\ SO_4^{2-} + 4\ H^+$$

Excess acidity and associated soluble heavy metals and sulfates produced in the reaction is the source of what has historically been termed “acid mine drainage” (Singer and Stumm, 1970). In order to prevent spoil materials from discharging net acidic water, pyritic materials are sometimes mixed with alkaline (e.g. calcite or dolomite) containing materials. While this practice improves discharge pH, it also generates an appreciable amount of Ca, Mg, and HCO_3^- (USEPA, 2011) in addition to sulfate per the reactions shown above.

$$2\ CaCO_3 + 2\ H^+ \rightarrow 2\ Ca^{2+} + 2\ HCO_3^-$$

$$2\ CaMgCO_3 + 2\ H^+ \rightarrow Ca^{2+} + Mg^{2+} + 2\ HCO_3^-$$

Sulfate is common in regional discharge waters, but original mineral sources (e.g. gypsum) are scarce in the unweathered rocks of the study area. Surface mining can cause pyrite weathering rates to increase more than 600% versus natural weathering rates (Brady et al., 2000). Thus, sulfate presumably results from the oxidation of trace sulfides present in the rocks; ferric iron in the groundwater can also oxidize sulfides even in the absence of oxygen. The oxidation reactions are also catalyzed at low pH by Fe-oxidizing bacteria (Singer and Stumm, 1970), which rapidly replenish Fe^{3+}, which then directly oxidizes pyrite in a coupled reaction. Similar direct pyrite oxidation reactions are driven by Mn^{4+} in solution (Evangelou, 1995).

A review study by Calkins et al. (1994) found that "high-sulfur coal usually contains mineral sulfur, which is largely iron pyrite, but can also include other metal sulfides and sulfates, and in some cases small amounts of elemental sulfur". In addition, a variety of types of organic-S compounds were noted to occur. Their study went to on to describe sulfide minerals as including pyrite (FeS_2), the dimorphic marcasite (FeS_2), sphalerite (ZnS), galena (PbS), chalcopyrite ($CuFeS_2$), pyrrhotite ($Fe_{1-x}S$), arsenopyrite (FeAsS) and others. Pyrite was found to be the dominant sulfur compound in coal, occurring as both finely disseminated framboids 10 to 40 µm in diameter and as larger massive aggregates up to boulder size. Framboidal pyrite is much more reactive than aggregate pyrite on a wt/wt basis, so the ratio of framboidal pyrite to aggregate pyrite is perhaps as important to sulfate and overall TDS release as is total-S contents. The review by Calkins et al. (1994) also showed that some minor amounts of sulfate may also occur in coal as barite ($BaSO_4$), gypsum ($CaSO_4 \cdot 2H_2O$), anhydrite ($CaSO_4$), a number of different Fe-sulfates (e.g. jarosite), and other sulfate compounds. While the Calkins et al. study only reviewed coal samples, it is reasonable to assume coal-associated materials, such as underclays, fireclays, flint clays, and interburden layers that are high in S likely contain similar S compounds. Thus, while framboidal pyrite oxidation likely provides the main source of sulfate in the study area, a number of other S compounds also contribute to sulfate release.

Field Indicators for TDS Prediction

Previous studies have suggested that simple mine spoil indicators observable in the field can predict both overall SC and specific ionic elution potentials. Rock type is one such readily observable trait. Daniels et al. (2016) concluded that rock type significantly affected bulk mine spoil SC; generally black shales > mudstones > mixed rock types > sandstones. Agouridis et al. (2012) found the average leachate SC in field-scale plots to be higher from mixed shale and sandstone plots (1,224 µS cm^{-1}) than from both weathered (829 µS cm^{-1}) and unweathered (1,032 µS cm^{-1}) sandstone plots. Thus, fine-grained rocks, such as shales and mudstones, generally produce significantly higher SC than coarse-grained sandstones.

Brown, weathered spoils are generally lower in SC than gray, unweathered spoils and color is tied closely to weathering status. Agouridis et al. (2012) found the average leachate SC in field-scale plots from gray spoils to be significantly higher (1,032 µS cm^{-1}) than brown spoils (829 µS cm^{-1}). Orndorff et al. (2010; 2015) found weathered samples to generally be orangish to brownish and unweathered samples to generally be grayish. In 2016, Daniels et al. described weathered spoils as brown and unweathered spoils as gray and found that weathered spoils produced lower peak leachate SC (~ 750 µS cm^{-1}) than unweathered spoils (> 1500 µS cm^{-1}). Saturated paste SC was highly predictive (R^2 = 0.85) of peak leachate SC produced from unsaturated leaching columns. Daniels et al. (2014) also summarized column leaching results from over 50 spoils and coal mine refuse materials from the Central Appalachians and found weathered samples to have lower pH and SC. Orndorff et al. (2010) found weathered and unweathered spoil saturated paste SC to range from 200 to 560 µS cm^{-1} and 40 to 348 µS cm^{-1}, respectively. In short, color, weathering status, and SC potential are closely related; brown, weathered spoils generally produce lower leachate SC than gray, unweathered spoils.

Weathered spoils are generally lower in pH than unweathered spoils (Daniels et al. 2016; Orndorff et al., 2015), so it would seem that lower pH materials would generally have a lower SC, but this is generally not the case. In fact, some studies have shown that pH per se is a poor predictor of SC. Odenheimer et al. (2014) reported saturated paste pH to have a very weak association with TDS ($R^2 = 0.12$). Orndorff et al. (2010) noted that column leachates from spoils containing higher levels of reduced sulfides produced higher levels of leachate SC across a range of pH values (~ 4.5 to 8.5). Spoils containing high levels of reduced sulfide-S commonly produce leachates with moderately acidic pH values (Skousen et al., 2002) and high SC (Orndorff et al. 2010). Since both high sulfide-S spoils (high SC) and weathered spoils (low SC) produce low pH, pH is generally a poor indicator of SC per se.

In conclusion, limited work has been published to date that would allow the mining industry to reliably separate low and high TDS materials at a given mine site. Previous findings suggest that rock type, color, and weathering status are all possibly useful predictors of both mine spoil SC and ionic concentrations, but most studies published to date have analyzed bulk mine spoils that have been blasted and transported, limiting sample details and, in turn, the statistical comparisons that can be made. Thus, more research is needed to accurately predict TDS elution potentials of Appalachian mine spoils using field indicators.

Geology of the Pottsville and Breathitt Groups in Central Appalachia

Coal beds occur in large extent throughout the Pennsylvanian aged rocks in the Central Appalachians (Fig. 2.2). The Pennsylvanian system can be subdivided into the Pottsville, Allegheny, Conemaugh, and Monongahela groups. The Pottsville group is the dominant coal bearing group in southwestern Virginia, eastern KY, and southern West Virginia, which is further subdivided into the Lee, Norton, and Wise Formations in Virginia and the Pocahontas, New River, and Kanawha Formations in West Virginia (USGS, 2012). The Breathitt group is the equivalent to the Pottsville group in Kentucky and is composed of the Grundy, Pikeville, Hyden, Four Corners, and Princess formations. This study focused on the Pottsville group and the associated formations of the Breathitt group (Fig. 2.3) since these groups contain the dominant coal beds being mined in the Central Appalachians. Brady et al. (2000) describe the Pottsville group as generally dominated by sandstone, with lesser amounts of claystones, mudstones, and shale. The Pottsville Group was also noted to have less than 1% calcareous rock and a greater amount of siderite than other calcareous mineral components.

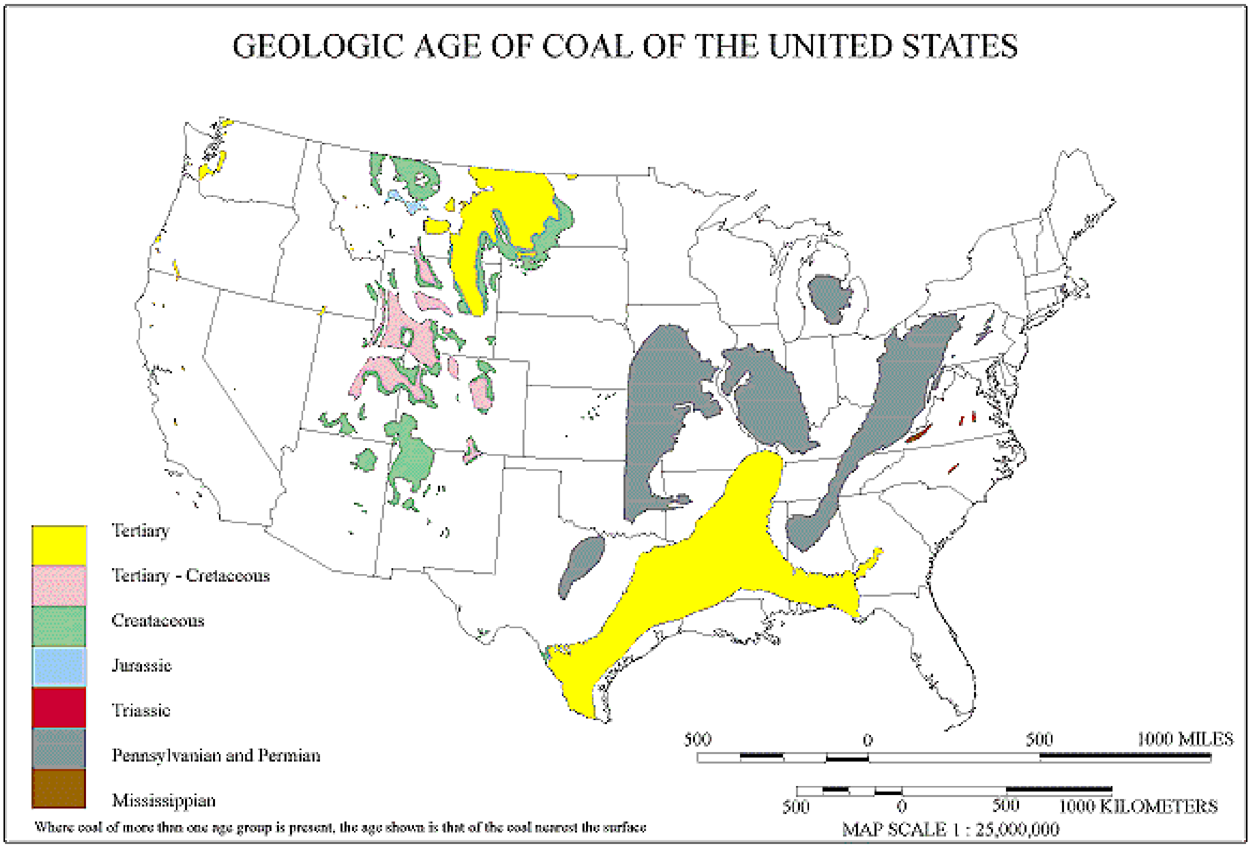

Figure 2.2. Map of the contiguous United States showing the geologic ages of major coal reserves. "Where coal of more than one age group is present, the age shown is that of the coal nearest the surface." Modified from Tully (1996).

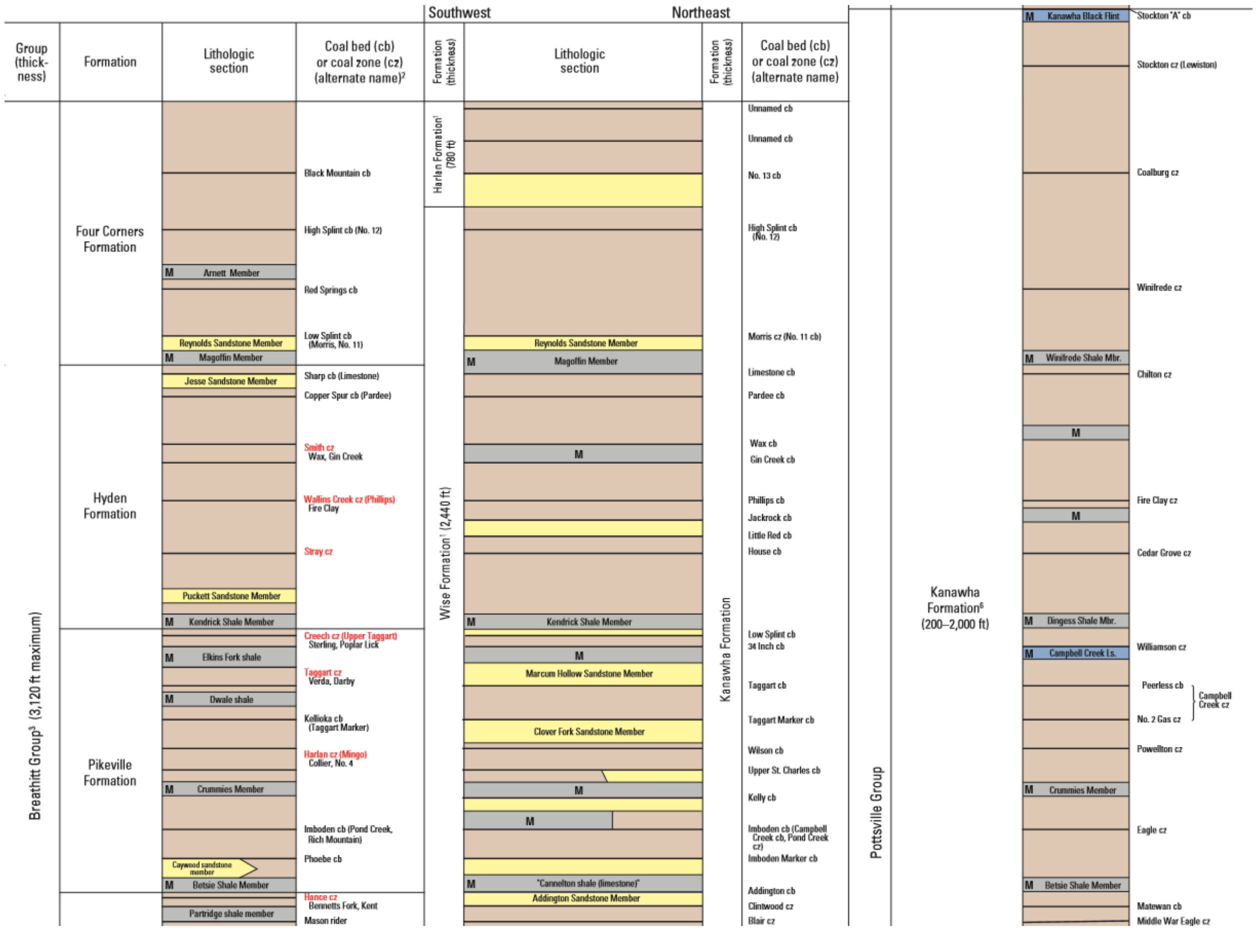

Figure 2.3. Stratigraphic correlation chart with common nomenclature. Left to right KY, Southwest VA, and WV (Modified from Ruppert et al., 2010).

Pocahontas Formation

The maximum thickness of the Pocahontas formation in WV is up to 229 meters (750 feet) (USGS, 2012). The dominant geologic materials consist of gray colored shales and siltstones. Sandstones are light gray, fine to medium grained, micaceous, and feldspathic. The Pocahontas formation corresponds roughly to the lower Lee formation in VA, but is dominated by the Warren Point sandstone in KY.

New River Formation

The New River Formation can be correlated to the lower Norton formation. The dominant rock type is sandstone, followed by shale, siltstone, coal, and minor limestone components. Sandstones in the formation are described as light to medium-light gray, micaceous, feldspathic, and very fine to coarse grained. Siltstones and shales range in color from medium to light gray to black. Limestone, where present, is medium-gray in color and occurs in thin discontinuous beds. Coal locally grades into black carbonaceous shale in places (USGS, 2012). The New River formation loosely corresponds to the upper Lee formation in VA, but in KY the Sewanee and Bee Rock sandstones dominate these strata.

Kanawha Formation

The extensive Kanawha formation is roughly equivalent to the Norton, Wise, and Harlan formation in VA and the Grundy, Pikeville, Hyden, and Princess formations in KY. The formation includes up to the top of the Kanawha black flint. The Kanawha black flint is notable as a distinct horizon that is a valuable benchmark to mining engineers. It is generally around three meters (10 feet) thick, has conchodial fracture, and has a dark bluish-black color. Sandstone in the Kanawha Formation is feldspathic, micaceous, fine- to coarse-grained, and light to medium gray. Siltstone and shale occur to lesser extent and are medium to dark gray in color. Interbedding of rock types is common (USGS, 2012).

Lee Formation

Quartzose sandstones mark the top and bottom of the formation, with another prominent quartzarenite located near the middle. Intertonguing of strata is common throughout the formation. The primary rock type is quartz arenite, followed by sandstone, conglomerate, siltstone, shale, and coal. The quartz arenite is a very resistant rock, described as white in color, fine to coarse grained, and even conglomeratic in places. The sandstone is feldspathic, micaceous, light gray in color, and has a fine to medium grain. The shales and siltstones are medium to dark gray and highly interbedded (USGS, 2012). Corresponding strata in KY are dominated by several massive sandstone strata (i.e. Warren Point, Sewanee, Bee Rock sandstones), but the Pocahontas and New River formations in WV are roughly equivalent.

Norton Formation

This formation is dominated by a mixed sequence of interlayered siltstone and shale, with lesser amounts of sandstone and coal. The bottom 61-90 meters (200-300 feet) is generally a siltstone/shale mix. Siltstones and shales are light to medium gray and contain siderite. Sandstones are feldspathic, micaceous, argillaceous, very fine to coarse-grained, and light to medium gray in color (USGS, 2012). Powell and Larsen (1985) studied the Norton formation in Buchanan County, VA and found the predominant minerals to be quartz, plagioclase feldspar, potassium feldspar, muscovite, chlorite, siderite, and calcite (as cement and clasts in sandstone strata). Sulfur was also reported to be generally very low (< 0.1 %) in most strata and presumably occurred as pyrite. The Gladeville sandstone defines the boundary between the Norton and Wise formations. The Gladeville sandstone is generally a medium gray to white, fine to medium grained, massively bedded, quartzose, feldspathic, micaceous, carbonaceous sandstone that ranges from 9-15 m (30-50 feet) thick (USGS, 2012). The Norton formation in VA is roughly equivalent to the lower Kanawha formation in WV and the Grundy formation in KY.

Wise Formation

The Wise Formation roughly correlates to the middle Kanawha Formation in WV and the Pikeville, Hyden, and the lower Four Corners formations in KY. It is dominated by sandstone, followed by siltstone and lesser amounts of shale and coal. The sandstone is feldspathic, micaceous, argillaceous, carbonaceous in places, and fine to coarse grained. The color can range from medium gray to light gray to moderate and pale yellowish-brown (USGS, 2012). Siltstones and shales throughout the formation are light olive gray to medium dark gray to grayish black. Siderite and ironstone can be found as thin beds or nodules.

Harlan Formation

Sandstone is the primary rock type, but siltstone and shale are also abundant. The sandstone is feldspathic, argillaceous, and somewhat quartzose, with a medium gray color. Siltstones and shales vary in color from medium or dark gray to brown or reddish-brown. Coal beds are commonly intertongued throughout the siltstone and shale strata (USGS, 2012). The Harlan formation in VA corresponds to the upper Kanawha formation in WV and the upper Four Corners formation in KY.

Weathered Mantle

Physical weathering of rock strata is much more intensive near the surface, primarily through the long term effects of unloading (via geologic erosion) and release of confining pressures. As materials are unloaded or eroded from the surface, geostatic vertical forces decrease, allowing geologic strata beneath to expand, causing "stress-relief fracturing" (Borchers and Wyrick, 1981) in the material. These vertical and horizontal cracks or fractures open pathways for oxygen, water, organisms, and other weathering agents to penetrate otherwise confined layers.

Geologic materials close to the Earth's surface are also exposed to a much more intensive chemical weathering environment than deeper strata that are protected from water and oxygen. Oxygenated water from the surface percolates down through bedrock fracture zones (Kipp and Dinger, 1987) and increases oxidation rates. Infiltration and percolation of the net surplus of precipitation (precipitation ranges from 100-127 cm annually in the study area according to the National Climatic Data Center, 2009) also drive hydration, carbonation, dissolution, cation exchange, oxidation, and hydrolysis reactions. Organic acids are also generated in elevated rates near the surface, originating from forest litters, plant roots, and leaf through-fall (Younger, 2004), further intensifying near-surface chemical weathering reactions. Thus, the weathered mantle capping the Earth's surface is exposed to more intensive, long-term physical and chemical weathering compared to bedrock strata deep below the surface.

Long-term weathering has leached soluble mineral phases from the surface zone in most areas of the Pottsville and Breathitt groups. Dissolution (via carbonation) and oxidation reactions mobilize carbonates and pyrites, respectively. The net surplus of precipitation carries the mobilized ions out of the upper layers, leaving behind largely inert materials. Kleinmann (2000) found groundwater flowing through the weathered zone to contain low amounts of dissolved solids and alkalinity. Several studies have noted the extent of this weathered zone throughout the Appalachian Plateau. Kleinmann (2000) described the weathered zone as extending to 5 to 20 m below the surface, but typically being on the order of 6 to 12 m thick. Another study (Smith et al., 1974) found the weathered zone to vary in thickness, but generally to be about six m thick.

Brady et al., (1988) discovered the absence of calcareous rocks to a depth of seven m. Weathering was found to extend 10 to 20 m below the surface the study by Hawkins et al. (1996). Daniels et al. (2016) also noted the depth of weathered materials to generally extend 10 to 20 m below the surface. Less than 3% $CaCO_3$ and less than 0.5% total sulfur was found within six m of the surface by Brady et al. (2000), while higher amounts of carbonates and S were found in deeper strata. Singh et al. (1982) noted a loss of alkaline earth elements down to a six m depth. Kirkaldie (1991) observed a weathered zone extending 8.8 m deep in sandstone, but only 3.3 m in shale, suggesting that coarser lithologies support a deeper weathered mantle. Agouridis et al. (2012) compared discharge waters from weathered, unweathered, and mixed spoils in large (> 0.5 ha) field lysimeters. The weathered spoil discharge water was found to have significantly lower pH and EC values, as well as lower concentrations of most studied ions. Similarly, Orndorff et al. (2015) reported significantly higher TDS release from unweathered versus weathered materials from the same strata and location. Thus, it has been shown repeatedly that TDS is significantly lower in weathered spoils compared to unweathered mine spoils and that the depth of weathering generally extends 3.5 to 20 m below the surface, generally depending on site specific lithology.

Soils

Hard rock strata ultimately weather to soil, but high relief in the study area and weathering resistant strata commonly lead to thin soils in the study area. Soil surveys are available for most counties in the Central Appalachian region online at the USDA-NRCS website (http://soils.usda.gov/). Soils in the region are commonly Entisols, Inceptisols, Alfisols, and Ultisols, depending on site-specific soil forming factors (Table 2.2). Parent material has a large influence on soil formation in the area. Residual soils formed out of sandstone often occur along ridges and rocky slopes. These soils generally have a sandy surface and a sandy subsurface. Examples of sandstone soils would be Marrowbone and Matewan soils (both Typic Dystrudepts). Residual soils formed out of shale/siltstone commonly have a loamy or silty surface and subsurface. Berks (Typic Dystrudepts) and Gilpin (Typic Hapludults) soils are examples of shale/siltstone soils. Colluvial soils such as Highsplint (Typic Dystrudepts) and Shelocta (Typic Hapludults) soils occur on lower side slopes and footslope positions and are variable in texture (Fig. 2.4). All locally occurring soils are commonly high in rock fragments (e.g. >15%, often >35%). Clay minerals such as kaolinite, vermiculite, and to a lesser extent smectite, form from the weathering of primary minerals and accumulate in the subsurface in many of the soils (i.e. Alfisols and Ultisols). Soils in the study area are generally of mixed clay mineralogy, so no one specific clay type dominates (Wagner, 2009). Thus, a number of soil forming processes are at work in the Central Appalachians and soils vary highly across the landscape.

Table 2.2. Common soil series (soil name) and taxonomic classes listed in the 2009 Buchanan County, Virginia soil survey (Wagner, 2009). These soils provide a good representation of soils found throughout the Appalachian coalfields.

Soil name	Family or higher taxonomic class
Berks	Loamy-skeletal, mixed, active, mesic Typic Dystrudepts
Calvin	Loamy-skeletal, mixed, active, mesic Typic Dystrudepts
Cedarcreek	Loamy-skeletal, mixed, active, acid, mesic Typic Udorthents
Cloverlick	Loamy-skeletal, mixed, active, mesic Typic Dystrudepts
Cotaco	Fine-loamy, mixed, semiactive, mesic Aquic Hapludults
Fiveblock	Loamy-skeletal, mixed, semiactive, nonacid, mesic Typic Udorthents
Gilpin	Fine-loamy, mixed, active, mesic Typic Hapludults
Grigsby	Coarse-loamy, mixed, active, mesic Dystric Fluventic Eutrudepts
Highsplint	Loamy-skeletal, mixed, active, mesic Typic Dystrudepts
Itmann	Loamy-skeletal, mixed, semiactive, acid, mesic Typic Udorthents
Kaymine	Loamy-skeletal, mixed, active, nonacid, mesic Typic Udorthents
Lily	Fine-loamy, siliceous, semiactive, mesic Typic Hapludults
Marrowbone	Coarse-loamy, mixed, semiactive, mesic Typic Dystrudepts
Matewan	Loamy-skeletal, mixed, active, mesic Typic Dystrudepts
Oriskany	Loamy-skeletal, siliceous, semiactive, mesic Typic Hapludults
Philo	Coarse-loamy, mixed, active, mesic Fluvaquentic Dystrudepts
Rough	Loamy, mixed, active, acid, mesic Lithic Udorthents
Sewell	Loamy-skeletal, mixed, semiactive, acid, mesic Typic Udorthents
Shelocta	Fine-loamy, mixed, active, mesic Typic Hapludults
Stonecoal	Loamy-skeletal, mixed, semiactive, nonacid, mesic Typic Udorthents
Udorthents	Udorthents
Wallen	Loamy-skeletal, siliceous, active, mesic Typic Dystrudepts
Wharton	Fine-loamy, mixed, active, mesic Aquic Hapludults

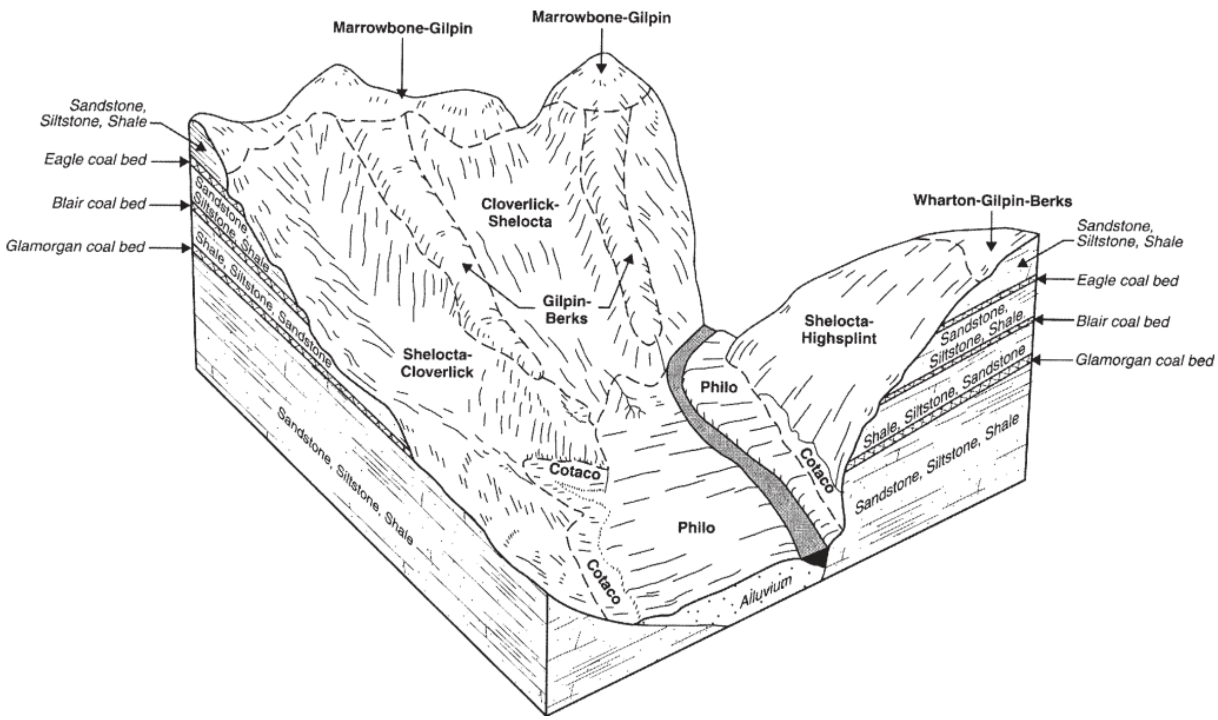

Figure 2.4. Diagram of a typical sequence of soils in the study area. Several common soil series, along with the associated parent materials and landscape positions are illustrated. Figure modified from the soil survey of Buchanan County, Virginia (Wagner, 2009).

References

Agouridis, C. T., P. N. Angel, T. J. Taylor, C. D. Barton, R. C. Warner, X. Yu, and C. Wood. 2012. Water quality characteristics of discharge from reforested loose-dumped mine spoil in Eastern Kentucky. J. Environ. Qual. 41:454–468.

American Petroleum Institute. 1998. The toxicity of common ions to freshwater and marine organisms. Document 0300–029. Washington, DC. Available at http://www.worldcat.org/title/toxicity-of-common-ions-to-freshwater-and-marine-organisms/oclc/52999702

Brady, K.B.C., J.R. Shaulis, and V.W. Skema. 1988. A study of mine drainage quality and prediction using overburden analysis and paleoenvironmental reconstructions, Fayette County, Pennsylvania. US Bureau of Mines Information Circular 9183, pp. 33-43.

Brady, K. B., T. Kania, M. W. Smith, and R. J. Hornbeger. 2000. Coal mine drainage prediction and pollution prevention in Pennsylvania. *In* Proc., West Virginia Surface Mine Drainage Task Force Symposium. 2000. Univ. of West Virginia, Morgantown, WV.

Borchers, J. W. and G. G. Wyrick. 1981. Application of stress-relief-fracturing concepts for monitoring the effects of surface mining on groundwater in Appalachian Plateau valleys. p. 443-449. *In* Proc., Nat. Symp. on Surface Mining Hydrology, Sedimentology, and Reclamation, Lexington, KY. 7-11 Dec. 1981. Univ. of Kentucky, Lexington, KY.

British Petroleum. 2010. BP statistical review of world energy. Available at http://www.bp.com/liveassets/bp_internet/globalbp/globalbp_uk_english/reports_and_publications/statistical_energy_review_2011/STAGING/local_assets/spreadsheets/statistical_review_of_world_energy_full_report_2012.xlsx

Calkins, W.H. 1994. The chemical forms of sulfur in coal: A review. Fuel. 73 (4): 475-484.

Chapman, P.M., H. Bailey, and E. Canaria. 2000. Toxicity of total dissolved solids associated with two mine effluents to chironomid larvae and early life stages of rainbow trout. Env. Toxicol. Chem. 19:210-214.

Clean Water Act (CWA). 33 U.S.C. §1252.

Cormier, S.M., G.W. Suter and L. Zheng, 2013. Derivation of a benchmark for freshwater ionic strength. Env. Toxicol. Chem. 32:263-271.

Daniels, W.L., M. Beck, M.J. Eick and Z.W. Orndorff. 2009. Predicting Contaminant Leaching Potentials for Central Appalachian Overburden and Coal Refuse Materials. Final Report - OSM Applied Science Research Program, December 2009. Available at http://landrehab.org/ItemDetails.aspx?DataItemID=bFJ7oBteh8k%3d

Daniels, W.L., C.E. Zipper, and Z.W. Orndorff. 2014. Predicting release and aquatic effects of total dissolved solids from Appalachian USA coal mines. Int. J. Coal Sci. Technol. 1:152-162.

Daniels, W. L., C. E. Zipper, Z. W. Orndorff, J. Skousen, C. D. Barton, L. M. McDonald, and M. A. Beck. 2016. Predicting total dissolved solids release from Central Appalachian coal mine spoils. Environ. Poll. 216: 371-379.

EIA. 2012. Recoverable reserves at producing mines, estimated recoverable reserves, and demonstrated reserve base by mining method. U.S. Energy Information Administration. Available at http://www.eia.gov/coal/annual/xls/table15.xls.

Evans, D. M., C. E. Zipper, P. F. Donovan, and W. L. Daniels. 2014. Long-Term trends of specific conductance in waters discharged by coal-mine valley fills in Central Appalachia, USA. J. Am. Water Res. Assoc. 50 (6): 1449-60.

Evangelou, V.P. 1995. Pyrite Oxidation and its Control. CRC Press, NY, 293 p.

Hawkins, J.W., K.B.C. Brady, S. Barnes, and A.W. Rose. 1996. Shallow ground water flow in unmined regions of the northern Appalachian Plateau: Part 1. Physical characteristics. p. 42-51. In: Daniels et al. (Eds.), Proc., American Society for Surface Mining and Reclamation, Knoxville, TN, May 18-23, 1996, ASMR, Lexington, KY. Available at http://www.asmr.us/Publications/Conference%20Proceedings/1996/.

Howard, J.L. 1979. Physical, Chemical, and Mineralogical Properties of Mine Spoil Derived from the Wise Formation, Buchanan County. Virginia. M.S. Thesis, Va. Poly. Inst. & State Univ., Blacksburg, VA.

Kennedy, A.J., D.S. Cherry, and C.E. Zipper. 2005. Evaluation of ionic contribution to the toxicity of a coal-mine effluent using *Ceriodaphnia dubia*. Arch. Environ. Contam. Toxicol. 49:155−162.

Kipp, J. A. and J. S. Dinger. 1987. Stress-relief fracture control of ground-water movement in the Appalachian Plateaus. p.423-438. *In* Proc., of the Fourth Annual Eastern Regional Ground Water Conference, Focus on Eastern Regional Ground Water Issues Burlington, Vermont. 14-16 July, 1987. Univ. of KY, Lexington, KY.

Kirkaldie, L. 1991. Paleoweathering and differential erosion beneath glacial materials in Pennsylvania. Bull. of the Assoc. of Engineering Geologists, 28-2: 203-209.

Kleinmann, R.L. (Ed.), 2000. Prediction of water quality at surface coal mines. The National Mine Land Reclamation Center, Morgantown, WV. Available at http://www.arcc.osmre.gov/resources/pubs/1998-RKleinmann-PredictionWaterQuality.pdf

Larsen, D. and R. Mann. 2005. Origin of high manganese concentrations in coal mine drainage, eastern Tennessee. J. Geochem. Explor. 86:143–163.

Lee, G., J.M. Bigham, and G. Faure. 2002. Removal of trace metals by coprecipitation with Fe, Al, and Mn from natural waters contaminated with acid mine drainage in the Ducktown Mining District, Tennessee. Appl. Geochem. 17(5):569−581.

Mount, D. R., J. M. Gulley, J. R. Hockett, T. D. Garrison, and J. M. Evans. 1997. Statistical models to predict the toxicity of major ions to *Ceriodaphniadubia*, *Daphnia magna*, and fathead minnows (*Pimephalespromelas*). Environ. Toxicol. Chem. 16:2009-2019.

NADP (National Atmospheric Deposition Program). 2012. National Atmospheric Deposition Program 2011 annual summary. NADP Data Report 2012-01.Illinois State Water Survey, University of Illinois at Urbana-Champaign, IL. Available at http://nadp.sws.uiuc.edu/lib/data/2011as.pdf.

National Climatic Data Center. 2009. Climatography of the U.S. No. 81 - Supplement # 3 Maps of Annual 1961-1990 Normal Temperature, Precipitation and Degree Days. http://www.ncdc.noaa.gov/oa/documentlibrary/clim81supp3/clim81.html.

Odenheimer, J., J. Skousen, L.M. McDonald, D.J. Vesper, M. Mannix, and W. L. Daniels. 2014. Predicting release of total dissolved solids from overburden material using acid-base accounting parameters. Geochem. Explor. Env. A. 15: 131-137.

Orndorff, Z.W., W.L. Daniels, M. Beck, and M.J. Eick. 2010. Leaching potentials of coal spoil and refuse: Acid-base interactions and electrical conductivity. p. 736-766. *In* R.I. Barnhisel (ed.) Proc. Am. Soc. Min. Reclam., Pittsburgh, PA. 5-11 Jun. 2010. ASMR, Lexington, KY.

Orndorff, Z.W., W. L. Daniels, C.E. Zipper, M. Eick, and M. Beck. 2015. Column evaluation of Appalachian coal mine spoils' temporal leaching behavior. Environ. Poll. 204: 39-47.

Palmer, M. A., and K. L. Hondula. 2014. Restoration as mitigation: Analysis of stream mitigation for coal mining impacts in southern Appalachia. Environ. Sci. Technol. 48 (18): 10552-60.

Pond, G.J. 2010. Patterns of Ephemeroptera taxa loss in Appalachian headwater streams (Kentucky, USA). Hydrobiologia 641:185–201.

Pond, G. J., M. E. Passmore, F. A. Borsuk, L. Reynolds, and C. J. Rose. 2008. Downstream effects of mountaintop coal mining: comparing biological conditions using family- and genus-level macroinvertebrate bioassessment tools. J. North Am. Benthol. Soc. 27:717–737.

Pond, G.J., M. E. Passmore, N.D. Pointon, J.K. Felbinger, C.A Walker, K.J. Krock, J.B. Fulton, W.L. Nash. 2014. Long-term impacts on macroinvertebrates downstream of reclaimed mountaintop mining valley fills in Central Appalachia. Environ. Manag. 54: 919-933.

Powell, J.D. and J.P. Larson, 1985. Relation between groundwater and mineralogy in the coal-producing Norton Formation of Buchanan County, Virginia. U.S. Geol. Survey Water-Supply Paper 2274. Reston, VA. Available at http://pubs.usgs.gov/wsp/2274/report.pdf.

Reaver, N. G., and S. V. Khare. 2014. Imminence of peak in US coal production and overestimation of reserves. Int. J. of Coal Geol. 131: 90-105.

Rose, A.W. and C.A. Cravotta, III. 1998. Geochemistry of coal mine drainage. p. 1.1−1.22. *In* Brady et al. (eds.) Coal Mine Drainage Prediction and Pollution Prevention in Pennsylvania. Pennsylvania Department of Environmental Protection, Harrisburg, PA.

Ruppert, L. F., M. H. Trippi, and E. R. Slucher. 2010. Correlation Chart of Pennsylvanian Rocks in Alabama, Tennessee, Kentucky, Virginia, West Virginia, Ohio, Maryland, and Pennsylvania Showing Approximate Position of Coal Beds, Coal Zones, and Key Stratigraphic Units. U.S. Geological Survey Scientific Investigations Report 2010–5152, 9 p., 3 plates, available at http://pubs.usgs.gov/sir/2010/5152/.

Singer, P.C. and W. Stumm. 1970. Acidic mine drainage: the rate-determining step. Science. 167:1121-1123. Available at http://www.jstor.org/stable/1728684.

Singh, R.N., W.E. Grube, Jr., R.M. Smith, and R.F. Keefer. 1982. Relation of pyritic sandstone weathering to soil and minesoil properties. p. 193-208. *In;* J.A. Kittrick et al. (eds), Acid Sulfate Weathering. Soil Sci. Soc. Am. Spec. Pub 10, Madison, WI.

Skousen, J., J. Simmons, L.M. McDonald and P. Ziemkiewicz. 2002. Acid-base accounting to predict post-mining drainage quality on surface mines. J. Environ. Qual. 31:2034 - 2044.

Skousen, J.G., A. Sexstone, P. F. Ziemkiewicz. 2000. Acid mine drainage control and treatment. pp. 131-168. *In:* R.I. Barnhisel et al. (Eds.), Reclamation of Drastically Disturbed Lands. Agronomy Mono. No. 41. ASA-SSSA, Madison, WI, USA.

SMCRA (Surface Mining Control and Reclamation Act). 1977. P.L. 95-87. Revision 2006. 25 U.S.C. § 1201.

Smith, R.M., W.E. Grube, Jr., T. Arkle, Jr., and A. Sobek. 1974. Mine Spoil Potentials for Soil and Water Quality. U.S. Environ. Protection Agency, Project No.S800745, EPA-670/2-74-070.

Timpano, A. 2011. Levels of Dissolved Solids Associated with Aquatic Life Effects in Headwater Streams of Virginia's Central Appalachian Coalfield Region. M.S. Thesis, Va. Poly. Inst. & State Univ., Blacksburg, VA.

Timpano, A. J., S. H. Schoenholtz, D. J. Soucek, and C. E. Zipper. 2015. Salinity as a limiting factor for biological condition in mining-influenced Central Appalachian headwater streams. J. of the Am. Water Res. Assoc. 51 (1): 240-50.

Tully, J.K. 1996. Coal fields of the conterminous United States: U.S. Geological Survey Open-File Report 96–92, 1 map, scale 1:5,000,000, available at http://pubs.usgs.gov/of/1996/of96-092/

US Court of Appeals. 2013. Mingo Logan Coal Company v. USEPA. Appeal from the United States District Court for the District of Columbia (No. 1:10-cv-00541).

USEPA (U.S. Environmental Protection Agency). 2005. Mountaintop mining/valley fills in Appalachia. Final programmatic environmental impact statement. U.S. Environmental Protection Agency, Region 3, Philadelphia, PA. Available at https://www3.epa.gov/region03/mtntop/eis2005.htm.

USEPA (U.S. Environmental Protection Agency). 2011. The effects of mountaintop mines and valley fills on aquatic ecosystems of the Central Appalachian coalfields (2011 Final). U.S. Environmental Protection Agency, Washington, DC. Available at http://cfpub.epa.gov/ncea/cfm/recordisplay.cfm?deid=225743.

USEPA (U.S. Environmental Protection Agency). 2012. Spruce no. 1 surface mine discharge of dredged or fill materials (404). Decision by Federal District Court for the District of Columbia. Available at http://water.epa.gov/lawsregs/guidance/cwa/dredgdis/spruce.cfm.

USEPA (U.S. Environmental Protection Agency). 2013. Final petition for rulemaking to set water quality standards to protect Appalachian waters from mining waste and harmful levels of conductivity. Petitions to the Office of Water. Available at http://www2.epa.gov/aboutepa/petitions-office-water.

USGS (U.S. Geological Survey). 1997. What is acid rain?. Available at http://pubs.usgs.gov/gip/acidrain/2.html.

USGS (U.S. Geological Survey). 2012. Geologic maps of US states. Available at http://mrdata.usgs.gov/geology/state/.

Wagner, D.F. 2009. Soil survey of Buchanan county, Virginia. USDA-NRCS.

Wunsch, D.R. 1993. Ground-water geochemistry and its relationship to the flow system at an unmined site in the eastern Kentucky coal field. Thesis series 5. Kentucky Geological Survey, Lexington, KY.

Younger, PL. 2004. Environmental impacts of coal mining and associated wastes: A geochemical perspective. Geol. Soc. 236:169−209.

Chapter 3. Geochemical Characteristics of Appalachian Soils and Underlying Bedrock

Abstract

Surface coal mining is often associated with elevated total dissolved solids (TDS) levels in Appalachian headwater receiving streams, which is generated by rainwater percolating through blasted mine spoils. The objective of this study was to analyze the geochemical differences among low, medium, and high TDS generating strata; I hypothesized elemental concentrations would vary significantly among these samples. Thirty-three vertical weathering sequences were sampled from eight coal mines throughout the central Appalachian coalfields; each distinct layer of soil and weathered and unweathered rocks was collected from each sequence, for a total of 204 samples. A saturated paste extract from each crushed sample was analyzed for specific conductance (SC), pH, and elemental concentrations. SC was used as a proxy for TDS and samples were grouped as relatively low (< 300 µS cm^{-1}), medium (300 to 999 µS cm^{-1}), or high (> 1000 µS cm^{-1}) in TDS potential for comparison. No differences were found in overall TDS potentials among sites. Both low- and high-TDS samples occurred across a range of pH values and pH ranged from 2.39 to 8.94. Sulfate, Ca, Mg, K, Na, Cl, and HCO_3^- were the dominant ions found in the saturated paste extractions. The conventional SC to TDS conversion factor (0.64) underestimates the actual mass load of ions in solution; this study indicates a 1:1 relationship. Iron, Al, K, Mg, Ca, and S dominated microwave-assisted acid digests, but only weak correlations existed between acid digest and saturated paste extract ion concentrations. Low-TDS potential samples generally produced higher levels of citrate-dithionite extractable Al and Fe than high TDS samples due to their pre-weathered nature. Some sandstones were studied in thin

section and were generally quartz-rich subarkoses or sublitharenites and high in weatherable feldspars, which likely contribute to TDS production. In summary, my initial hypotheses were confirmed; geochemical properties for the samples ranged widely and increases in overall SC were generally related to the release of sulfate, Ca, and Mg; and to a lesser extent, Cl, K, and Na. I recommend special attention be given to reducing reactive sources of S, Ca, and Mg in spoils in direct contact with drainage waters.

Introduction

Total dissolved solids (TDS) have emerged as one of the leading environmental concerns for the Appalachian coal industry. Multiple court actions involving the EPA (USEPA, 2011; USEPA, 2012; US Court of Appeals, 2013; USEPA, 2013) demonstrate the regulatory and public focus on this topic. The concentration of major ions in mined streams can be 10 times that of unmined reference streams (USEPA, 2011). Elevated concentrations include sulfate, Ca, Mg, Mn, and HCO_3^-. Orndorff et al. (2010; 2015) found Ca, K, Mg, Na, sulfate, and to be the dominant ions released at highest concentrations from mine spoils in column leaching studies. Public attention has been drawn by several recent studies (e.g. Chapman et al., 2000; Kennedy et al., 2005; Pond et al., 2008) showing mining-related increases in TDS concentrations to have negative impacts on stream aquatic life, particularly benthic macroinvertebrates. As described in these studies, the detailed relationship between TDS concentrations and in-stream effects for aquatic life is still under debate, but is not the focus of this paper.

Regardless of specific concentrations and in-stream effects, elevated TDS concentrations in receiving streams generated by Appalachian surface coal mining have been studied and documented at many separate locations (Pond et al., 2014; USEPA, 2011). As native soils are disturbed and hard bedrock is blasted apart to expose coal seams, rainwater and oxygen are available for infiltration and to drive weathering reactions with the freshly exposed materials (Brady et al., 2000). Part of this TDS generation is unavoidable as part of the mining process; however, if potentially high TDS materials can be identified and isolated, perhaps overall TDS loads to adjacent streams can be reduced.

In addition to overall TDS, some studies have shown that individual ions have different toxicities to aquatic life. Mount et al. (1997) found that the relative ion toxicity for *Ceriodaphnia dubia*, *Daphnia magna*, and fathead minnows (*Pimephales promelas*) was K > HCO_3^- = Mg > Cl > sulfate. Therefore, more complete geochemical characterization of the rock spoils generated by mine reclamation can provide further insight into the geologic sources of specific TDS pollutants; unfortunately, studies in this area are lacking, giving rise to the current study.

Saturated paste specific conductance (SC) values are commonly used as a proxy for TDS because TDS is expensive and laborious to analyze. SC can be accurately and rapidly measured with relatively inexpensive instruments (Timpano et al., 2015). As discussed above, environmental effects thresholds of SC between 300 and 500 µS cm^{-1} have been documented and underpin current regulatory proposals (Pond et al., 2008; Timpano et al., 2015). When analyzing for TDS directly, however, samples must be filtered, weighed, oven dried, and weighed again – a very tedious and time consuming process (APHA, 1999). However, SC and TDS are linearly related and virtually all field and laboratory measurements are made with SC. A common equation used for the conversion of SC to TDS in HCO_3 systems is as follows (Evangelou, 1995):

$$\text{TDS (mg L}^{-1}\text{)} = 640 * \text{SC (dS m}^{-1}\text{)}$$

In sulfate-dominated systems, however, the ratio of SC to TDS is generally closer to 1:1. Daniels et al. (2009) showed SC and TDS to be directly and linearly related with a slope approaching 0.95. Daniels et al. (2016) reported that the peak SC for leachates emitted from 39 mine spoils had a very strong correlation with saturated paste SC. Orndorff et al. (2015) found that weathered spoils released lower SC levels than unweathered spoils and that the mean SCs of all 15 spoils studied decreased rapidly from an initial peak of 1468 µS cm^{-1} to 247 µS cm^{-1}.

Thus, the scientific evidence indicates that S, Mg, and Ca dominate overall changes in SC both in mining influenced streams and in direct mine leachate studies. At the beginning of this study, I hypothesized that saturated pastes extracted directly from crushed mine spoils would also be dominated by S, Mg, and Ca and reflect field-scale contributions to local waters. Further, I suggested that saturated paste concentrations for individual ions would vary significantly among low, medium, and high SC samples. The overall objective of this research was to analyze the geochemical properties of a range of Central Appalachian soil and bedrock layers and to compare their properties to differences in the elemental concentrations of saturated paste extracts from a range of low, medium, and high SC samples.

Materials and Methods

Sample Collection and Preparation

Thirty-three vertical weathering sequences were sampled from eight surface coal mines throughout the central Appalachian coalfields (Table 3.1; Fig. 3.1). Twenty-five of these represented unique geologic strata and the remaining eight sequences were replications collected from five of the sites. Sites were selected based on local coal mining companies' willingness to offer site access, but every effort was made to select a wide range of sites throughout the Pottsville and Breathitt groups in the Central Appalachians. Some mining operations covered areas large enough to allow multiple weathering sequences to be collected from different elevations representing different geologic formations, while the size and layout of some operations limited sampling to one weathering sequence. Actual sampling locations at each mine were largely determined by the physical constraints of being able to safely reach the samples. Sites were selected that had been mined within the past five years. In short, samples were collected from recently surface mined areas throughout the Central Appalachians for a total of 33 weathering sequences.

Table 3.1. County, geologic formation, coal bed, and depth of weathering for all 33 sites sampled. See Figure 2.3 for the relative stratigraphic position of these locations.

Site ID	County	Geologic Formation	Coal Bed	Depth of Weathering (m)
1	Buchanan, VA	Wise	Clintwood / Eagle	15.9
2a	Wise, VA	Wise	Low Splint	14
2b	Wise, VA	Wise	Low Splint	14
2c	Wise, VA	Wise	Low Splint	6
3	Wise, VA	Wise	Data Not Provided	12.9
4a	Pike, KY	Breathitt	Data Not Provided	3.9
4b	Pike, KY	Breathitt	Data Not Provided	3.8
4c	Pike, KY	Breathitt	Data Not Provided	9
5	Pike, KY	Breathitt	Data Not Provided	3
6	Pike, KY	Breathitt	Data Not Provided	10
7	Pike, KY	Breathitt	Data Not Provided	1.8
8	Logan, WV	Kanawha	Stockton	3
9	Logan, WV	Kanawha	Stockton	3
10	Breathitt, KY	Four Corners	Peach Orchard	3.6
11	Knott, KY	Four Corners	Peach Orchard	2.5
12	Knott, KY	Four Corners	Peach Orchard	6.8
13	Knott, KY	Four Corners	Peach Orchard	0.7
14	Buchanan, VA	Norton	Raven Rider	11.5
15	Buchanan, VA	Norton	Raven 1, 2, 3	3
16	Dickenson, VA	Norton	Raven 1, 2, 3	6
17	Buchanan, VA	Data Not Provided	Data Not Provided	8.8
18	Pike, KY	Pikeville	Elkhorn 3 rider	5.5
19	Pike, KY	Pikeville	Upper Amburgey	6.5
20	Pike, KY	Pikeville	Data Not Provided	6.5
21a	Buchanan, VA	Norton	Raven 3	8.8
21b	Buchanan, VA	Norton	Raven 3	6.7
21c	Buchanan, VA	Norton	Raven 3	6.7
22a	Dickenson, VA	Norton	Raven 1	4.9
22b	Dickenson, VA	Norton	Raven 1	4.9
22c	Dickenson, VA	Norton	Raven 1	4.9
23	Claiborne, TN	Slatestone	Rich Mt. A	8.2
24	Claiborne, TN	Indian Bluff	Rider above Jelico	1.5
25	Wise, VA	Harlan	No. 13	6.7
		Average weathering depth (m)		**6.5**

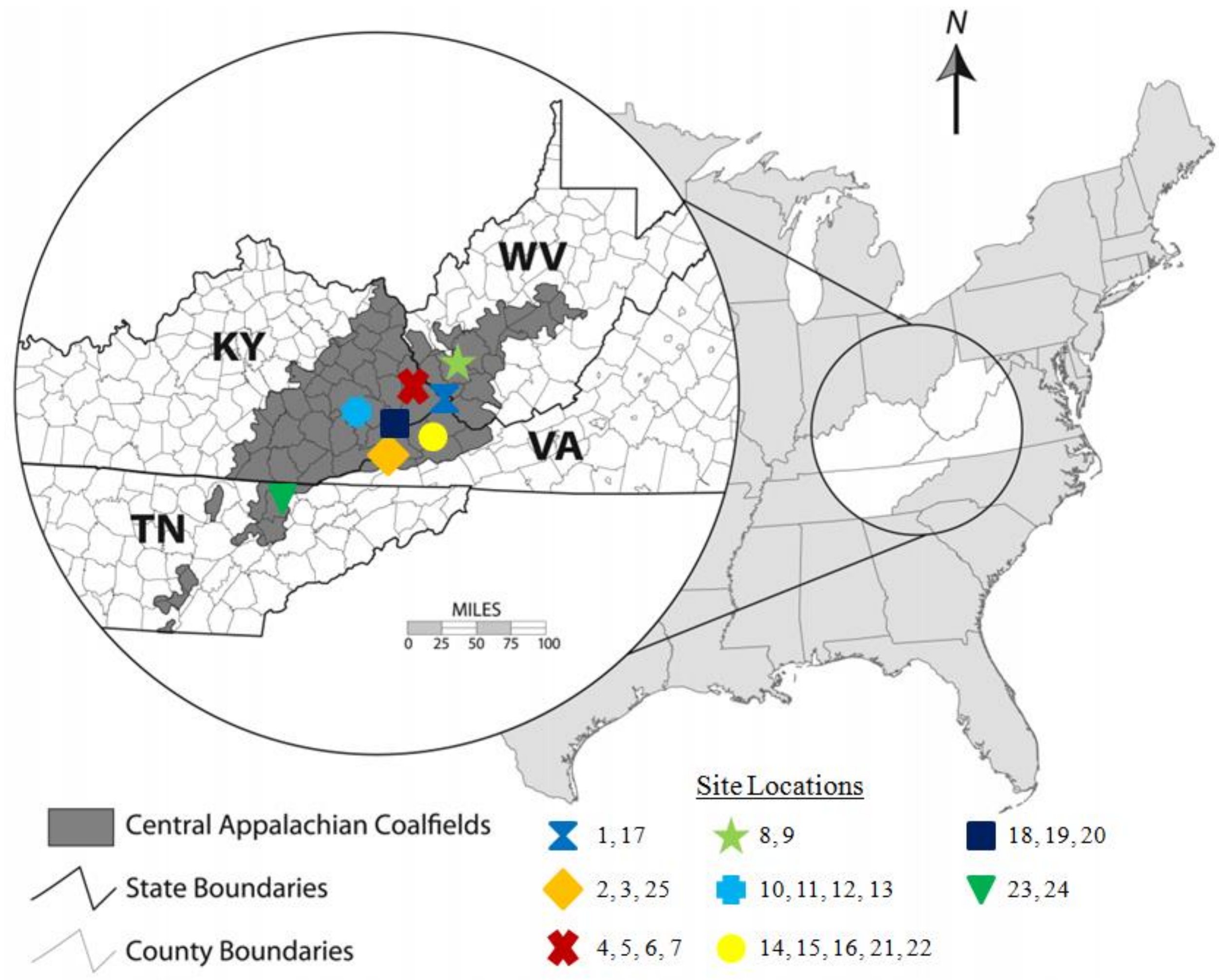

Figure 3.1. The central Appalachian coalfields with site locations indicated for the current study. Modified from USEPA, 2011.

For each "weathering sequence", strata were sampled down through the mining column from the soil surface through fractured, weathered rock into the unweathered lower rock strata. Locations were selected where the native soil and bedrock were still intact and in-situ. Soil samples were dug by hand auger and bedrock samples were removed with a rock hammer from freshly mined highwalls. Sampling generally extended at least 15-30 m below the surface, depending on the physical accessibility of each location. Some weathering sequences were sampled from drill cores (~ 5 cm diameter) rather than from highwalls. In this case, all "rippable" soil and rock layers were bulldozed away before drilling, so the weathering sequences sampled from drill cores did not contain the uppermost soil and rock layers. Each distinct layer was collected from each weathering sequence, for a total of 204 individual samples, and mechanically crushed to < 2 mm using a swinging jaw crusher. The samples were then subsampled for certain analyses, such as total-S, and further ground to a < 0.05 mm powder using a mechanical mortar and pestle.

Saturated Paste Extractions

Saturated paste extractions were used to determine saturated paste SC, pH, and ionic composition. Deionized water was added to samples crushed to < 2 mm to form a saturated paste and allowed to equilibrate for 2 hours (Rhoades, 1996). Liquid was then extracted from the soil/water slurry using vacuum filtration. The resulting extract was tested for SC and pH. Samples were sorted into categories of low SC (0-299 $\mu S\ cm^{-1}$; n = 120), medium SC (300-999 $\mu S\ cm^{-1}$; n = 52), and high SC (1,000+ $\mu S\ cm^{-1}$; n = 32) for comparison. These general groupings were made based upon (a) the general distribution of SC values across the data set and (b) the reported lower environmental effects threshold of 300 $\mu S\ cm^{-1}$ as discussed earlier.

The saturated paste extract was also analyzed for individual ionic concentrations. A subsample was transferred into a test tube and preserved by adding 8N nitric acid for a final approximate acidity of 3%. Elemental concentration was then determined by USEPA, 2007 method SW 846 6020A, revision 1, using a Thermo Electron Corporation ICP-MS, X-Series. Each extract was then analyzed for total Al, As, Ca, Cl, Co, Cu, Fe, K, Mg, Mn, Mo, Na, Ni, P, Se, Sr, and Zn. A separate subsample was analyzed for S content utilizing USEPA, 2001 method SW 846 6010B, revision 2, using a Spectro ARCOS ICPES Model FHS16 with CETAC ASX-520 autosampler. Sulfur was assumed to be in the form of sulfate in the saturated paste extract for mass comparison of ions. The saturated paste extract SC was then compared to individual ion concentrations as detected by ICP.

Microwave Assisted Acid Digestion and Total Sulfur

USEPA's Method 3051A, Revision 1 (USEPA, 2007) was used to determine the "environmentally available" elemental concentration. Historically, these data were reported as “total elemental analysis”. However, while this method uses a strong acid solution with microwave digestion, it does not fully dissolve quartz, certain silicates, titanium oxides, zircon, alumina, and certain other oxides, so it is not currently considered by USEPA to effectively represent a "total elemental" analysis. Regardless, this method does provide a relative estimate of the total mass amount of major and minor elements present in the samples for comparison to the saturated paste extracts. For this study, a two g sample was digested and elemental concentrations determined using a Thermo Electron Corporation ICP-MS, X-Series USEPA method SW 846 6020A, revision 1, for Al, As, Ca, Cu, Fe, K, Mg, Mn, Mo, Ni, and Zn.

Total Sulfur (Total-S) was determined on a separate powder-ground, air-dry subsample with a LECO S632 Sulfur Analyzer, which uses dry combustion and infrared analysis to determine the total-S content. Results were reported on a percent and ppm (mg kg^{-1}) basis. Speciation of the different forms of S was beyond the scope and budget of this research, but the common forms of S in the study area are discussed in the results below.

Citrate Dithionite Extractable Aluminum, Iron, and Manganese

Citrate-dithionate (CD) extractable Fe/Mn/Al was determined according to NRCS Soil Survey Laboratory Methods (USDA-NRCS, 2004). For each sample, 0.75 g of < 2 mm, air-dry material was added to a 50 mL centrifuge tube along with 0.4 g of sodium dithionite and 25 mL 0.57 M sodium citrate solution. The samples were then placed on a shaker at 200 oscillations per minute for 12-16 hours, allowed to settle overnight, and then centrifuged for 15 minutes at 4000 rpm. Finally, Al, Fe, and Mn were determined on a clear aliquot of the extract by ICP-AES.

Hydrogen Peroxide pH and Specific Conductivity

A novel method to test pH and SC was employed to determine the usefulness of the method to predict geochemistry of the soil and bedrock materials following exposure to oxidation. The method used was a modified version of the standard 1:1 water:soil technique for measuring EC and pH described in the NRCS Soil Survey Laboratory Methods (USDA-NRCS, 2004) and similiar to field tests that have been developed for acid sulfate soils (Ahern et al., 2004). Commercially available H_2O_2 (3%) was used in place of the water in the method. The basic concept was to oxidize reduced sulfides and accelerate acid-base reactions to produce TDS. Five g of air-dry material ground < 2 mm was added to a test tube. Next, five mL of H_2O_2 was added to the test tube and stirred for one minute. The sample was stirred again at 10 minutes and at 20 minutes and then tested for SC and pH at 30 minutes. Samples which were high in organic matter, sulfides, or manganese reacted vigorously with the peroxide and much of the liquid added generated foam. Topsoil samples high in organic matter also soaked up a large amount of the liquid. In such cases where the amount of liquid remaining was not enough to test, an additional five mL of DI water was added. Samples were simultaneously tested using the standard 1:1 water method for SC and pH for comparison.

Mehlich Dilute Double Acid Extractable Ions

In addition to the other specialized analyses described here, the samples were also sent to Virginia Tech's Extension Soil Testing Laboratory (VTSTL) for routine soil testing. The VTSTL provides water pH, buffer pH, CEC by summation, and Mehlich 1 extractable concentrations of Al, B, Ca, Cu, Fe, K, Mg, Mn, and Zn. Water pH is determined on a 1:1 (vol/vol) ratio pH measurement. The elemental concentrations are determined by adding Mehlich 1 dilute, double acid solution (0.05 N HCl and 0.025 N H_2SO_4), shaking for five minutes, and then analyzing with ICP-AES (Maguire, 2011).

Petrographic Thin Section Analysis

Fourteen sandstone samples were selected for additional optical analysis by petrographic thin section analysis using reflected light microscopy. Samples were chosen where there was a clear relationship between weathered and unweathered strata from the same location. These 14 samples were sent to the National Petrographic Service, Inc. and stained to aid in the analysis of porosity, ferruginous carbonate, and calcite. Upon return, 300 to 400 point counts were made for each sample (by Dr. K. Eriksson; Virginia Tech committee member) to determine detailed mineralogy using a grid system on a mechanical stage.

Statistical Analyses

JMP Pro 11.0 Statistical Discovery software from SAS was used for statistical analysis. A p value ≤ 0.05 was considered significant. Initial analysis revealed the data had several strong outliers, unequal variances, unequal sample sizes between categories, and was also skewed strongly to the left (with many more low than high TDS samples) – all of which challenged the assumptions for normality, so non-parametric statistical tests were chosen. The non-parametric Kruskal-Wallis one-way analysis of variance test was used to compare median values to determine overall significant differences. The Steel-Dwass method was used to compare median values between individual categories. Spearman's nonparametric rank correlation method was used to test relationships between ions and overall TDS. For ICP-MS analysis, concentration values below the specified limits of detection (LOD) for each element were handled according to the method described by Croghan and Egeghy (2003) and replaced with half the LOD.

Results and Discussion

Saturated Paste Extractions

The saturated paste extract SC analysis revealed large differences between individual samples. No significant differences in the mean saturated paste SC between sites were found (p = 0.09), but site 18 contained several samples with much higher values for overall SC (Fig. 3.2). Six extreme outliers were excluded from the 204 sample set for the statistical analyses presented below using a cutoff value of > 1 for Cook's Distance outlier analysis, leaving a total of 198 samples. These six outliers were from sites 10, 18, and 20 and contained variety of rock types, including one coal, three dark gray shales, one dark gray sandstone, and one brown sandstone sample. Across all of the sites, the SC ranged from 23 µS cm^{-1} to 4,690 µS cm^{-1} and the mean and median SC were 503 µS cm^{-1} and 204 µS cm^{-1}, respectively.

These saturated paste SC results agree with other, similar studies. Daniels et al. (2014) analyzed three coal mine spoils and three coal refuse samples and found the saturated paste SC to range from 1,261 µS cm^{-1} to 2,820 µS cm^{-1}. A joint study with samples from Virginia, Kentucky, and West Virginia (Odenheimer et al., 2014) presented 41 mine spoils (and one coal refuse) which ranged in saturated paste SC from 26 µS cm^{-1} to 2415 µS cm^{-1} for the mine spoils and even higher for the coal refuse sample, 3,505 µS cm^{-1}. Daniels et al. (2016) studied 39 weathered and unweathered mine spoils and found saturated paste SC to range from 87 µS cm^{-1} to 7,370 µS cm^{-1}. Orndorff et al. (2015) analyzed a smaller set of 15 weathered and unweathered mine spoils from Virginia and reported saturated paste SC to range from 264 µS cm^{-1} to 3560 µS cm^{-1}.

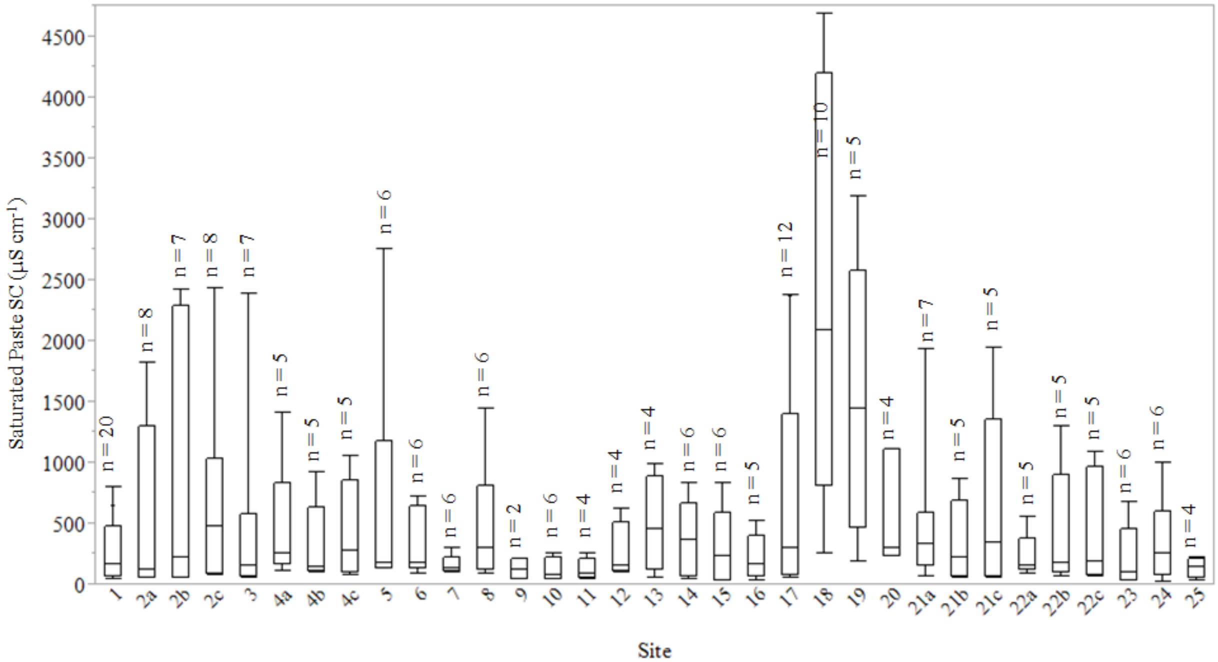

Figure 3.2. Quantile box plots of mean saturated paste specific conductance by site summarizing the range and the 25th, 50th (median), and 75th percentiles of the data. Letters represent site replications. Samples of each distinct layer (topsoil, subsoil, weathered bedrock, and unweathered bedrock) were collected from the soil surface down into clearly unweathered materials. The total number of samples was 198 and "n" represents the number of samples collected at each site. Soil layers were not collected for sites 9, 17, 18, 19, and 25. Six extreme outliers were found at sites 10 (1), 18 (4), and 20 (1) and are not included here. While site 18 contained many of the highest SC samples, no significant differences were found among sites.

Samples with both low and high pH values produced moderate to high SC values (Fig. 3.3), although a slight difference in mean pH was found between samples with low SC compared to samples with medium and high SC ($p < 0.005$). Samples with relatively low SC levels returned a significantly lower mean pH value (6.17) compared to samples with relatively medium and high SC levels (7.13 and 7.08, respectively). This was presumably due to their pre-weathered nature and loss of reaction products over time. However, samples in each category did range widely in pH, which limits the usefulness of pH as an indicator of TDS potential since both weathered samples that produced low TDS and acid-forming spoils that produced very high TDS produced low pH extracts. This is discussed further in Chapter 4.

Previous studies report similar findings. Roberts et al. (1988) found unweathered overburden pH to range from 6.5 to 8.2 and weathered overburden pH to range from 4.5 to 6.0. Odenheimer et al. (2014) found pH to range from 4.1 to 8.3 for 41 mine spoil and coal refuse samples and also showed a poor relationship (R^2=0.12) between calculated TDS and saturated paste pH. In 2010, Orndorff et al. showed that column leachates from samples with higher levels of S contained higher levels of TDS across a range of pH levels.

Saturated paste SC had a strong correlation (r_s = 0.90; Fig. 3.4) with the sum of all ions analyzed (sum of ICP-MS elements + sulfate + HCO_3^-). The regression equation for this relationship, Y = 109.3 + 1.045X, shows that the ratio of this relationship was close to 1:1 for approximately 90% of the samples. In addition to the direct results reported below, this relationship clearly reinforces the fact that for mine spoil systems where sulfate is the dominant anion, the conventional SC to TDS conversion factor (e.g. 0.64) significantly underestimates the total mass ionic load. Several individual elements also had a strong relationship with the overall salinity of the saturated paste extracts. Spearman's nonparametric rank correlation coefficients for saturated paste SC vs. HCO_3^-, Ca, Cl, K, Mg, Na, and sulfate were 0.59, 0.90, 0.01, 0.71, 0.92, 0.65, and 0.88, respectively, and Ca, Mg, and sulfate also had a very strong correlation with overall TDS. While Ca and Mg showed a slightly stronger correlation than sulfate with SC, comparing the results on a mass basis revealed more details.

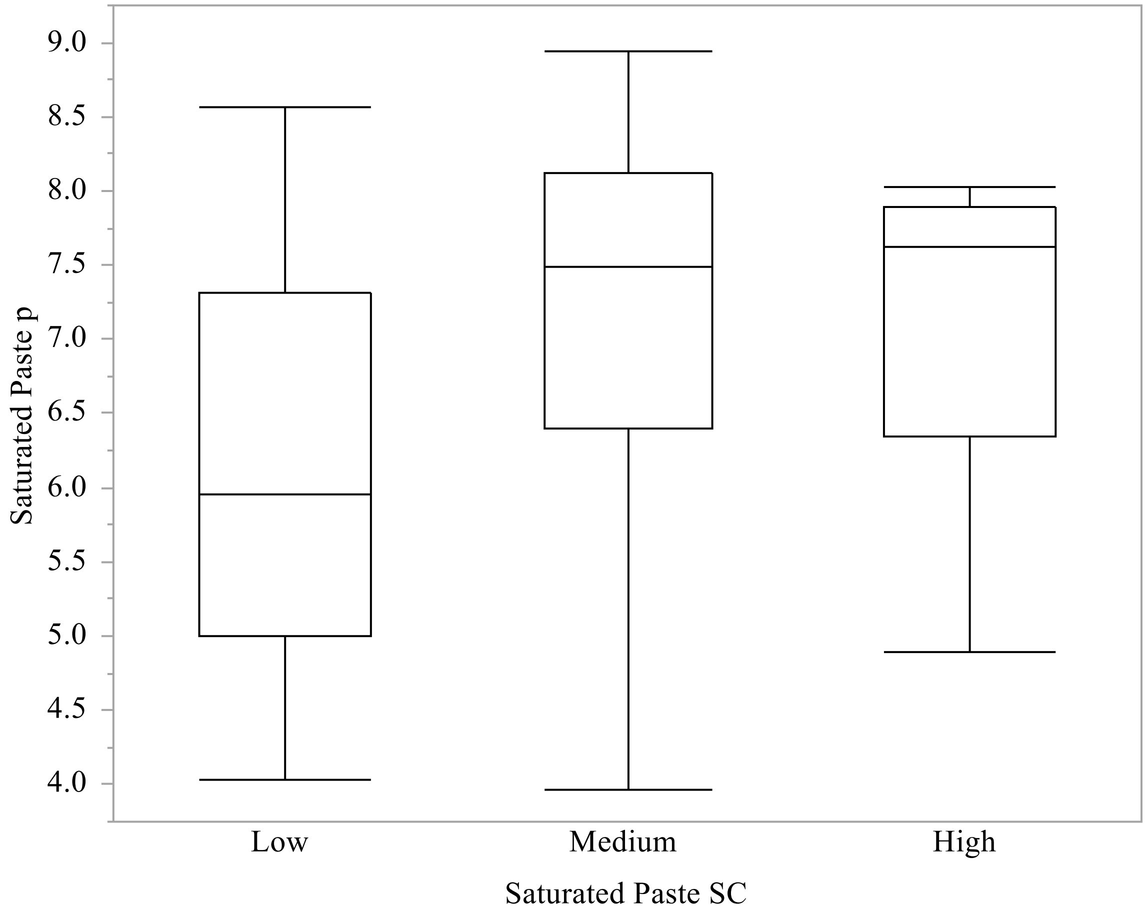

Figure 3.3. Quantile box plots of mean saturated paste pH by relative saturated paste SC levels summarizing the range and the 25th, 50th (median), and 75th percentiles of the data. Samples are sorted by saturated paste specific conductance into categories of low (< 300 µS cm^{-1}; n = 120), medium (300 - 999 µS cm^{-1}; n = 52), and high (≥ 1,000 µS cm^{-1}; n = *32*). Medium and high SC samples were higher in pH (p < 0.005) compared to low SC samples.

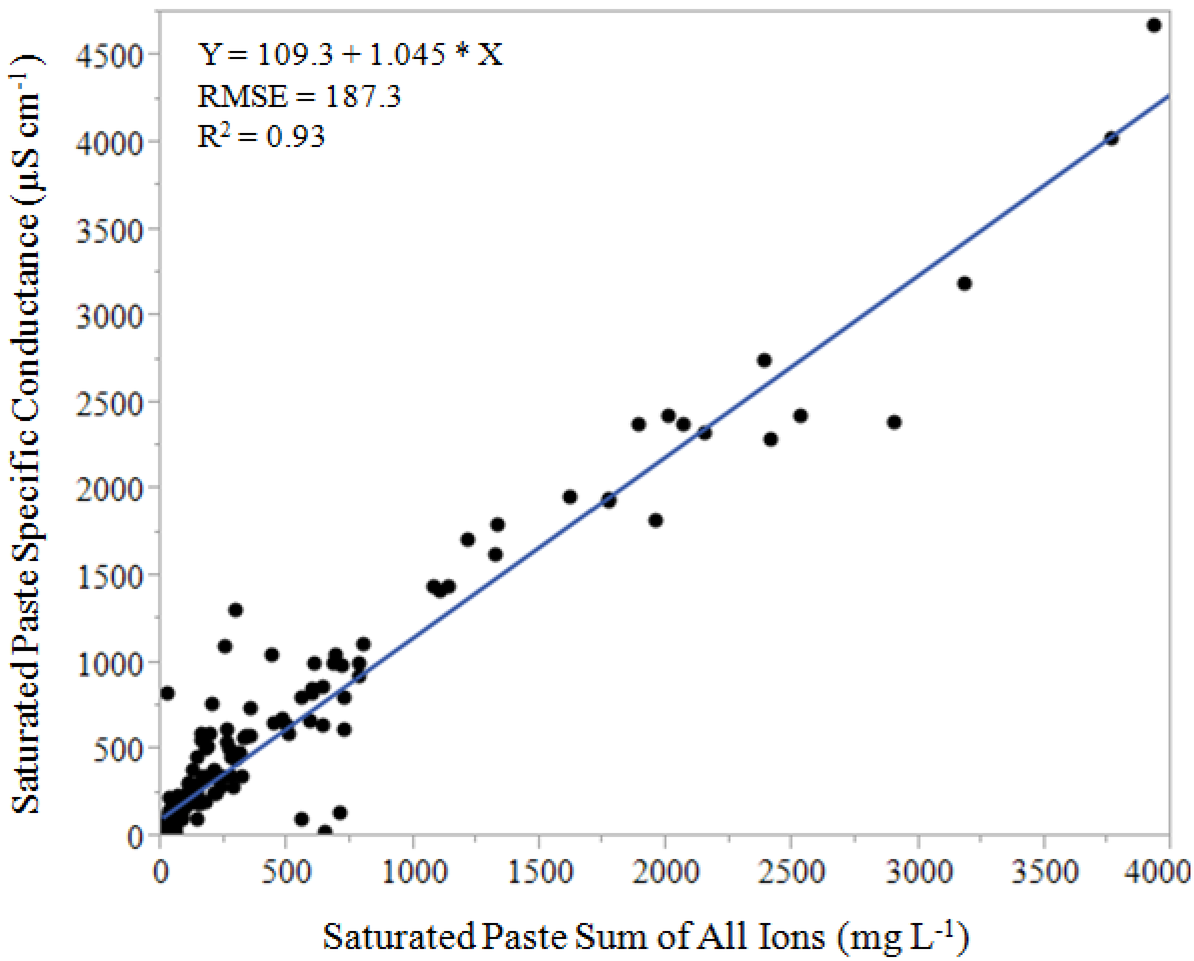

Figure 3.4. Saturated paste SC versus the sum of all of the ions analyzed (sum of ICP-MS elements + sulfate + HCO_3^-). Saturated paste SC had a strong correlation (r_s= 0.90) with the sum of all of the ions analyzed (sum of ICP-MS elements + sulfate + HCO_3^-). The regression equation for this relationship, Y = 109.3 + 1.045X, shows that the ratio of this relationship is close to 1:1 for approximately 93% of the samples. Spearman's rho nonparametric rank correlation gave similar results (r_s = 0.90).

Sulfate, Ca, Mg, K, Cl, Na, and HCO_3^- were found to be the largest contributors to overall TDS on a mass basis, making up 65%, 13%, 7%, 5%, 3%, 2% and 1% of total TDS, respectively (Fig. 3.5). These seven ions alone constituted 97% of calculated TDS mass on average across all of the samples. Sulfate, Ca, Mg, K, and Na increased significantly from low, to medium, to high SC levels (all $p < 0.004$). Sulfate means for low, medium, and high SC levels were 24 mg L^{-1}, 217 mg L^{-1}, and 1310 mg L^{-1}, respectively. The means for Ca of 8 mg L^{-1}, 52 mg L^{-1}, and 231 mg L^{-1}, for low, medium, and high SC levels, respectively. Magnesium mean values were low (5 mg L^{-1}), medium (26 mg L^{-1}), and high (141 mg L^{-1}). Potassium levels for low, medium, and high SC samples had means of 13 mg L^{-1}, 26 mg L^{-1}, and 42 mg L^{-1}, respectively. Sodium means were 5 mg L^{-1}, 13 mg L^{-1}, and 18 mg L^{-1}, respectively. Thus, as saturated paste SC increases, so does the concentration of sulfate, Ca, Mg, K, Cl, Na, and HCO_3^-.

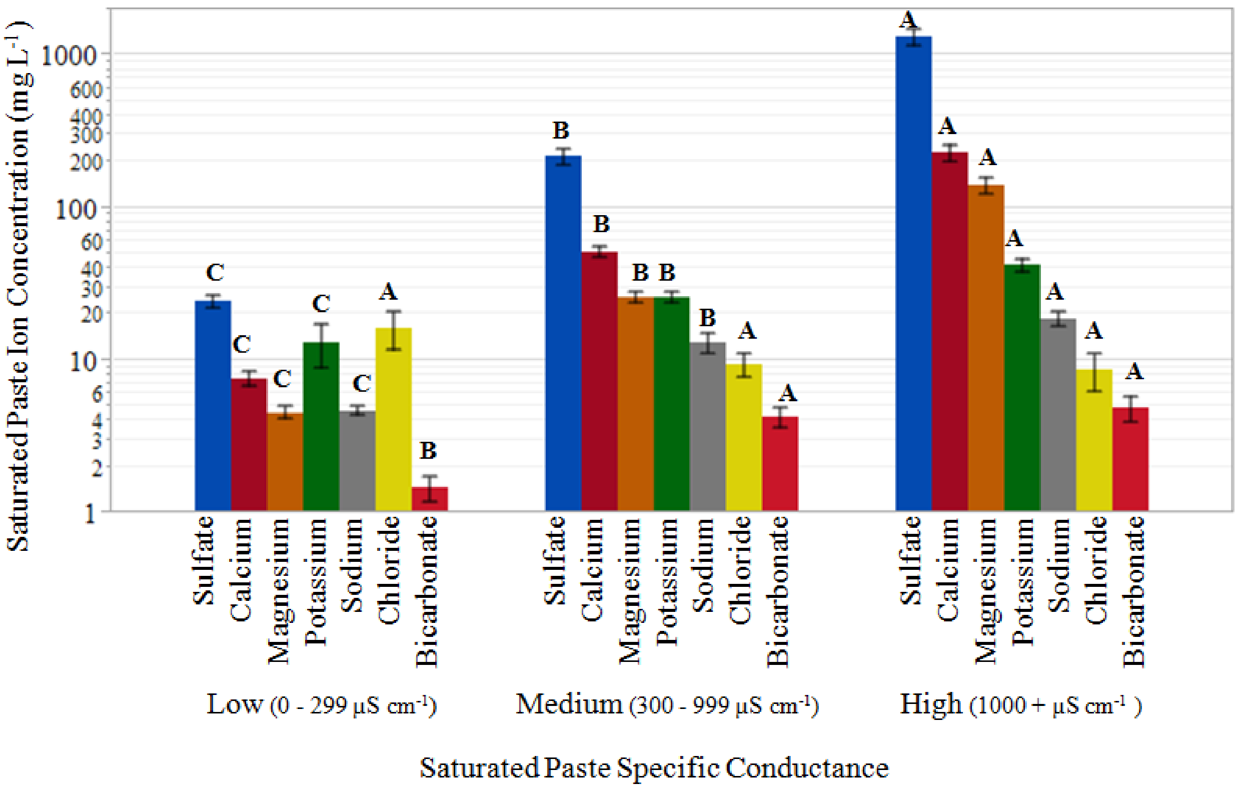

Figure 3.5. Saturated paste ion concentration versus saturated paste specific conductance for major ions. Samples are sorted by saturated paste specific conductance into categories of low (< 300 µS cm^{-1}; n = 120), medium (300 - 999 µS cm^{-1}; n = 52), and high (≥ 1,000 µS cm^{-1}; n = 32). Different letters indicate significantly different (α = 0.05) concentrations for individual ions across the low, medium, and high categories. Error bars represent one standard error above and below the mean.

In contrast, Cl and HCO_3 did not increase regularly and proportionally with increases in overall TDS. Chloride was not significantly different (all $p > 0.64$) between low, medium, and high SC samples, with means of 16 mg L^{-1}, 9 mg L^{-1}, and 9 mg L^{-1}, respectively. HCO_3^- was significantly lower for samples with low SC levels than for medium and high SC levels ($p < 0.001$), with means of 1 mg L^{-1} for low, 4 mg L^{-1} for medium, and 5 mg L^{-1} for high SC samples.

Previous studies have found these same elements to be the main contributors to TDS. Skousen et al. (2000) found Ca, K, Mg, Na, sulfate, and HCO_3^- to be the main ions at neutral pH ranges, in addition to Al, Fe, and Mn at lower pH ranges. USEPA (2011) found sulfate, Ca, Mg, Mn, and HCO_3^- to be among the elevated parameters in streams associated with valley fills compared to unmined or reference stream areas. Daniels et al. (2009) and Orndorff et al. (2015) reported Ca, K, Mg, Na, sulfate and HCO_3^- were the dominant ions in mine spoil leachate solutions.

Many of the trace elements showed a poor relationship with SC, maintaining similar levels across low, medium, and high SC samples (Fig. 3.6). However, Si was significantly higher in low SC extracts when compared with medium and high SC extracts ($p < 0.004$). Manganese and Fe had significantly higher average means for high SC samples compared to the medium and low SC samples. Mean Mn levels were 816 µg L^{-1}, 1581 µg L^{-1}, and 4847 µg L^{-1}, while Fe was 374 µg L^{-1}, 398 µg L^{-1}, and 4676 µg L^{-1} for low, medium, and high SC levels, respectively ($p < 0.04$). Aluminum, P, Zn, and Cu showed no significant differences between SC levels ($p > 0.08$). Strontium had significantly different values for each of the low, medium, and high SC levels, with means of 40 µg L^{-1}, 380 µg L^{-1}, and 753 µg L^{-1}, respectively (all $p < 0.001$). Nickel, Se, and Mo were significantly higher in high and medium SC extracts than in low SC extracts, with $p <$

0.001. Nickel had means of 11 μg L^{-1}, 41 μg L^{-1}, and 254 μg L^{-1}; Se had means of 3 μg L^{-1}, 59 μg L^{-1}, and 115 μg L^{-1}; and Mo had means of 2 μg L^{-1}, 5 μg L^{-1}, and 52 μg L^{-1} for low, medium, and high SC samples, respectively. Mean As was unexpectedly significantly higher at medium SC levels (2 μg L^{-1}) than in low or high level extracts (0.7 and 0.9 μg L^{-1}, respectively), with $p < 0.05$. Thus, while some of the trace elements varied significantly with changes in sample TDS potential, these elements only made minor contributions to changes in overall TDS.

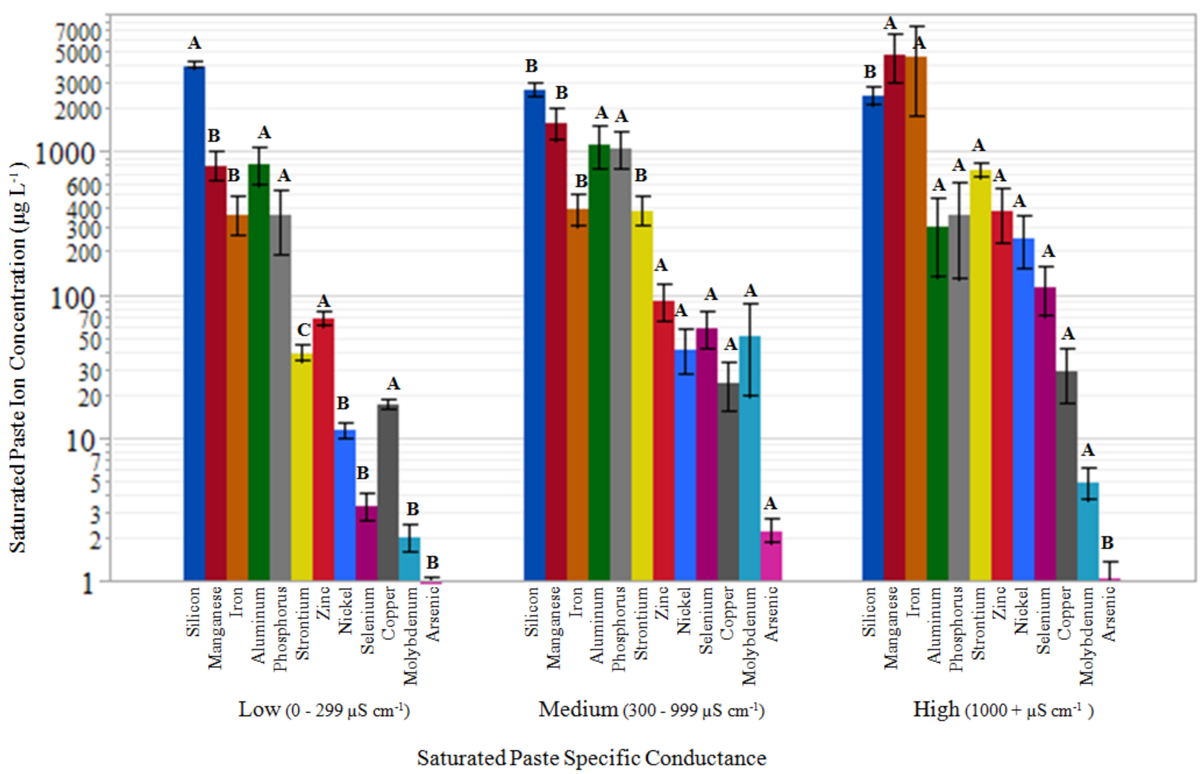

Figure 3.6. Saturated paste ion concentration versus saturated paste specific conductance for trace elements. Samples are sorted by saturated paste specific conductance into categories of low (< 300 μS cm^{-1}; n = 120), medium (300 - 999 μS cm^{-1}; n = 52), and high (≥ 1,000 μS cm^{-1}; n = *32*). Error bars represent one standard error above and below the mean. Different letters indicate significantly different (α = 0.05) concentrations for individual ions across the low, medium, and high categories.

Microwave-Assisted Acid Digestion and Total Sulfur

Total S concentrations increased significantly from low, medium, to high SC levels, with means of 0.03%, 0.09%, and 0.26%, respectively (all $p < 0.001$; Fig. 3.7). Sulfur forms were not differentiated for this study. A-horizon (or "topsoil") samples, coal samples, and other coal associated materials, such as fireclays, likely contained some amount of organic S in addition to reduced forms (including sulfides) and generally contained higher levels of Total-S than other samples. Freney et al. (1961) showed that 1% or less of S in the topsoils studied was in reduced forms, such as sulfide; rather it was generally found in an organic form. Calkins (1994) showed S contents by percent (on a mass basis) and speciation in various U.S. coals. Illinois No. 6 contained 1.06% pyritic-S, 0.12% sulfate, and 2.17% organic-S, for a total of 3.35% total-S. Ohio No. 6 coal contained 1.15% pyritic-S, 0.03% sulfate, and 2.01% organic-S, for a total of 3.19% total-S. Daniels (2014) found total-S to range from 0.23% to 1.25% in mine spoil materials and from 0.76% to 7.00% in coal refuse materials. Orndorff et al. (2015) reported 15 mine spoils from Virginia to range from 0.02% to 0.34% total-S. So, while total-S concentrations were lower than some samples noted in previous studies, the current samples generally fell within the normal range of total-S concentrations for the study area.

Elements present in the highest concentrations from the EPA 3051A microwave-assisted acid digest included Fe, Al, K, Mg, and Ca, followed by total-S (listed highest to lowest concentration); total-S values presented here represent a higher recovery rate than the other elements. Mean values for Ca, K, Al, and Fe were significantly higher for medium and high SC samples than low SC samples ($p < 0.02$). Mean values for Ca and K were 0.17%, 0.55%, and 0.61% and 0.56%, 0.75%, and 0.99% for low, medium, and high SC samples, respectively. Low, medium, and high SC samples had mean Al and Fe concentrations of 2.52%, 3.00%, and 3.64% and 2.39%, 3.36%, and 3.92%, respectively. Magnesium concentrations increased significantly from low (0.28%), medium (0.58%), to high (0.80%) SC levels, with all $p < 0.001$. Daniels et al. (2009) used a similar digestion method and found the following ranges in elemental concentrations for 25 coal refuse and mine spoil samples: Mg 0.17-0.97%; Ca 0.08-1.26%; Fe 1.77-4.50%; K 0.18-0.36%; Al 0.70-1.81%. The results from the current study generally fell within these same ranges. So, there was a shift in the dominant ions present in the environmentally available elemental digests compared to the saturated paste deionized water extracts. The microwave-assisted acid digests were dominated by Fe and Al, but the saturated paste extracts using only deionized water were dominated by S, Mg, and Ca. These results reflect the more rapid initial weathering of minerals containing elements such as S, Mg, and Ca over other more stable oxide minerals containing Fe and Al which are released by the strong acid used for the microwave-assisted acid digest.

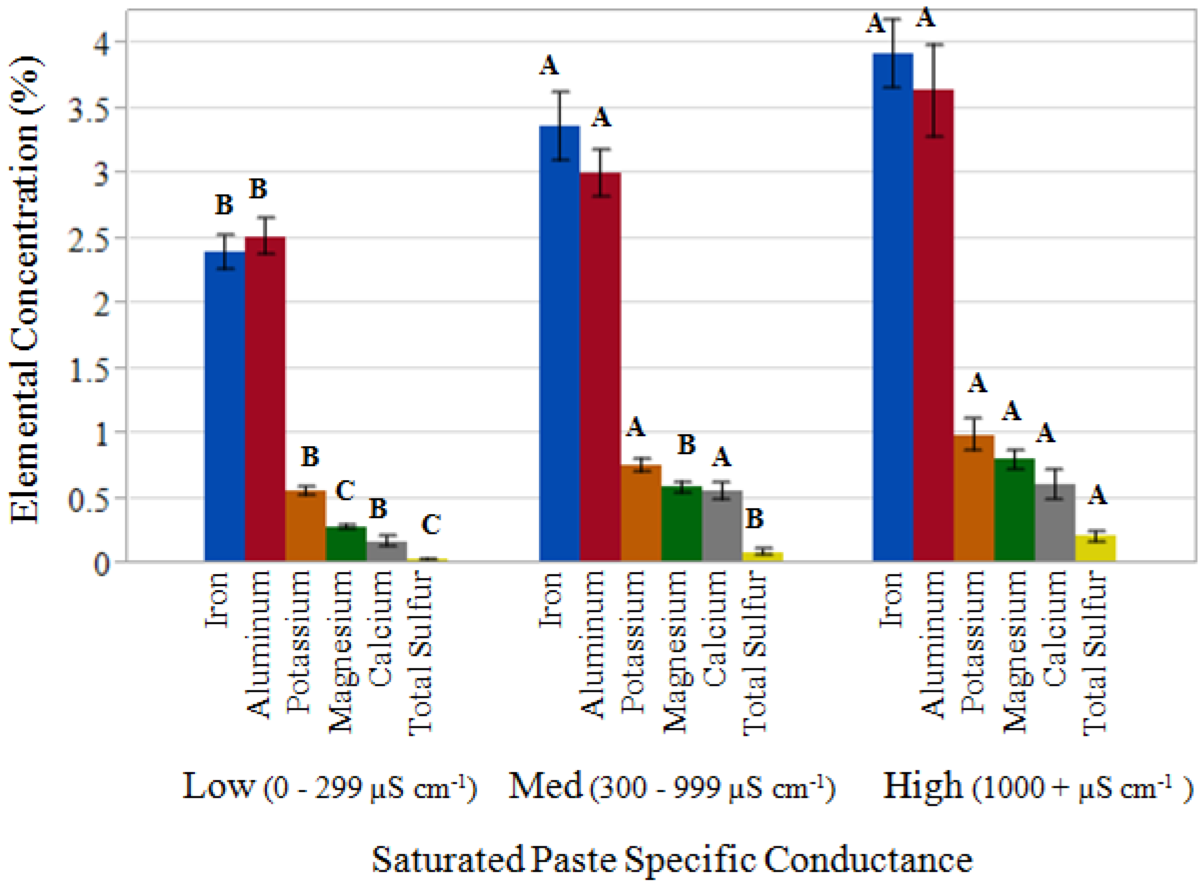

Figure 3.7. Mean microwave-assisted acid digest ion concentration and total-S concentration versus saturated paste specific conductance for dominant ions. Total-S data represents a total recovery technique. All other elements are represented on an environmentally available basis. Samples are sorted by saturated paste specific conductance into categories of low (< 300 µS cm^{-1}; n = 120), medium (300 - 999 µS cm^{-1}; n = 52), and high (≥ 1,000 µS cm^{-1}; n = 32). Error bars represent one standard error above and below the mean. Different letters indicate significantly different (α = 0.05) concentrations for individual ions across the low, medium, and high categories.

Total-S and acid digest Ca and Mg concentrations all had significant (p < 0.001) correlations with the corresponding saturated paste extract concentrations (Figs. 3.8, 3.9, and 3.10). Total-S had a moderate correlation (r_s=0.66) with the saturated paste sulfate. The acid digest Ca had a moderately strong correlation (r_s=0.75) with the saturated paste extract Ca, but the acid digest

Mg was weakly correlated (r_s=0.46) with saturated paste extract Mg. All other correlations between environmentally available element concentrations and saturated paste extract concentrations were weak (r_s < 0.4). Thus, increases in the amount and weatherability of S, Ca, and Mg-bearing minerals within a sample accounted for the largest increases in overall TDS.

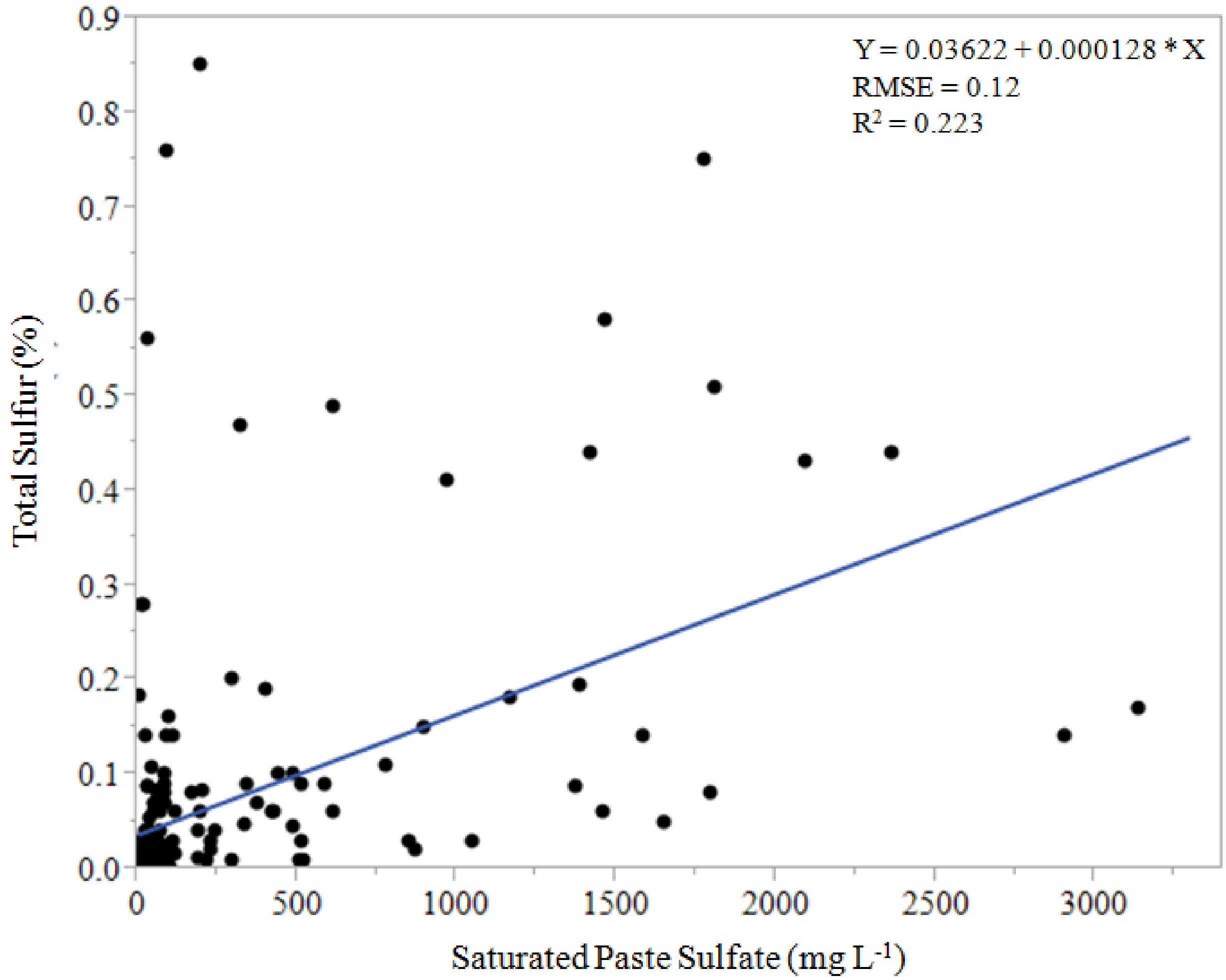

Figure 3.8. Total-S versus saturated paste sulfate for 198 samples. Total-S had a significant effect on saturated paste sulfate (p < 0.001). Spearman's rho nonparametric rank correlation produced a much stronger relationship (r_s = 0.67) than the simple linear regression shown above.

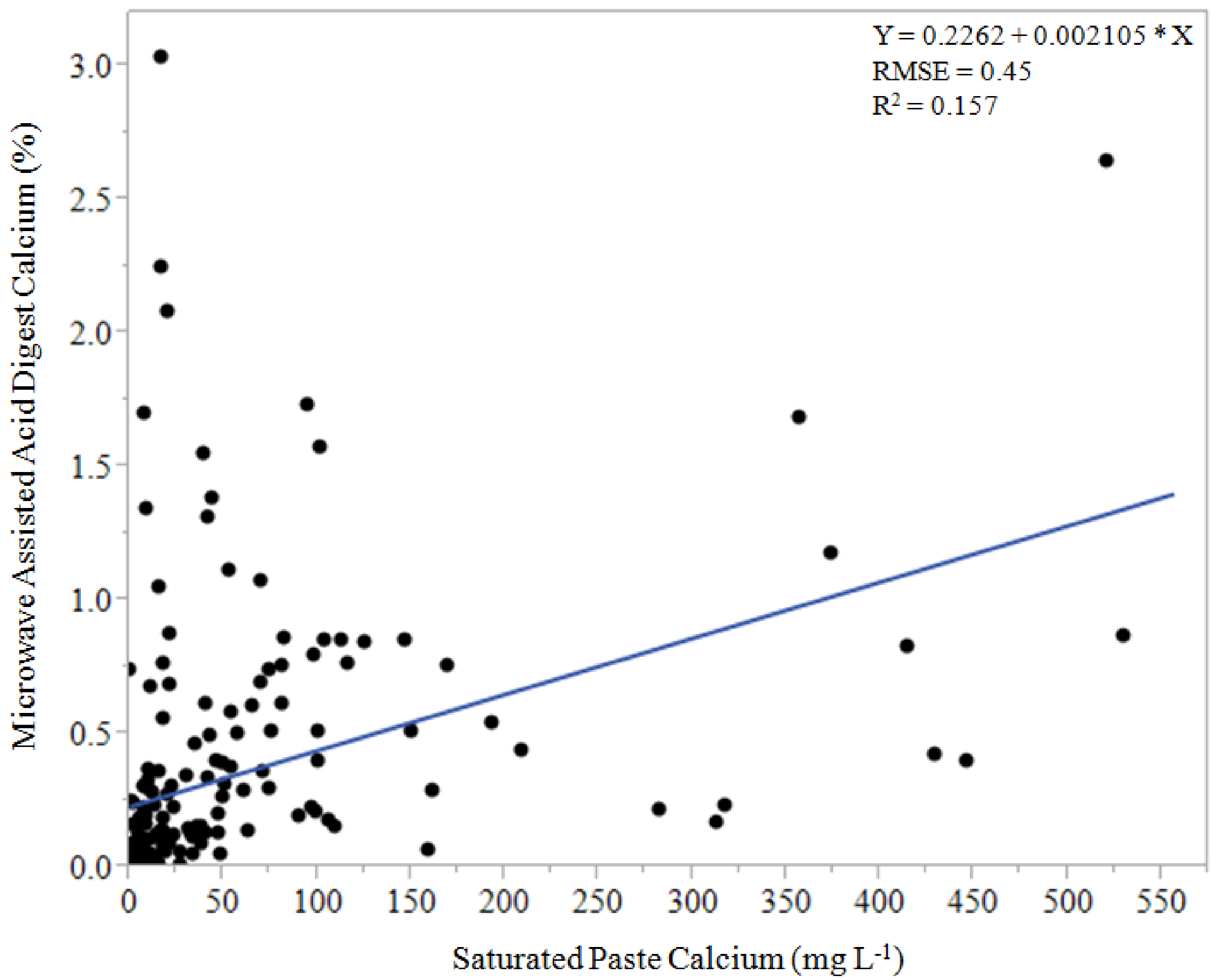

Figure 3.9. Microwave-assisted acid digest (environmentally available) Ca versus saturated paste Ca for 198 samples. Environmentally available Ca had a significant effect on saturated paste Ca (p < 0.001). Spearman's rho nonparametric rank correlation produced a much stronger relationship (r_s = 0.75) than the simple linear regression shown above.

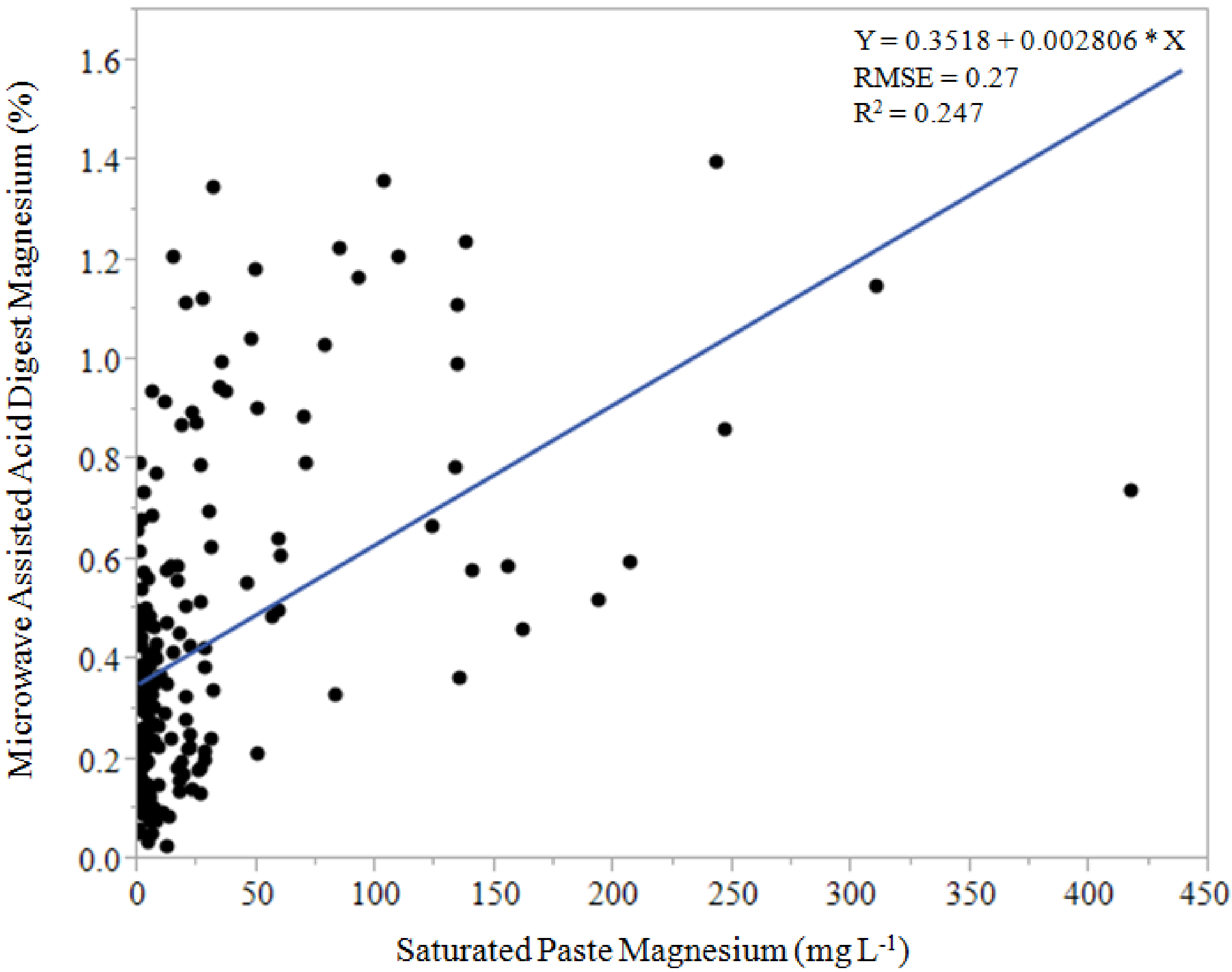

Figure 3.10. Microwave assisted acid digest (environmentally available) Mg versus saturated paste Mg for 198 samples. Environmentally available Mg had a significant effect on saturated paste Mg ($p < 0.001$). Spearman's rho nonparametric rank correlation produced a much stronger relationship ($r_s = 0.47$) than the simple linear regression shown above.

Manganese, P, Na, Zn, Cu, Ni, As, Mo, and Se (listed from highest to lowest concentration) were all minor constituents of the digest solution (Fig. 3.11). Manganese, P, Ni, Cu, Zn, and Mo were all significantly higher for medium and high SC samples compared to low SC samples, with $p < 0.02$. Manganese and P averages were 398 mg kg^{-1}, 897 mg kg^{-1}, and 768 mg kg^{-1} and 321 mg kg^{-1}, 659 mg kg^{-1}, and 720 mg kg^{-1}, for low, medium, and high SC samples, respectively. Mean values for Na and Zn were 179 mg kg^{-1}, 272 mg kg^{-1}, and 369 mg kg^{-1} and 60 mg kg^{-1}, 169 mg

kg^{-1}, and 107 mg kg^{-1} for low, medium, and high SC samples, respectively. Molybdenum averaged 0.65 mg kg^{-1}, 1.14 mg kg^{-1}, 0.99 mg kg^{-1} for low, medium, and high SC samples, respectively. Copper averaged 33 mg kg^{-1}, 41 mg kg^{-1}, 40 mg kg^{-1} for low, medium, and high SC samples, respectively. Nickel varied from 21 mg kg^{-1} in low, to 39 mg kg^{-1} in medium, to 37 mg kg^{-1} in high SC samples. Arsenic levels were significantly different (all $p < 0.03$) across all three SC levels, with means of 5 mg kg^{-1}, 6 mg kg^{-1}, and 10 mg kg^{-1} for the low, medium, and high SC samples, respectively. Selenium levels were not significantly different across SC levels ($p > .05$). The means for Se across SC levels were: 0.5 mg kg^{-1} for low, 0.4 mg kg^{-1} for medium, and 0.5 mg kg^{-1} for high. One additional extreme outlier (from site 24) for As, Se, and Mo was removed prior to analysis for As, Se, and Mo. Thus, while some significant differences did occur among saturated paste SC levels, mass concentrations of these nine elements generally had little apparent influence on the overall TDS-generation potential (as indicated by saturated paste SC) of the samples.

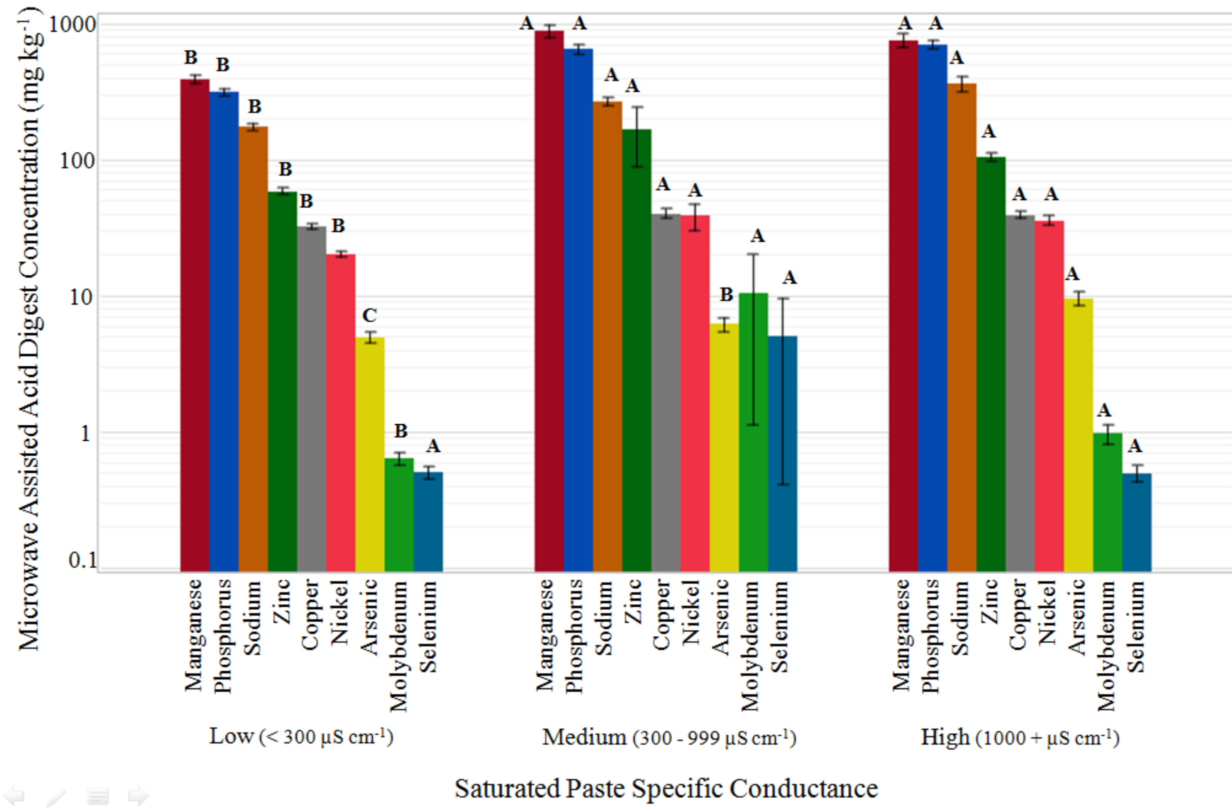

Figure 3.11. Mean microwave assisted acid digest ion concentration sorted by relative saturated paste specific conductance for trace elements. Data represents an environmentally available basis and not a total recovery. Samples are sorted by saturated paste specific conductance into categories of low (< 300 µS cm^{-1}; *n* = 120), medium (300 - 999 µS cm^{-1}; *n* = 52), and high (≥ 1,000 µS cm^{-1}; *n* = *32*). Error bars represent one standard error above and below the mean. Capital letters indicate means significantly different at α = 0.05 for individual ions among low, medium, and high SC levels.

Citrate Dithionite Extractable Aluminum, Iron, and Manganese

Citrate dithionite extractable Fe and Al proved to be a useful indicator of weathering status, and thus, of saturated paste SC and TDS production potential. Both CD extractable Fe and Al were significantly lower in medium and high SC samples than low SC samples (*p* <0.09; Fig. 3.12). Low SC samples had 10,451 mg kg^{-1} Fe compared to medium SC samples with 7,068 mg kg^{-1}

and high SC samples with 6,880 mg kg^{-1} extractable Fe. The CD extractable Al averages for low, medium, and high SC samples were 558 mg kg^{-1}, 908 mg kg^{-1}, and 3093 mg kg^{-1}, respectively. Means for CD-extractable Mn were similar across SC levels, 382 mg kg^{-1} for low, 524 mg kg^{-1}, for medium, and 313 mg kg^{-1} for high. Medium and low levels showed a slight significant difference in Mn (p = 0.05), but differences between other levels had p > 0.41. So, samples with high amounts of CD extractable Fe and Al were generally low in TDS potential; however, some samples with low TDS potential also contained low amounts of CD extractable Fe and Al. As discussed further in Chapter 4, highly weathered samples produced lower TDS overall and have higher levels of CD extractable Fe and Al due to increased levels of weathered Fe/Al oxides. The CD extraction analysis can be a helpful predictor of weathering status and thus, of TDS, but results should be interpreted with caution and other tests should be used in conjunction when possible.

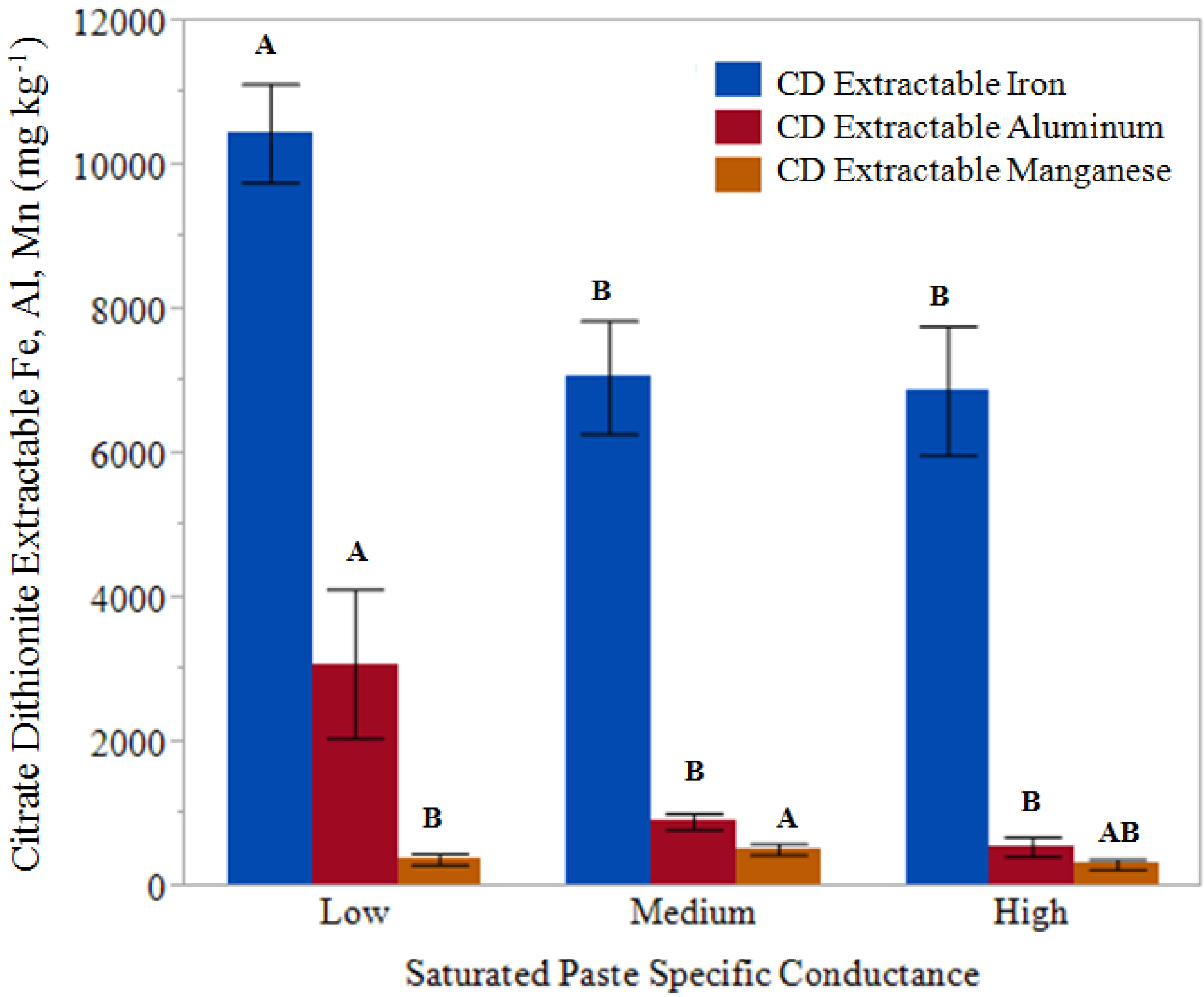

Figure 3.12. Mean CD extractable Fe, Al, and Mn sorted by relative saturated paste specific conductance. Samples are sorted by saturated paste specific conductance into categories of low (< 300 µS cm^{-1}; *n* = 120), medium (300 - 999 µS cm^{-1}; *n* = 52), and high (≥ 1,000 µS cm^{-1}; *n* = *32*). Error bars represent one standard error above and below the mean. Capital letters indicate means significantly different at α = 0.05 for individual ions among low, medium, and high SC levels.

Hydrogen Peroxide pH and Specific Conductance

The H_2O_2 method for evaluating mine spoils turned out to be not viable for distinguishing between low and high TDS samples. A slight significance was detected in the difference of water versus H_2O_2 SC between medium and low SC levels, but generally no useful trends were found (Fig. 3.13). The mean changes in pH were 0.4, 0.6, and 0.8 for the low, medium, and high SC samples, respectively (Fig. 3.14). Although there was a significant difference in water minus H_2O_2 pH between high and low SC samples (p = 0.03), no useful trends were detected. Further trials with stronger (> 3% H_2O_2) may reveal these tests to be more useful, but further testing is needed.

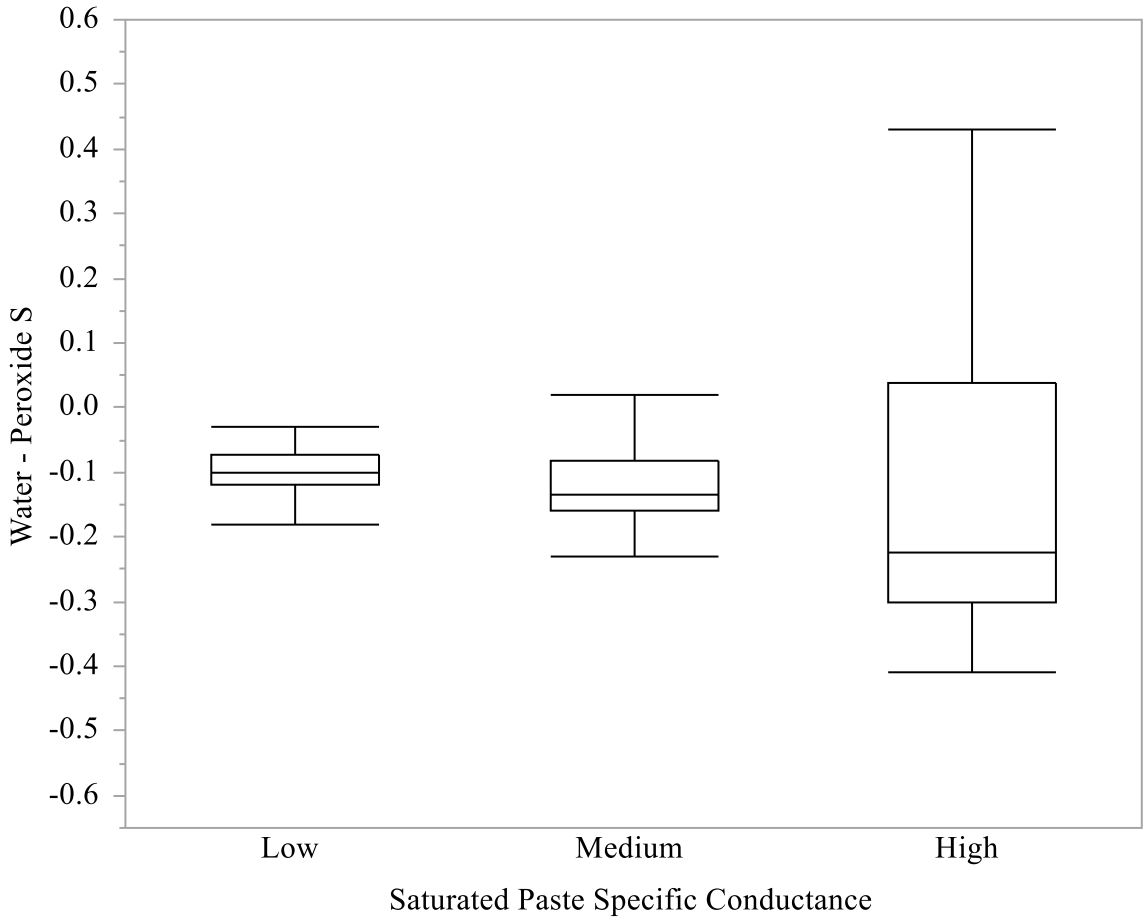

Figure 3.13. Quantile box plots of mean difference of water minus peroxide SC by relative saturated paste SC levels summarizing the range and the 25th, 50th (median), and 75th percentiles of the data. Samples are sorted by saturated paste specific conductance into categories of low (< 300 µS cm^{-1}; n = 120), medium (300 - 999 µS cm^{-1}; n = 52), and high (≥ 1,000 µS cm^{-1}; n = *32*). A slight difference between medium and low levels was observed, but generally no useful patterns were found.

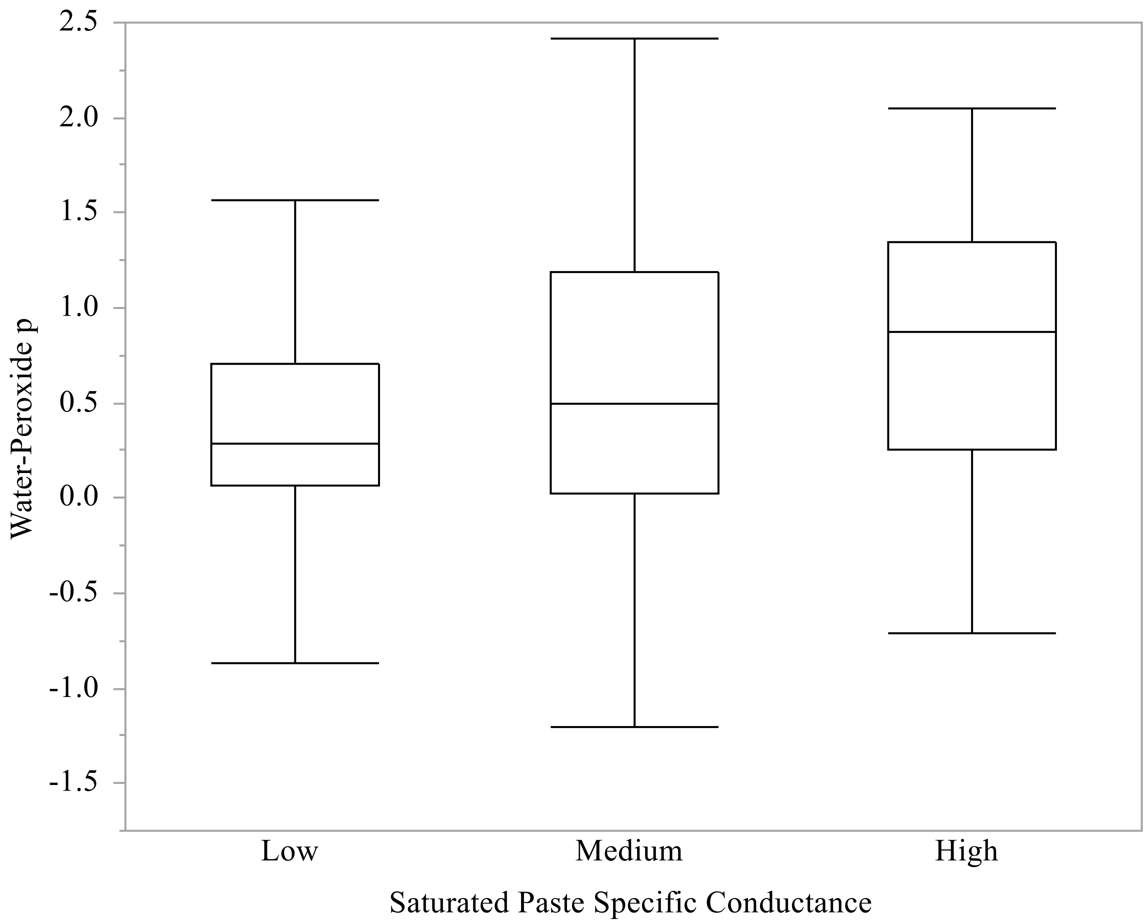

Figure 3.14. Quantile plot of mean differences in water minus peroxide pH by relative saturated paste SC levels summarizing the range and the 25th, 50th (median), and 75th percentiles of the data. Samples are sorted by saturated paste specific conductance into categories of low (< 300 µS cm^{-1}; n = 120), medium (300 - 999 µS cm^{-1}; n = 52), and high (≥ 1,000 µS cm^{-1}; n = 32). There was a significant difference in water minus peroxide pH between high and low SC samples (p = 0.03).

Mehlich Dilute Double Acid Extractable Ions

Samples from this study were sent to the VTSTL primarily for quick, general chemical characterization and most of the results revealed no significant statistical relationships beyond those discussed above for the other analyses. Interestingly though, the VTSTL Mg rating proved to be quite effective at separating out high SC samples (Fig. 3.15). While the Kruskal-Wallis test revealed no significant differences between Mg ratings, nearly all of the medium and high SC samples were confined to the very high Mg rating. The very high Mg rating did, however, also include many low SC samples. So, as noted for many of the other TDS predictors previously, the VTSTL Mg Rating should be used in conjunction with other indicators and should not be relied on individually to predict TDS release potentials.

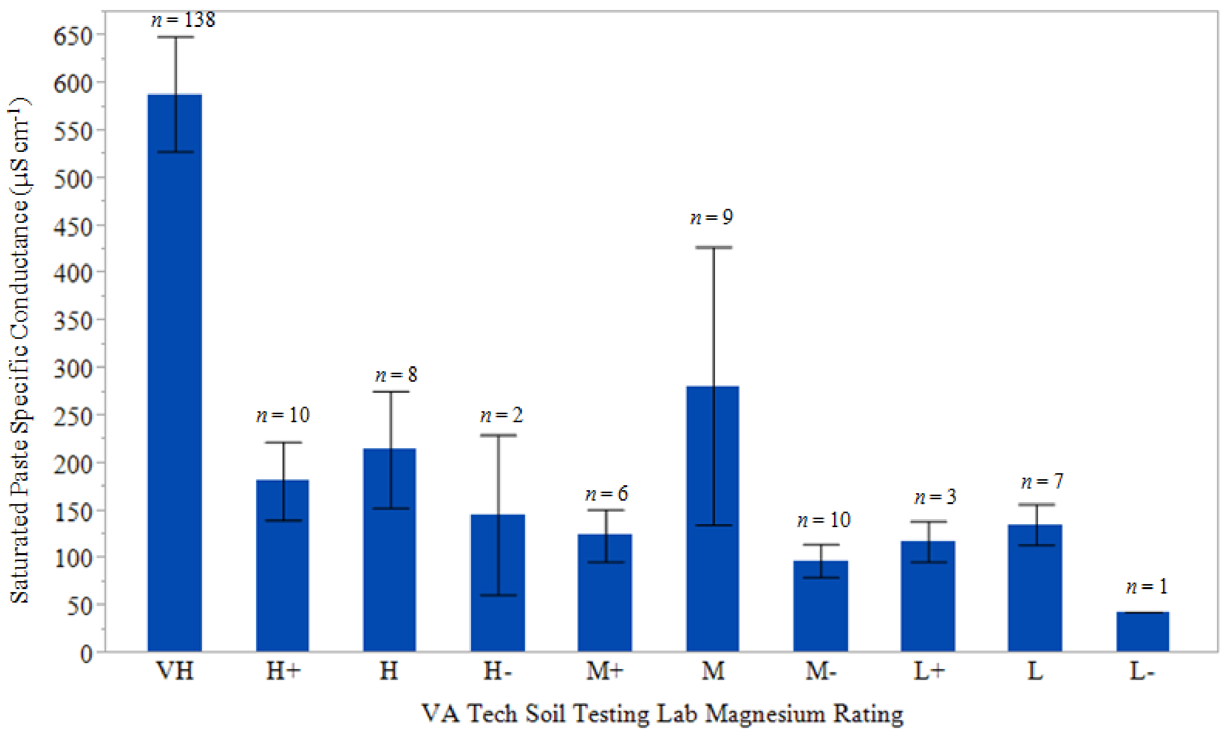

Figure 3.15. Mean saturated paste specific conductance versus VTSTL Mg rating. (L = Low, M = Medium, H = High, VH = Very High). No significant differences were calculated between Mg ratings, but nearly all of the medium and high SC samples were confined to the very high rating. Error bars represent one standard error above and below the mean.

Petrographic Thin Section Analysis

Highly weathered and fresh, unweathered samples originating from the same geologic strata showed little differences in thin section analysis (Table 3.2). The fourteen samples analyzed were generally quartz rich subarkoses or sublitharenites. Quartz occurred as monocrystalline and polycrystalline forms and was the most common framework grain. Feldspars were also abundant and occurred as plagioclase, orthoclase, and microcline. Feldspars were often replaced by kaolinite. Lithic fragments were interestingly found to generally be metamorphic in nature. Carbonate cements were rare, suggesting Ca in saturated paste extracts and field leachates may originate from feldspar hydrolysis rather than from carbonates. Siderite cements were somewhat rare and were only found as rims coating some framework grains. Microcline and plagioclase were found to be weathering much more than chlorite and muscovite. Oxidation of siderite cements and ferruginous carbonate cements was evident in some samples.

The fact that no obvious differences were found between weathered vs. nonweathered samples from the same strata was surprising. However, this may simply indicate that the relative amount of rock mineral volume that actually weathers and contributes to TDS is (a) very small relative to total volume, (b) that the majority of weathering is occurring in silt and clay sized mineral grains that were too fine to be identified, or (c) insufficient samples were analyzed to separate weathering effects. Regardless, the combined point count data indicate that the sandstones selected for thin section analysis contained a large component of weatherable feldspars along with metamorphic fragments which most likely are major contributors to the mixed ion load observed in the saturated paste extracts. This reinforces the conclusions reached by Ondorff et al.

(2015) that TDS generation by these spoils is not solely related to pyrite oxidation and carbonate neutralization reactions.

Table 3.2. Point counts for thin section analysis of selected weathered and unweathered samples. Sample ID represents site number - individual sample number. Data provided by K. Eriksson.

Sample ID	Weathered/Unweathered	Monocrystaline Quartz	Polycrystaline Quartz	K-spar	Altered K-spar	K-spar to Kaolinite	Plagioclase	Altered Plagioclase	Plagioclase to Kaolinite	Metamorphic Lithics	Sedimentary Lithics	Muscovite	Biotite	Chlorite	Chert	Limonite/Goethite	Pyrite	Heavies	Porosity	Sillimanite cement	Siderite	Carbonate cement/replacement	Kaolinite cement
1-10	W	191	25	21	4	1	5	14		23		9	1	7	3	4			3	1	5		3
1-11	W	183	20	21	1	3	10	34		19		7		9		7		1	8	2	7	2	2
1-12	W	204	12	11	2		13	34	1	17	2	12		3	6	3	1		1		4		6
1-13	W	174	18	9	1	1	8	21		25	1	14	3	12	2	2			17		6	4	1
1-14	W	159	4	6	3		11	41		48		12		4	2	6		1	16	1	2	1	
1-16	U	198	26	9		1	8	16		41	2	19	1	10		7	2		23		3	1	1
2a-5	W	166	14	11	2		7	17		65	1	20		9	5	9		1	13		6	3	
2a-6	W	181	7	7	4		17	30	1	51		23	1	5	6	9	1	1	17		8	1	2
4c-3	W	167	41	9		4	7	37	1	33	3	7		4	1	15			32	5	1	1	12
4c-5	U	159	43	10	2	6	3	31	4	39	1	9	1	5	2	11	1		19	2	4	1	19
6-2	W	171	55	11	1	11	5	49		20		11		7	2	16		1	40	7	7	1	22
6-3	W	157	52	8		12	1	31		40		21	2	5		10			32	3	7		13
9-2	W	189	31	9	41	30	3	4		50	1	10	2	8	2	2			30	1	2		19
9-3	U	199	23	13	34	27	5	1	1	44	1	17		4		5		1	41	3	8	4	14

Spoil Geochemical vs. Extract Properties

Previous studies (Daniels et al., 2014; Orndorff et al. 2015; Skousen et al., 2000) have clearly identified sulfate, bicarbonate, Ca, Mg and K as the dominant components of TDS in circumnetural regional mine waters. These studies also report that early leachates are dominated by sulfate, Ca, and Mg and then bicarbonate slowly replaces sulfate as the dominant anion over extended leaching events. Sulfate is clearly being generated by trace sulfide oxidation in these materials and carbonates are the commonly assumed source of Ca and Mg (Skousen et al., 2000; Daniels et al., 2014). However, petrographic analyses of sandstone samples (Table 3.2) revealed only limited carbonates as secondary cements, counter to what was expected based on the earlier work of Howard (1979). While siderite was noted at low levels in a number of samples, it is doubtful that it was plentiful or reactive enough to supply the relatively large mass of Ca and Mg observed in the SC extracts. However, feldspars (both intact and weathered/altered) were common in the sandstones (Table 3.2) and presumably were also found in the finer grained rocks. Rapid feldspar weathering could provide substantial Ca and K to these extracts, but we would also expect significant Na release along with that which was not observed here. Thus, I can only assume that the high Ca release is coming from a combination of direct carbonate dissolution and rapid acid-base neutralization reactions driven by pyrite oxidation along with a mix of other currently unknown sources. I also assume that K release is occurring via a combination of feldspar hydrolysis and mica weathering since muscovite was also common in the sandstones (Table 3.2).

Identification of the source of the relatively high levels of Mg release to these solutions poses more difficulty than for Ca. While a certain amount of the Mg may be contributed by siderite, these rocks also contained a relatively large assemblage of metamorphic lithic fragments which could contain Mg-bearing chlorites and low to moderate levels of chlorite were also noted as primary grains in the sandstones. Trioctahedral (Mg-rich) chlorite is also a relatively weatherable 2:1 mineral phase in acidifying systems and therefore could be a potentially major source of Mg release (Murakami et al., 1996). However, the fact that the VTSTL (dilute double acid) extracts for high SC samples also extracted large amounts of Mg indicates that the primary source of the Mg may be in an acid-soluble mineral component, which again points to a carbonate source rather than a 2:1 mineral weathering mechanism.

The overall release of the majority of trace elements was (a) relatively low and (b) varied little across the observed SC range for most elements. It is commonly assumed (Skousen et al., 2000; Kittrick et al., 1982) that the majority of trace elements (e.g. As, Cu, Cr, Mo, Ni, Se, etc.) are found substituted into pyrite or other sulfide minerals and are released during acid sulfate weathering processes. It is also possible that Se is found as a primary Se zero-valent species in highly reduced and non-weathered rocks of this region (J. Unrine, University of KY, Personal Communication). As discussed earlier, the primary source of Fe in the extracts is presumed to be via pyrite oxidation in the non-weathered rocks and then dissolution of secondary Fe-oxides in the weathered materials. The original source of Mn in the non-weathered rocks is most likely a combination of complex metal-carbonate secondary rock cements (Howard, 1979) and Mn containing primary minerals in the metamorphic lithic fragments.

It is notable that these spoil materials generate relatively low levels of Cl, but bicarbonate is present in moderate amounts in the higher pH samples. Longer-term column leaching trials on similar regional strata (Orndorff et al., 2015) indicate that bicarbonate does increase substantially over time as sulfate loadings diminish. This would indicate that either (a) there are secondary carbonates present in these rocks that were not readily identifiable by petrographic analysis or (b) other reactions such as feldspar hydrolysis are releasing enough alkalinity to solution to influence the carbonate/bicarbonate equilibrium reactions in solution.

Regardless of the actual mineral source of the Ca and Mg observed in these extracts, my results clearly support the recent conclusions by Daniels et al. (2016) that historic practices to intentionally blend high neutralization potential (carbonate containing) strata with acid-forming sulfidic strata to achieve net circumneutral mine drainage will lead to very high levels of TDS release regardless of associated moderate pH and low metal levels. Thus, a better alternative would be to indentify these high TDS strata and isolate them separately regardless of predicted net acid-base accounting balances as described by Skousen et al. (2002).

Conclusions

Geochemical characteristics of the 204 soil and rock samples analyzed for this study varied widely. Our results suggest the selection of the most suitable geologic strata for reclamation will have a significant influence on the type and amount of ion produced by initial rapid weathering reactions and release to leaching solutions. The sandstones studied in thin section were generally quartz rich subarkoses or sublitharenites that contained relatively large amounts of weatherable feldspars and other minerals. While some differences in saturated paste SC did occur from site-to-site, no significant differences were found in overall salinity among sites. Generally, pH was a poor predictor of SC and high SC values occurred in samples across a wide pH range. Sulfate, Ca, Mg, K, Na, Cl, and HCO3- were the dominant ions affecting overall TDS (listed in order of importance), all of which increased significantly from low to medium to high SC samples, except Cl. This study indicates a 1:1 relationship between SC and TDS; thus suggesting the conventional SC to TDS conversion factor (0.64) significantly underestimates the actual mass load of ions in solution. The microwave assisted acid digest showed Fe, Al, K, Mg, Ca, and S to be the most environmentally available elements in the samples, but analysis revealed only weak correlations between these data and ion release in the saturated paste extracts for most elements except S, Mg, and Ca. These trends suggest some elements, such as S, Mg, and Ca, are released preferentially via weathering while others such as Fe are retained, as would be expected. Trace elements for both saturated paste extractions and for the microwave-assisted acid digest varied little with overall changes in saturated paste SC and only made minor contributions to overall SC.

While the novel H_2O_2 TDS prediction method tested here revealed some significant differences, the results were largely unreliable as a prediction method. Samples with higher levels of CD-extractable Al and Fe were significantly pre-weathered and lower in SC making this a useful test for identifying weathering status and TDS potential. Nearly all of the high TDS potential samples scored a very high rating on the VTSTL Mg rating, proving it to be a very quick and cost effective test to identify high TDS samples. Future research into the thin section point count data may reveal more differences in weathered and unweathered sandstones.

Thus, as hypothesized, mine spoil saturated paste extracts were dominated by S, Mg, and Ca and individual ions varied significantly among low, medium, and high SC samples. Samples with high TDS potential were generally higher in saturated paste Ca, Mg, and sulfate, so in order to reduce overall TDS elution, I recommend identifying mine spoils that are high in S and reactive Ca and Mg mineral components as high TDS risk and not allowing their net-blending to achieve acid-base accounting balances. While all of the methods discussed above provide some insight into the TDS generation potential of samples individually, a combination of all of these methods will provide the most accurate analysis.

References

Agouridis, C. T., P. N. Angel, T. J. Taylor, C. D. Barton, R. C. Warner, X. Yu, and C. Wood. 2012. Water quality characteristics of discharge from reforested loose-dumped mine spoil in Eastern Kentucky. J. Environ. Qual. 41:454–468.

Ahern, C.R., A.E. McElnea, and L.A. Sullivan. 2004. Acid sulfate soils laboratory methods guidelines. *In* Queensland Acid Sulfate Soils Manual 2004. Department of Natural Resources, Mines and Energy, Indooroopilly, Queensland, Australia.

APHA (American Public Health Association). 1999. Standard methods for the examination of water and wastewater, 20th ed. American Public Health Assoc Press, Washington DC.

Brady, K. B., T. Kania, M. W. Smith, and R. J. Hornbeger. 2000. Coal mine drainage prediction and pollution prevention in Pennsylvania. West Virginia Surface Mine Drainage Task Force Symposium. Morgantown: Pennsylvania Department of Environmental Protection, Harrisburg, PA.

Calkins, W.H. 1994. The chemical forms of sulfur in coal: A review. Fuel. 73 (4): 475-484.

Chapman, P.M., H. Bailey, and E. Canaria. 2000. Toxicity of total dissolved solids associated with two mine effluents to chironomid larvae and early life stages of rainbow trout. Env. Toxicol. Chem. 19:210-214.

Croghan, C. and P. P. Egeghy. Methods of dealing with values below the limit of detection using SAS. *In* Proc. of Southeastern SAS User Group. September 22-24, 2003. St. Petersburg, FL.

Daniels, W.L., M. Beck, M.J. Eick and Z.W. Orndorff. 2009. Predicting contaminant leaching potentials for Central Appalachian overburden and coal refuse materials. Final Report to OSM Applied Science Research Program, December 2009. Washington, DC.

Daniels, W.L., Z. Orndorff, C. Ross, S. Koropchak, C. Zipper, D. Evans, and M. Eick. 2014. Correlation of TDS release potentials with field leaching behaviors for Appalachian coal mine spoils and coarse refuse. Final Report to the Office of Surface Mining, Reclamation, and Enforcement. Washington, DC.

Daniels, W. L., C. E. Zipper, Z. W. Orndorff, J. Skousen, C. D. Barton, L. M. McDonald, and M. A. Beck. 2016. Predicting total dissolved solids release from Central Appalachian coal mine spoils. Environ. Poll. 216: 371-379.

Evangelou, V.P. 1995. Pyrite Oxidation and its Control. CRC Press. 293 p.

Freney, J. R., G.E. Melville, and C.H. Williams. 1969. Extraction, chemical nature, and properties of soil organic sulphur. J. Sci. Food Agric. 20, 440-5.

Howard, J.L. 1979. Physical, Chemical, and Mineralogical Properties of Mine Spoil Derived from the Wise Formation, Buchanan County. Virginia. M.S. Thesis, Va. Poly. Inst. & State Univ., Blacksburg, VA.

Kennedy, A.J., D.S. Cherry, and C.E. Zipper. 2005. Evaluation of ionic contribution to the toxicity of a coal-mine effluent using *Ceriodaphnia dubia*. Arch. Environ. Contam. Toxicol. 49:155−162.

Kittrick, J. A., D. S. Fanning, and L. R. Hossner.. Division S-9. 1982. Acid sulfate weathering: Proceedings of a symposium. Soil Sci. Soc. Am. Vol. no. 10. Madison, Wis.

Maguire, R. O. and S. E. Heckendorn. 2011. Laboratory procedures: Virginia Tech soil testing laboratory. Virginia Cooperative Extension Publication 452-881. http://pubs.ext.vt.edu/452/452-881/452-881_pdf.pdf.

Mount, D. R., J. M. Gulley, J. R. Hockett, T. D. Garrison, and J. M. Evans. 1997. Statistical models to predict the toxicity of major ions to *Ceriodaphniadubia*, *Daphnia* magna, and fathead minnows (*Pimephalespromelas*). Environ. Toxicol. Chem. 16:2009-2019.

Murakami, T., H. Isobe, T. Sato, and T. Ohnuki. 1996. Weathering of chlorite in a quartz-chlorite schist .1. Mineralogical and chemical changes. Clays and Clay Minerals. 44 (2): 244-56.

Odenheimer, J., J. Skousen, L.M. McDonald, D.J. Vesper, M. Mannix, and W. L. Daniels. 2014. Predicting release of total dissolved solids from overburden material using acid-base accounting parameters. Geochem. Explor. Env. A. 15: 131-137.

Orndorff, Z.W., W.L. Daniels, M. Beck, and M.J. Eick. 2010. Leaching potentials of coal spoil and refuse: Acid-base interactions and electrical conductivity. p. 736-766. *In* R.I. Barnhisel (ed.) Proc. Am. Soc. Min. Reclam., Pittsburgh, PA. 5-11 Jun. 2010. ASMR, Lexington,KY. Available at http://landrehab.org/ItemDetails.aspx?DataItemID=kFSPPK%2fvYDY%3d.

Orndorff, Z.W., W. L. Daniels, C.E. Zipper, M. Eick, and M. Beck. 2015. Column evaluation of Appalachian coal mine spoils' temporal leaching behavior. Environ. Pollut. 204: 39-47.

Pond, G. J., M. E. Passmore, F. A. Borsuk, L. Reynolds, and C. J. Rose. 2008. Downstream effects of mountaintop coal mining: comparing biological conditions using family- and genus-level macroinvertebrate bioassessment tools. J. North Am. Benthol. Soc. 27:717–737.

Pond, G.J., M. E. Passmore, N.D. Pointon, J.K. Felbinger, C.A Walker, K.J. Krock, J.B. Fulton, W.L. Nash. 2014. Long-term impacts on macroinvertebrates downstream of reclaimed mountaintop mining valley fills in central Appalachia. Environ. Manag. 54: 919-933.

Rhoades, J. D. 1996. Salinity: Electrical Conductivity and Total Dissolved Solids. p. 417-435. *In* D. L. Sparks (ed.) Methods of Soil Analysis. Soil Science Society of America Book Ser. 5 Part 3. Chemical Methods. SSSA and ASA, Madison, WI.

Roberts J.A., Daniels W.L., Bell J.C., Burger J.A. 1988. Early stages of mine soil genesis in a Southwest Virginia spoil lithosequence. Soil Sci. Soc. Am. J. 52:716–723

Skousen, J., A. Sexstone, P. Ziemkiewicz. 2000. Acid mine drainage control and treatment *In* Barnhisel, R.I., et al. (Eds.), Reclamation of Drastically Disturbed Lands. Agronomy Mono. 621 No. 41. ASA-SSSA, Madison, WI, USA. pp. 131-168.

Skousen, J., J. Simmons, L. McDonald, P. Ziemkiewicz. 2002. Acid-base accounting to predict post-mining drainage quality on surface mines. J. Environ. Qual. 31, 2034-2044.

USDA-NRCS (U.S. Department of Agriculture - Natural Resource Conservation Service). 2004. Soil Survey Laboratory Methods Manual. Soil Survey Investigations Report No. 42 Version 4.0.

US Court of Appeals. 2013. Mingo Logan Coal Company v. USEPA. Appeal from the United States District Court for the District of Columbia (No. 1:10-cv-00541).

USEPA (U.S. Environmental Protection Agency). 2007. Inductively coupled plasma mass spectrometry, method 6020A, rev.1. In SW 846: Test Methods for Evaluating Solid Waste, Physical/Chemical Methods. USEPA, Office of Solid Waste, Washington, DC.

USEPA (U.S. Environmental Protection Agency). 2011. The effects of mountaintop mines and valley fills on aquatic ecosystems of the Central Appalachian coalfields (2011 Final). U.S. Environmental Protection Agency, Washington, DC. Available at http://cfpub.epa.gov/ncea/cfm/recordisplay.cfm?deid=225743.

USEPA (U.S. Environmental Protection Agency). 2012. Spruce no. 1 surface mine discharge of dredged or fill materials (404). Decision by Federal District Court for the District of Columbia. Available at http://water.epa.gov/lawsregs/guidance/cwa/dredgdis/spruce.cfm.

USEPA (U.S. Environmental Protection Agency). 2013. Final petition for rulemaking to set water quality standards to protect Appalachian waters from mining waste and harmful levels of conductivity. Petitions to the Office of Water. Available at http://www2.epa.gov/aboutepa/petitions-office-water.

Chapter 4. Field Indicators for the Prediction of Appalachian Soil and Bedrock Geochemistry

Abstract

Surface coal mining is associated with elevated total dissolved solids (TDS) levels in adjacent Appalachian headwater streams, which is caused by rainwater percolating through mine spoils during and after mining. This study was conducted to test the effectiveness of predictors, such as weathering status, color, rock type, reaction with HCl, and reaction with H_2O_2 to determine the relative overall TDS and ion-specific elution potential of a range of mine spoils. Thirty-three vertical weathering sequences were sampled from eight surface coal mines throughout the central Appalachian coalfields; 204 samples of soil and both weathered and unweathered bedrock were collected in total. Dark gray, very dark gray, and black samples had the highest levels of saturated paste Ca, Mg, specific conductance (SC), and sulfate. Saturated paste Ca, Mg, SC, sulfate, and Mg, and total-S varied significantly by rock type, generally coal > mudstone > shale > siltstone > sandstone > soil. Saturated paste HCO_3^-, Ca, Mg, SC, Se, and sulfate were significantly lower in B horizons, C horizons, and weathered R layers than in surficial A horizons and lower unweathered R layers. The shallowest shale or mudstone layer at each site formed an abrupt transition between weathered and unweathered materials and ranged from 0.7 m to 15.9 m (average 6.5 m) below the surface. Saturated paste Ca, Mg, SC, and sulfate were significantly lower in the weathered zone. Weathered samples were commonly yellowish brown and relatively high in CD-extractable Al, Fe, and Mn, while unweathered samples were commonly grayish or black. The HCl acid fizz test was a good predictor of CCE, but not of SC.

Saturated paste Ca, Mg, SC, Se, sulfate, and Total-S were significantly higher in samples that reacted with heat or violently to the H_2O_2 test, but As was significantly higher in samples that only produced foam. Overall, the samples varied widely in both physical and geochemical properties; surficial weathered sandstones and soils occurring above the shallowest shale or mudstone layer were generally browner in color and lower in both overall SC and individual ionic concentrations. We recommend using a combination of weathering status, color, rock type, and reaction with H_2O_2 to produce the best prediction of SC.

Introduction

Surface coal mining in Central Appalachia has historically drawn attention from environmental advocates, prompting regulatory action by governing officials. As the mining industry has systematically improved its practices and reclamation ability, the public focus for regulation has shifted over the years (USEPA, 2005). Historically, acid mine drainage and topographic contour replacement were major concerns, but reclamation methods have advanced and these problems are now managed effectively (Skousen et al., 2002). Over the past decade, total dissolved solids (TDS) release to headwater streams has emerged to be one of the new leading environmental concerns related to Appalachian mining (Pond et al., 2014; USEPA, 2011)

Surface mining can increase TDS in several ways. Neutralizing acid mine drainage with chemical reagents, such as sodium hydroxide, can be a direct source of TDS (USEPA, 2011), as can be the acidic drainage itself. Mixing alkaline and acid strata according to acid-base accounting parameters accounts for a major source of TDS (Daniels et al., 2016); while this practice leads to circumneutral discharge waters, the underlying chemical reactions result in the release of significant amounts of neutral salts. Many of the trace metals associated with acid mine drainage are not soluble at these higher pH ranges, but several elements have remained problematic. Sulfate has repeatedly been shown to be the dominant ion of concern, but Ca, Mg, K, Na, and HCO_3^- also generally make up a significant portion of the overall ionic concentration (Daniels et al., 2016; Larsen and Mann, 2005; Lee et al., 2002; Griffith et al., 2012; Mack et al., 2013; Orndorff et al., 2015; Skousen et al. 2000).

Both overall TDS and specific ionic concentrations have been associated with negative effects on aquatic life at levels that commonly occur in mine-influenced streams. While most coal mine drainage from active mines is no longer acidic, neutral to alkaline mine drainage has still been shown to have negative associations with aquatic life in mine-influenced watersheds (Bernhardt et al. 2011; Bernhardt et al. 2012; Hartman et al. 2005; Pond et al. 2008;; Timpano et al. 2011). The exact level at which effects on organisms begin to take place is still under debate, but, generally, the effects become more pronounced as TDS levels (as estimated by SC) increase (Pond et al. 2008; 2014). In addition to overall TDS, some studies (American Petroleum Institute, 1998) show that the concentrations of individual ions can be just as important. The relative ion toxicity for *Ceriodaphnia dubia*, *Daphnia magna*, and fathead minnows (*Pimephales promelas*) was shown to be K > HCO_3^- = Mg > Cl > sulfate (Mount et al., 1997). In a review of the literature, Goodfellow et al. (2000) attributed Ca, Mg, Na, and sulfate in mine effluents to $CaSO_4$, $MgSO_4$, and $NaSO_4$ compounds liberated by weathering spoil or mine processing wastes. Thus, it is not only important to investigate the source of overall TDS, but also the sources of specific ions.

Some previous work predicting TDS risk in coal mine effluents exists, but is generally limited in scope, has a limited sample set, or lacks valuable geologic details. Historically, past studies such as Skousen et al. (2002) concentrated mainly on preventing acid mine drainage and generally only described geochemical properties of rock spoils related to acid drainage risk, such as total-S and neutralization potential (NP). Since TDS has been shown to be produced across a range of acidic to alkaline conditions, this approach is of limited use for predicting TDS risk per se. Some work has been done, however, utilizing the total-S values from acid-base accounting (ABA) data to predict overall TDS. Generally, high total-S values indicate high TDS potential. Odenheimer et al. (2013) tested an alternative TDS prediction method by shaking samples with dilute nitric acid solution for two weeks. However, their study found the experimental weathering simulation "did not provide a useful TDS release prediction". The column study by Daniels et al. (2016) reported that saturated paste SC was a very strong predictor (R^2 = 0.85) for peak SC for lab column leachates from 39 mine spoils. Weathered samples have been shown to produce lower levels of TDS than unweathered samples (Agouridis et al., 2012; Daniels et al. 2016; Orndorff et al., 2015), but the designation of "weathered" is often not well defined and largely up to the sample collector. Soluble ions in these weathered, surficial soil and bedrock layers are dissolved as groundwater follows flow paths downward and laterally (Borchers et al., 1981, Kipp et al., 1987). Brown colored mine spoils (weathered rocks) have also been shown to produce less TDS than gray mine spoils (unweathered rocks) in some studies (Agouridis et al., 2012; Odenheimer et al., 2014). Samples with finer particles size (i.e. mudstones, shales) and coal-associated materials have been shown to produce higher TDS than sandstones (Orndorff et al., 2015). While these previous studies show that unweathered, gray, and fine-grained rocks generally have higher TDS potential than weathered, brown, and coarse-grained rocks, these studies use bulk run-of-the-mine samples that had been blasted apart, transported, and mixed during final mine site placement and grading. Thus, some TDS prediction studies have been published previously, but are limited in extent and the potential exists to expand on the current research.

While the studies reviewed above provide useful generalizations about Appalachian mine spoil geochemistry, they lack site-specific sample location details, such as depth, strata thickness, relation to other strata, and pre-excavation bedding characteristics, which can provide useful insights into the root sources of TDS and individual ionic concentrations. Based on the studies reviewed, I hypothesized that mine spoil color would significantly affect TDS potential and that gray spoils would generate more TDS than brown spoils. Further, I hypothesized that fine-grained rocks would produce higher ionic concentrations than coarse-grained rocks. I also predicted that the weathering boundary between weathered and unweathered materials would occur rather abruptly at some confining layer in the profile and that the weathered materials would be significantly lower in TDS potential than the unweathered materials below. Thus, the overall objective of this study was to develop and test quick, inexpensive field indicators for the prediction of geochemical properties of native central Appalachian soil and underlying bedrock materials. The related secondary objective was to gain a better understanding of the overall soil-geologic weathering processes that have occurred in situ over time in the field and then to relate that understanding to observed differences in mine spoil chemical and physical properties that could be recognized readily in the field.

Materials and Methods

Sample Collection, Preparation, and Lab Analyses

The sample set presented here represents the same sample set discussed in Chapter 3 and sample collection, preparation, and lab analysis methodologies are presented in detail there. In short, 33 vertical weathering sequences were collected throughout the central Appalachian coalfields to a depth of 15-30 m. Each distinct soil or geologic layer was collected for chemical and physical analysis, giving a total of 204 individual samples. The samples were analyzed for saturated paste As, Ca, Mg, SC, Se, and sulfate, Total-S, and CCE as described in Chapter 3. This chapter (4) concentrates on field description methods and they are discussed in detail below.

Color

Colors for soil and rock samples were recorded according to the Field Book for Describing and Sampling Soils, Version 3.0 (FBDSS) (Schoeneberger et al., 2012). Soil peds were broken open and lightly moistened. Next, the color of each soil ped was recorded. Rock samples were carefully broken open with a rock hammer to expose a fresh, unweathered face and also lightly moistened before coloring. Soil color charts were used to determine the hue, value, and chroma of each sample. In the case of variegated colors, each color was recorded along with varying percentages. In such cases of mixed colors in rock samples it was determined that the lowest chroma present was of most importance and that chroma was reported (e.g. a sandstone with both chroma one and chroma two colors would be reported as chroma one). Qualitative analysis comparing SC values revealed that the lowest chroma color present was generally a better indicator than the higher chroma present or an average of the two.

Rock Type

The study area's geologic structure is made up entirely of sedimentary rock types. Some limited limestone strata exist in the area (USGS, 2012), but no samples gathered for this study were limestone. Rocks were categorized according to particle size and organic content; they were sorted as conglomerate, sandstone, siltstone, mudstone, shale, or coal. Fireclays, underclays, flint clays, and mixed interburdens were grouped with the mudstones. While some technical differences do exist among these materials, local terminology often varies from area to area and these different terms are all largely being used for the same materials – generally materials associated with coal seams. Ambiguous fine-grained samples were identified by fracturing samples in the field with a rock hammer; highly fissile samples splitting along cleavage planes were grouped as shales and less fissile samples were grouped as mudstones.

Horizon Type

Horizons were named according to the FBDSS (Schoeneberger et al., 2012). Weathered topsoil horizons darkened by organic matter were labeled as A horizons. Thin leached zones of eluviation below the A horizon, traditionally labeled E horizons, were generally too thin to sample in the study area; in the few cases E horizons were encountered, the material was aggregated together with the A horizon samples. Weathered subsoil horizons showing significant alteration from the parent material were labeled as B horizons. Minimally weathered subsoil horizons and soft bedrock layers that could be excavated by shovel were labeled as C horizons and bedrock horizons were labeled as R layers. The transition from C horizon to R layer was made when the bedrock could no longer be dug by hand with a shovel. Soft bedrock layers that could be hand excavated by shovel were designated C horizons. Transitional horizons were sampled with the adjacent layers. Horizon subscripts were also assigned according to the FBDSS, but are not presented here.

Degree of Pre-Weathering

As noted above, the study area consists almost entirely of relatively flat-bedded sedimentary rocks. There is a great difference in hydraulic conductivity between rock types, generally related to particle size (Wunsch, 1993). Rock types with coarse grain sizes, such as sandstones and conglomerates, transmit water quickly; while rock types with finer grain sizes, such as mudstones and shales, tend to retard the movement of water (and oxygen). Thus, water and oxygen move freely down through the soil and bedrock until they encounter the first fine-grained rock layer. This fine-grained layer generally greatly retards the downward flow of water and oxygen, and then water tends to flow laterally along the upper boundary of the layer, often effectively making a seasonally-fluctuating saturated zone or "perched water table". During collection, samples were noted as occurring above or below this shallowest occurring fine-grained rock layer.

Hydrochloric Acid Reaction Test

The HCl reaction test was used as described in the FBDSS (Schoeneberger et al., 2012). Approximately 0.5 g of material was crushed and added to a disposable test tube. Enough 1N HCl was then added to completely submerge the sample (~5 mL). Samples were sorted into effervescence classes according to reaction with the acid as described in the FBDSS. Samples with no bubbles were labeled noneffervescent. Samples forming few bubbles were labeled very slightly effervescent. Samples forming numerous bubbles were labeled slightly effervescent. Samples forming a low foam or slight audible bubbles were labeled strongly effervescent and samples reacting with thick foam or very audible bubbles were labeled as violently effervescent. Samples were also qualitatively investigated in the field for carbonates by adding one drop of 1N HCl to each sample and any anomalies, such as fossils, shell fragments, and siderite nodules; HCl reactions were noted.

Hydrogen Peroxide Reaction Test

A modified method of the H_2O_2 reaction test described in the FBDSS (Schoeneberger et al., 2012) was used. Approximately 0.5 g of material was crushed and added to a disposable test tube. Enough 30% H_2O_2 was then added to completely submerge the sample (~5 mL). Samples were sorted into effervescence classes. Samples with no bubbles were labeled noneffervescent. Samples forming few bubbles were labeled very slightly effervescent. Samples forming numerous bubbles were labeled slightly effervescent. Samples forming a low foam or slight audible bubbles were labeled strongly effervescent and samples reacting with thick foam or very audible bubbles were labeled as violently effervescent. A second categorization system was also used; in addition to effervescence rankings, samples were sorted depending on the reaction type of foam, heat, violent, or cold reactions. Samples that boiled, frothed over, and generated extreme heat were labeled as "violent". Samples generating temperature levels below boiling were labeled as "heat". Both samples that produced no bubbles and those that bubbled vigorously, but produced no heat were labeled as "cold". Samples that generated visible amounts of foam, but produced no heat were labeled as "foam". As discussed in the results section below, this later categorization method was much more effective at differentiating between low and high TDS-generating samples.

Statistical Analyses

JMP Pro 11.0 Statistical Discovery software from SAS was used for statistical analysis. A *p* value ≤ 0.05 was considered significant. Initial analysis revealed the data had several strong outliers, unequal variances, unequal sample sizes between categories, and was also skewed strongly to the left (with many more low than high TDS samples) – all of which challenged the assumptions for normality, so non-parametric statistical tests were chosen. The non-parametric Kruskal-Wallis one-way analysis of variance test was used to compare median values between categories to determine overall significant differences. The non-parametric Steel-Dwass post-hoc test was used to compare median values between individual categories. Six extreme outliers were excluded from the 204 sample set for the statistical analyses presented below using a cutoff value of > 1 for Cook's Distance outlier analysis, leaving a total of 198 samples. These six outliers were from sites 10, 18, and 20 and contained variety of rock types, including one coal, three dark gray shales, one dark gray sandstone, and one brown sandstone sample.

Results and Discussion

Color

Color was a strong indicator of saturated paste SC. All but a few of the 204 samples were hue 10YR, so hue per se had little to no influence on SC. Chroma and value, however, both had significant affects on SC ($p < 0.0001$) (Fig. 4.1), but chroma was the best of the three at segregating high and low SC samples. Chroma generally had an inverse relationship with SC; low chroma samples had significantly higher ($p < 0.03$) SC than high chroma samples. The average SC for chroma 1 samples was 901 µS cm^{-1}, while the average SC for all other chroma levels was < 345 µS cm^{-1}. Value also had an inverse relationship with SC, but trends were less meaningful than chroma, with some of the highest SC levels occurring at a color value of 4.

A combination of value and chroma, denoted by soil color names, was also a strong indicator of saturated paste SC (Figs. 4.2 and 4.3). Dark gray (4/1) and very dark gray (3/1) samples had significantly higher mean SC than other colors, with an average SC of 1199 µS cm^{-1} and 992 µS cm^{-1}, respectively. While not significantly higher, black (2/1) samples averaged 891 µS cm^{-1} SC, also relatively high. All of the other colors averaged $\leq$ 553 µS cm^{-1}. In comparison, dark yellowish brown (4/6) was the most common weathered sandstone and subsoil color and averaged 156 µS cm^{-1}. In short, low chroma, low value samples produced high SC. High chroma, high value samples produced low SC. Dark gray to black colored samples produced high SC, and yellowish brown samples produced low SC.

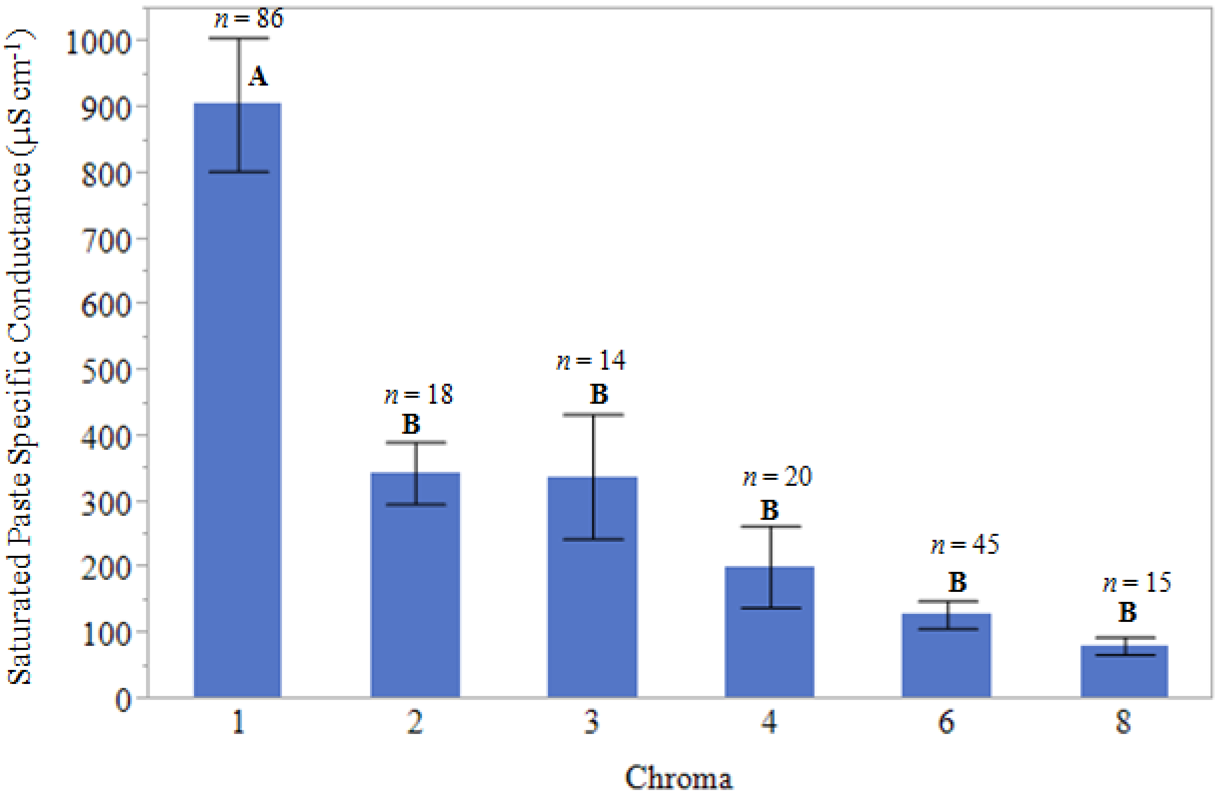

Figure 4.1. Mean saturated paste SC by Munsell© chroma for 198 soil and rock samples. Chroma 1 samples were signifantly higher ($p < .03$) in SC than higher chromas and nearly all of the high SC samples were chroma one. Error bars represent one standard error above and below the mean. Capital letters indicate means significantly different at $\alpha = 0.05$.

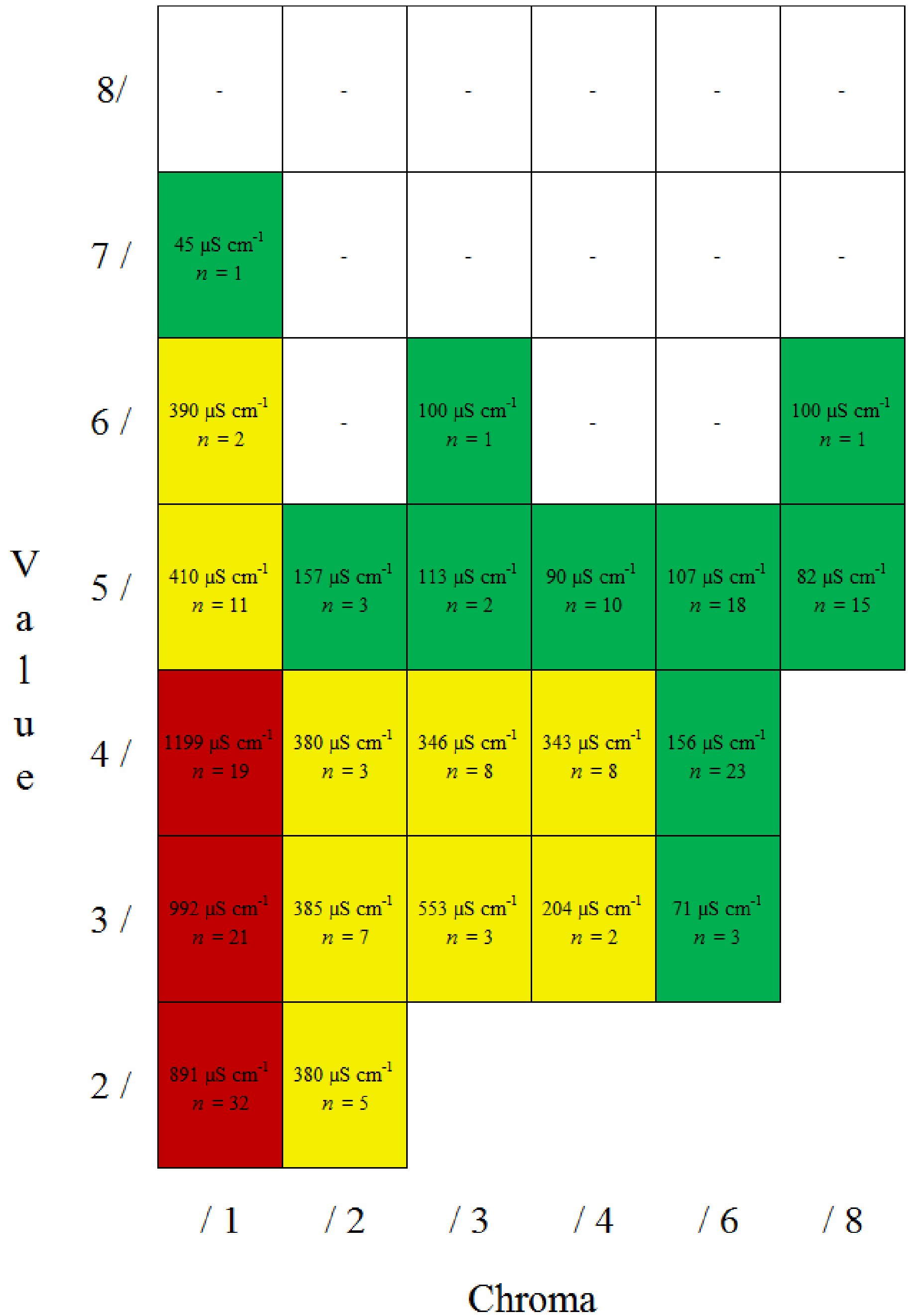

Figure. 4.2. Relationship of Munsell value and chroma to mean saturated paste SC (µS cm^{-1}) for the 10 YR hue page for 198 soil and rock samples. Green = relatively low SC, yellow = relatively moderate SC, and red = realtively high SC. For example, samples with value 2, chroma 1 averaged 891 µS cm^{-1} for saturated paste SC.

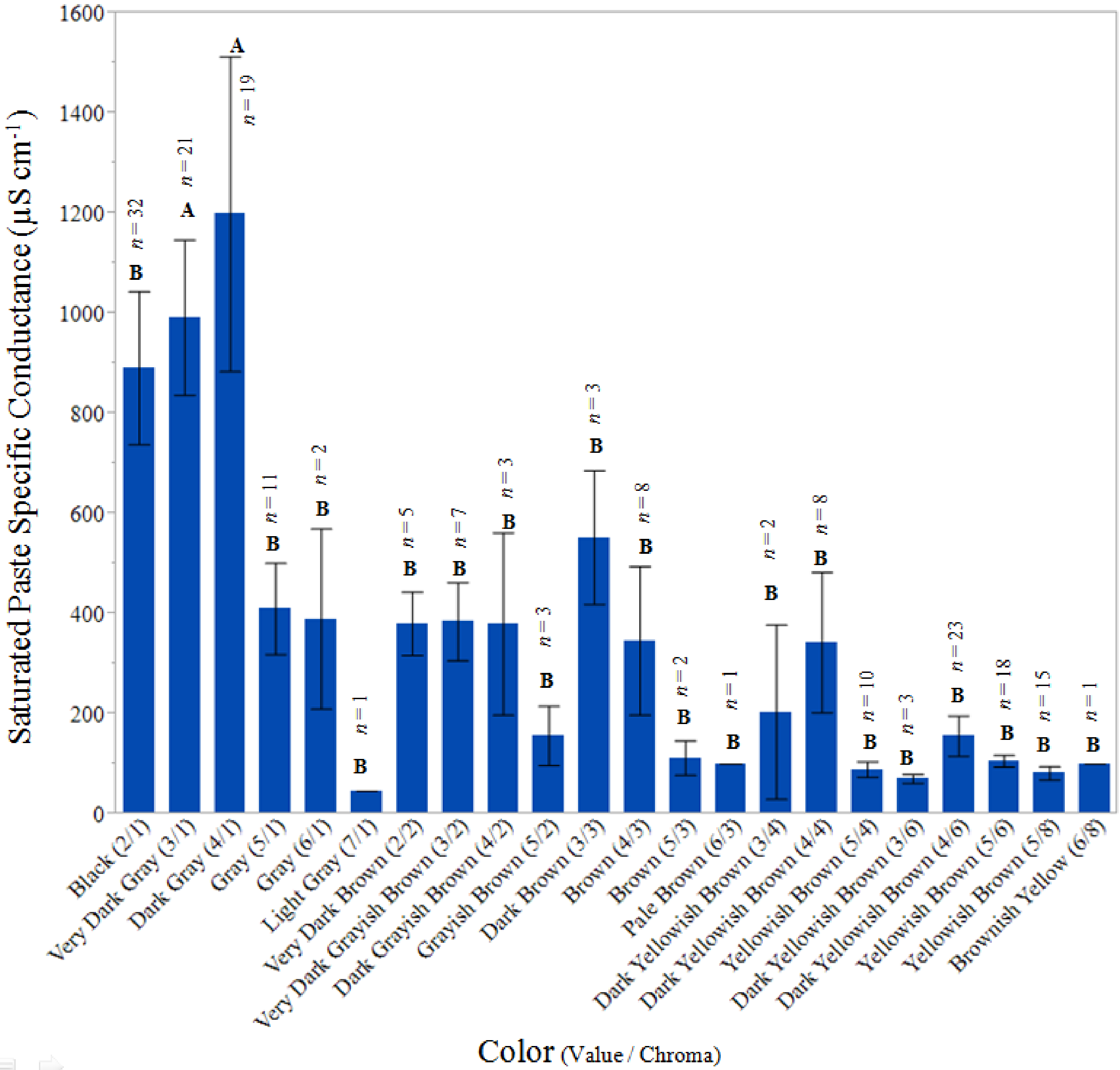

Figure. 4.3. Saturated paste SC (µS cm^{-1}) versus Munsell © color names for 198 soil and rock samples. Very dark gray and dark gray samples were significantly higher in SC than other samples, but black samples were also generally high in SC. Yellowish brown samples generally produced the lowest SC overall. Error bars represent one standard error above and below the mean. Capital letters indicate means significantly different at α = 0.05 across color names.

Chroma was also a reliable predictor of saturated paste sulfate, Ca, and Mg concentrations (Fig. 4.4); all of which were significantly higher in chroma 1 samples than other samples (p <0.001). Sulfate averaged 533 mg L^{-1} in chroma 1 samples and < 63 mg L^{-1} for all other chromas. Calcium averaged 93 mg L^{-1} for chroma 1 samples and < 37 mg L^{-1} for other chromas. Magnesium averaged 57 mg L^{-1} for chroma 1 samples and < 15 mg L^{-1} for all other chromas. Thus, chroma 1 samples had higher overall levels of saturated pasted extractable Ca and Mg and especially sulfate, which was an order of magnitude higher.

While most previous studies only provide anecdotal evidence between color and TDS, a few studies do provide simlilar results. Odenheimer et al. (2014) showed their estimated TDS parameter to generally decrease as chroma increased; simliar to the current study, the highest TDS samples were all confined to chroma one. Another study in Eastern Kentucky (Agouridis et al., 2012) detailed the differences in leachates from field-scale mine spoil lysimeter plots. Unweathered, gray sandstone spoil leachates were found to be higher in Ca, Mg, SC, and sulfate than weathered, brown sandstone spoil leachates. While these and other studies refer to predicting general geochemical traits by color, they either lack a large number of samples or only provide generalized colors for bulk samples, which had been blasted, mixed and transported before sampling. Thus, the results presented above reinforce previous findings with more detailed results and a larger sample set collected in situ and pre-mining disturbance.

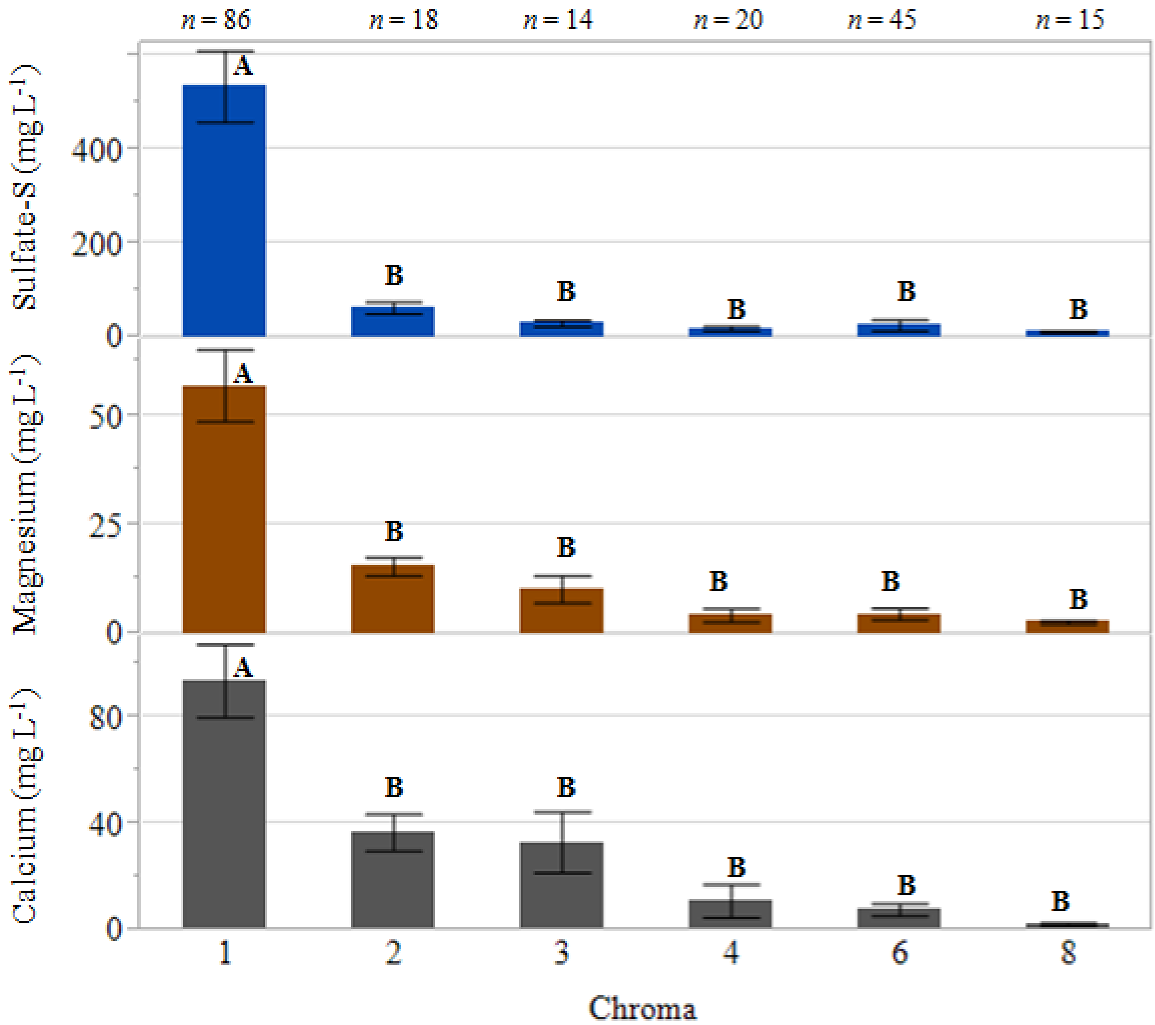

Fig. 4.4. Saturated paste Ca, Mg, and sulfate versus chroma. Chroma 1 samples produced significantly higher levels of saturated paste Ca, Mg, and sulfate than did higher chroma samples. Error bars represent one standard error above and below the mean. Capital letters indicate means significantly different at $\alpha = 0.05$ for each element.

Rock Type

Rock type had a significant effect ($p < 0.001$) on saturated paste SC (Fig. 4.5). Due to sample methodology and physical access, the number of coal seam samples collected was low, so one of the six outliers excluded from other analyses was included in the rock type analysis to increase the total number of coal samples (to $n = 3$). Due to low sample size and high variability in SC of coal samples collected, coal had a high standard error, but still had the highest average SC (2273 μS cm^{-1}). Mudstones (including fireclays, flintclays, and underclays) and shales generally had the next highest SC, followed by siltstones and siltstones interbedded with sandstone. Sandstone and soil samples had the lowest mean SC values of 410 μS cm^{-1} and 246 μS cm^{-1}, respectively.

Both saturated paste sulfate and total-S showed a similar trend to SC (Figs. 4.6 and 4.7) and were significantly different between rock types ($p < 0.001$); coals and mudstones were higher (2167 mg L^{-1} and 945 mg L^{-1}, respectively) than sandstones and soils (199 mg L^{-1} and 31 mg L^{-1}, respectively) for sulfate. Total-S was highest in coals (0.97%) and mudstones (0.21%) and lowest in sandstones (0.03%) and soils (0.04%). Interestingly, on average, Ca and Mg were higher in shale and mudstone samples than in coal samples, even though overall coal had much higher levels of SC. Magnesium averaged 74 mg L^{-1} in shale and mudstone samples, compared to 23 mg L^{-1} and 10 mg L^{-1} in sandstone and soil samples. Calcium averaged 220 mg L^{-1} in mudstone and 95 mg L^{-1} in shale samples, but only 34 mg L^{-1} in sandstone and 26 mg L^{-1} in soil samples. Thus, both overall saturated paste SC and individual ionic concentrations varied significantly by rock type; generally in the order of coal > mudstone > shale > siltstone > sandstone > soil.

Previous studies report similar results. Agouridis et al. (2012) found leachates in field-scale mine spoil plots to be higher in Ca, Mg, SC, and sulfate in a mixture of sandstone and shale compared to both weathered and unweathered sandstones. Daniels et al. (2016) studied 39 mine spoils and found rock type to have a significant effect on SC; generally black shales > mudstones > mix of rock types > sandstone.

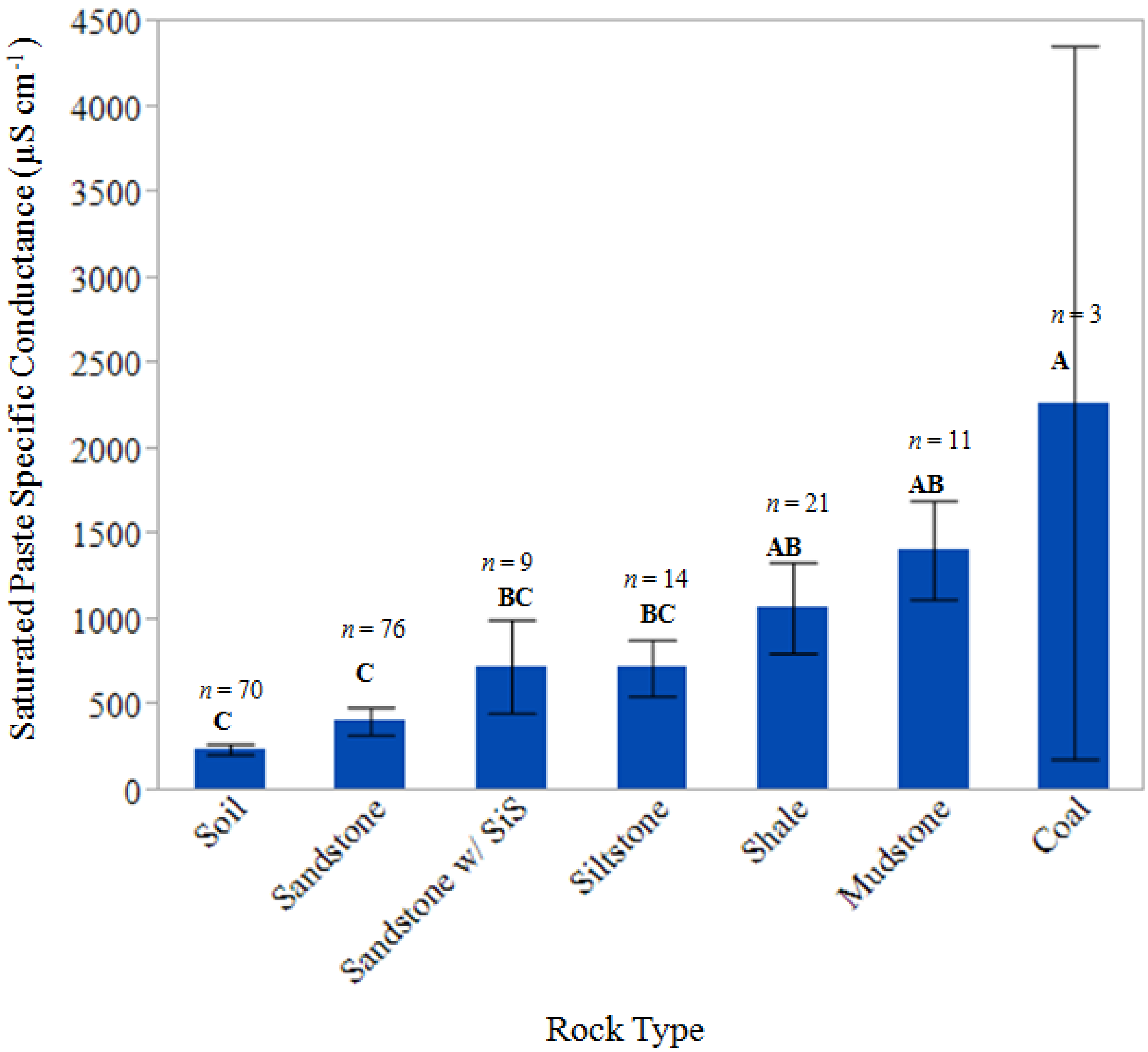

Figure. 4.5. Mean saturated paste SC (µS cm^{-1}) by rock type for 199 soil and rock samples. Fireclays, flint clays, underclays, and materials associated with coal seams are included under the "mudstone" category. Error bars represent one standard error above and below the mean. Capital letters indicate means significantly different at α = 0.05 across rock types.

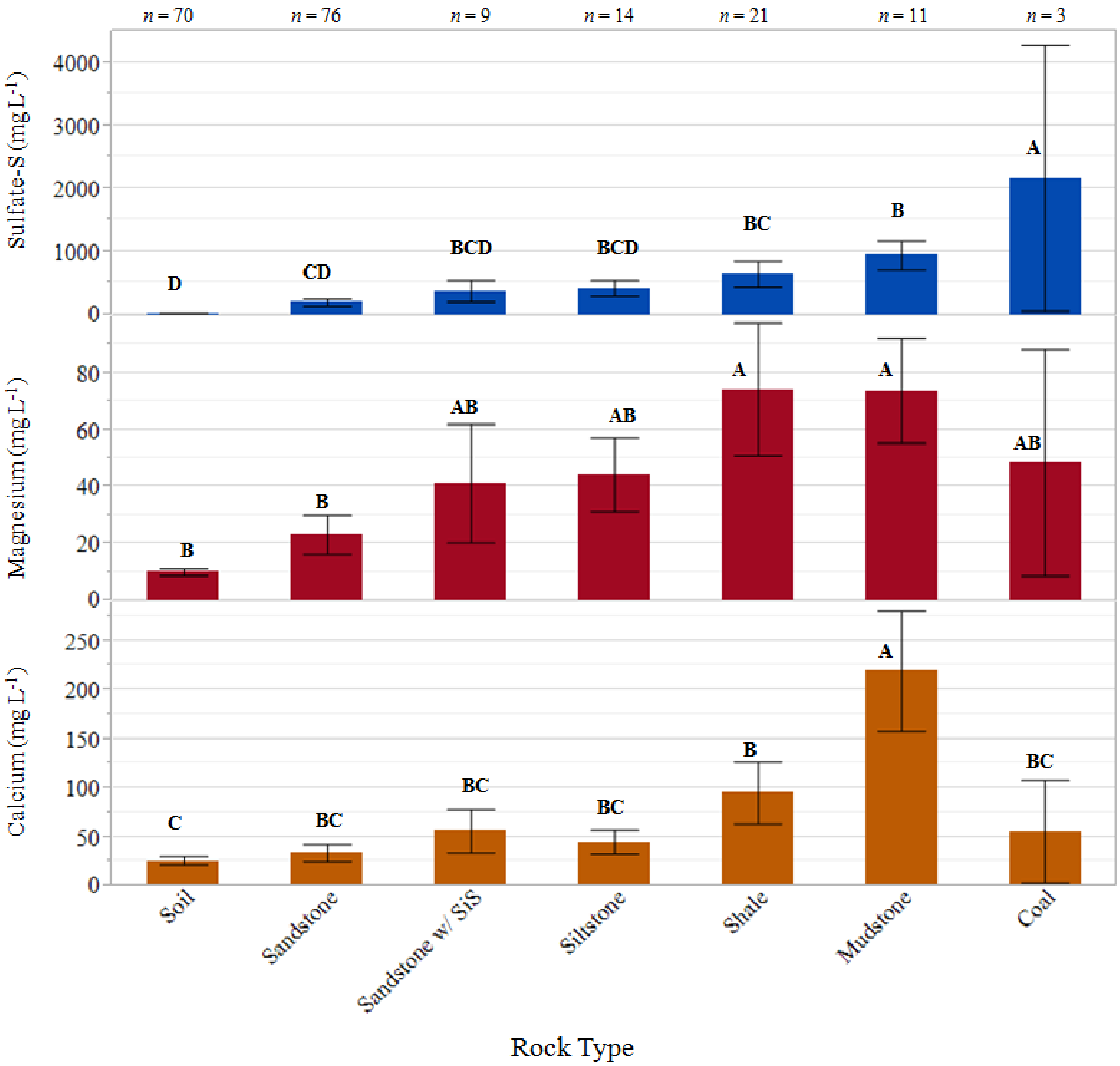

Figure. 4.6. Mean saturated paste Ca, Mg, and sulfate versus rock type for 199 soil and rock samples. Fireclays, flint clays, underclays, and materials associated with coal seams are included under the "mudstone" category. Error bars represent one standard error above and below the mean. Capital letters indicate means significantly different at α = 0.05 for each element.

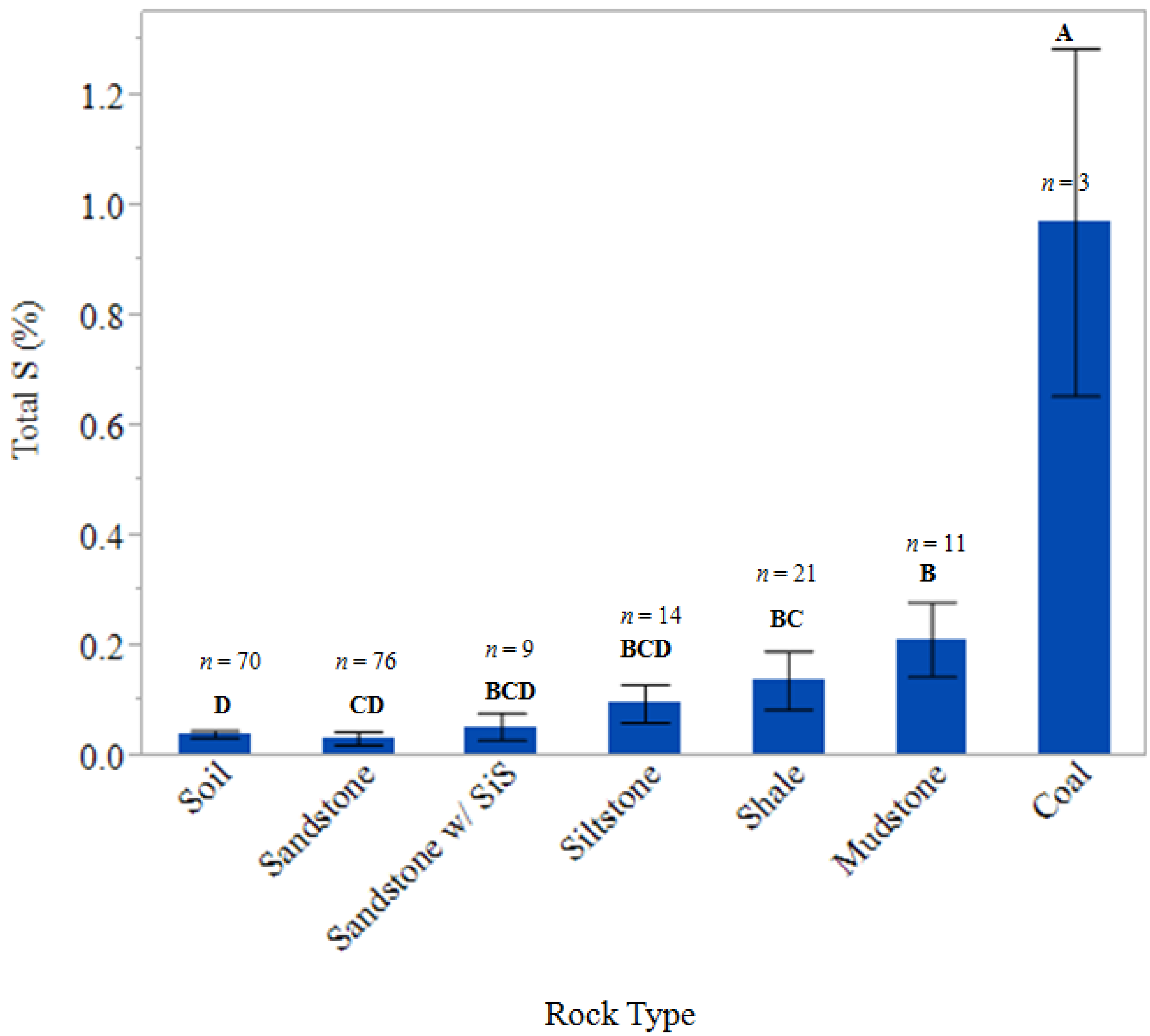

Figure. 4.7. Mean total-S versus rock type for 199 soil and rock samples. Fireclays, flint clays, underclays, and materials associated with coal seams are included under the "mudstone" category. Error bars represent one standard error above and below the mean. Capital letters indicate means significantly different at $\alpha = 0.05$ across rock types.

Horizon Type

Saturated paste SC was significantly different between horizon types ($p < 0.001$; Fig. 4.8). Subsoil B horizons were generally always low in SC and individual ion concentrations. Interestingly, A horizons (topsoils) were significantly higher in SC than B and C horizons. Unweathered R layers (bedrock layers) had the highest SC, but weathered R layers had similar SC levels to B and C horizons. Saturated paste sulfate, Mg, Ca, HCO_3^-, and Se (Figs. 4.9 and 4.10) all followed a similar trend by horizon type as for overall SC. In contrast, saturated paste As and P were significantly higher ($p < 0.01$) in A horizons than B, C, or R horizons/layers. So, soil horizons were generally lower than rock layers in saturated paste Ca, Mg, SC, and Se, but A horizon samples contained higher saturated paste Ca, Mg, SC, and Se levels than B or C horizons.

Presumably, organic nutrient cycling contributes to the higher ionic concentrations in A horizons; however, A horizons in the study area are commonly < 0.1 m thick and Appalachian surface mines commonly remove 100's of meters of overburden, so this thin layer of A horizon is likely of little consequence to overall TDS. Topsoil return provides many beneficial ecosystem properties to reclaimed mine soils, which would outweigh any negative impacts from a TDS perspective (Burger et al., 2005; Toy and Daniels, 1998). Topsoil has higher water holding capacity, better compaction resistance, and high organic matter content compared to subsoil and bedrock mine spoils. Elevated levels of TDS in the rooting zone will also contribute positively to soil fertility levels; after revegetation, many of these potential TDS pollutants will be tied up in organic nutrient cycles, preventing them from leaching. Thus, while B horizons, C horizons, and weathered R layers can be reliably used as sources of low-TDS mine spoil, A horizons contain many beneficial properties and the topsoil should be returned where economically feasible.

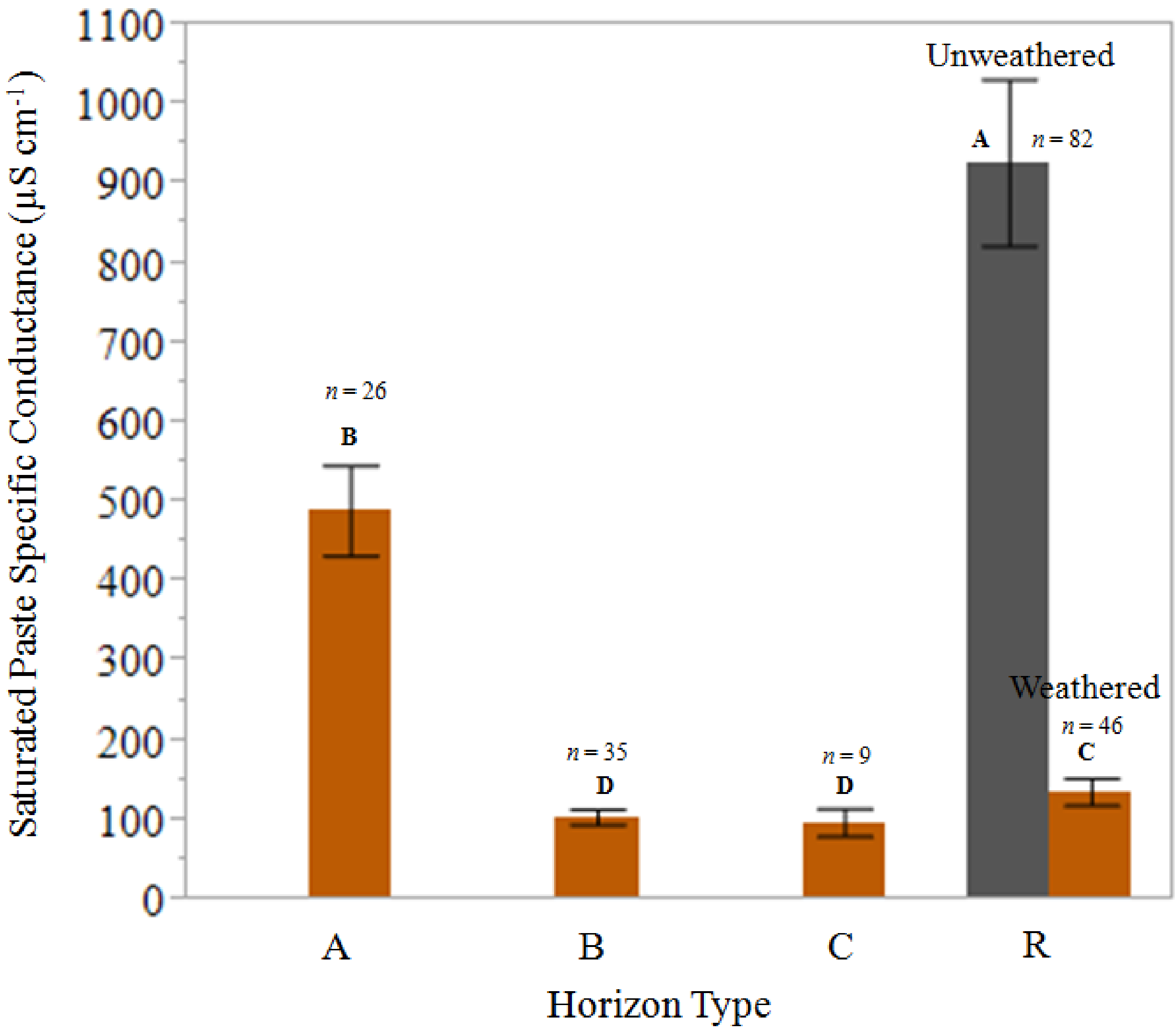

Figure. 4.8. Mean saturated paste SC (µS cm^{-1}) by horizon type for 198 soil and rock samples. The R layers (bedrock) are also sorted into weathered and unweathered categories. Error bars represent one standard error above and below the mean. Capital letters indicate means significantly different at α = 0.05.

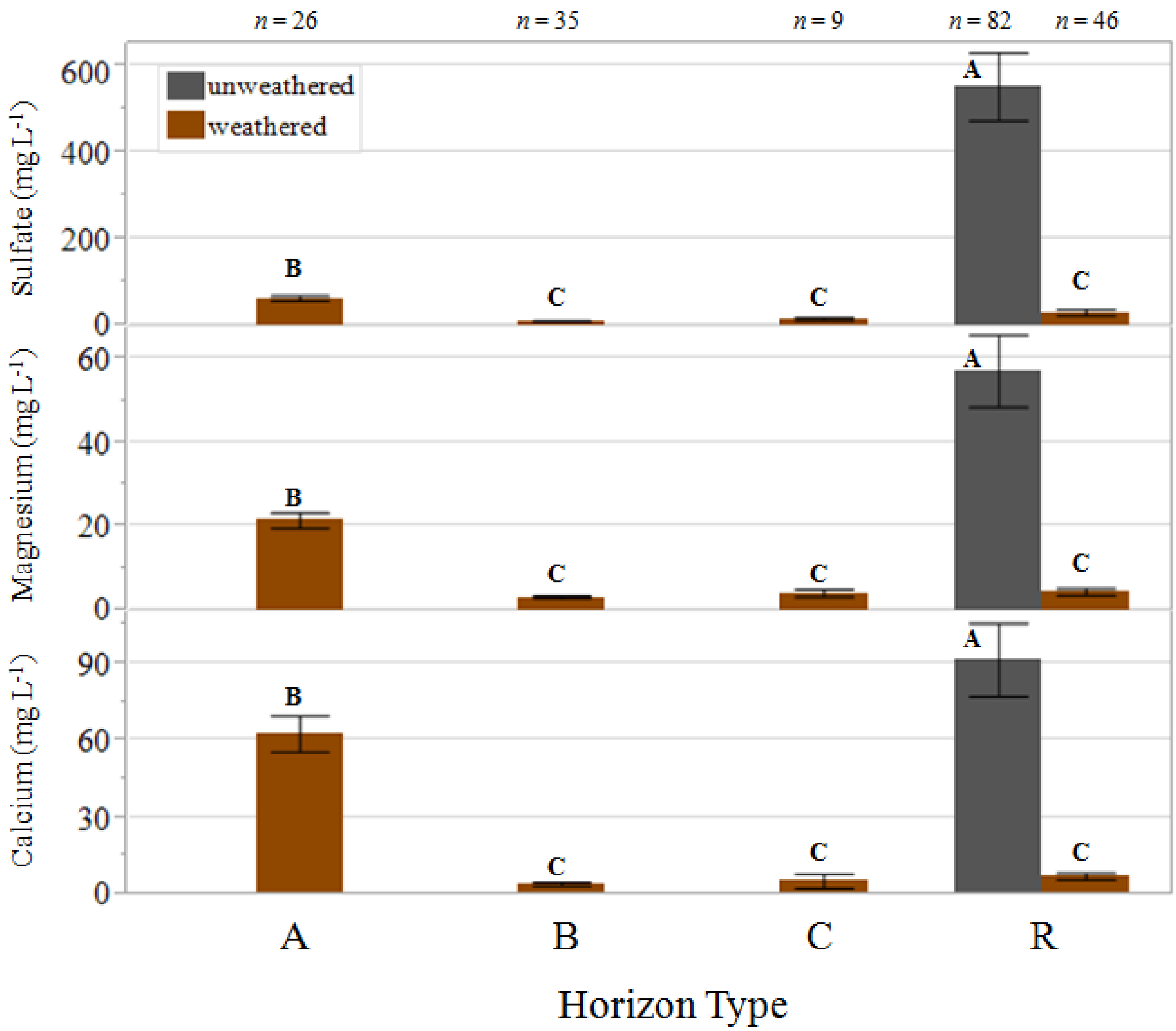

Figure. 4.9. Mean saturated paste Ca, Mg, and sulfate by horizon type for 198 soil and rock samples. The R layers (bedrock) are also sorted into weathered and unweathered categories. Error bars represent one standard error above and below the mean. Capital letters indicate means significantly different at $\alpha = 0.05$ for each element.

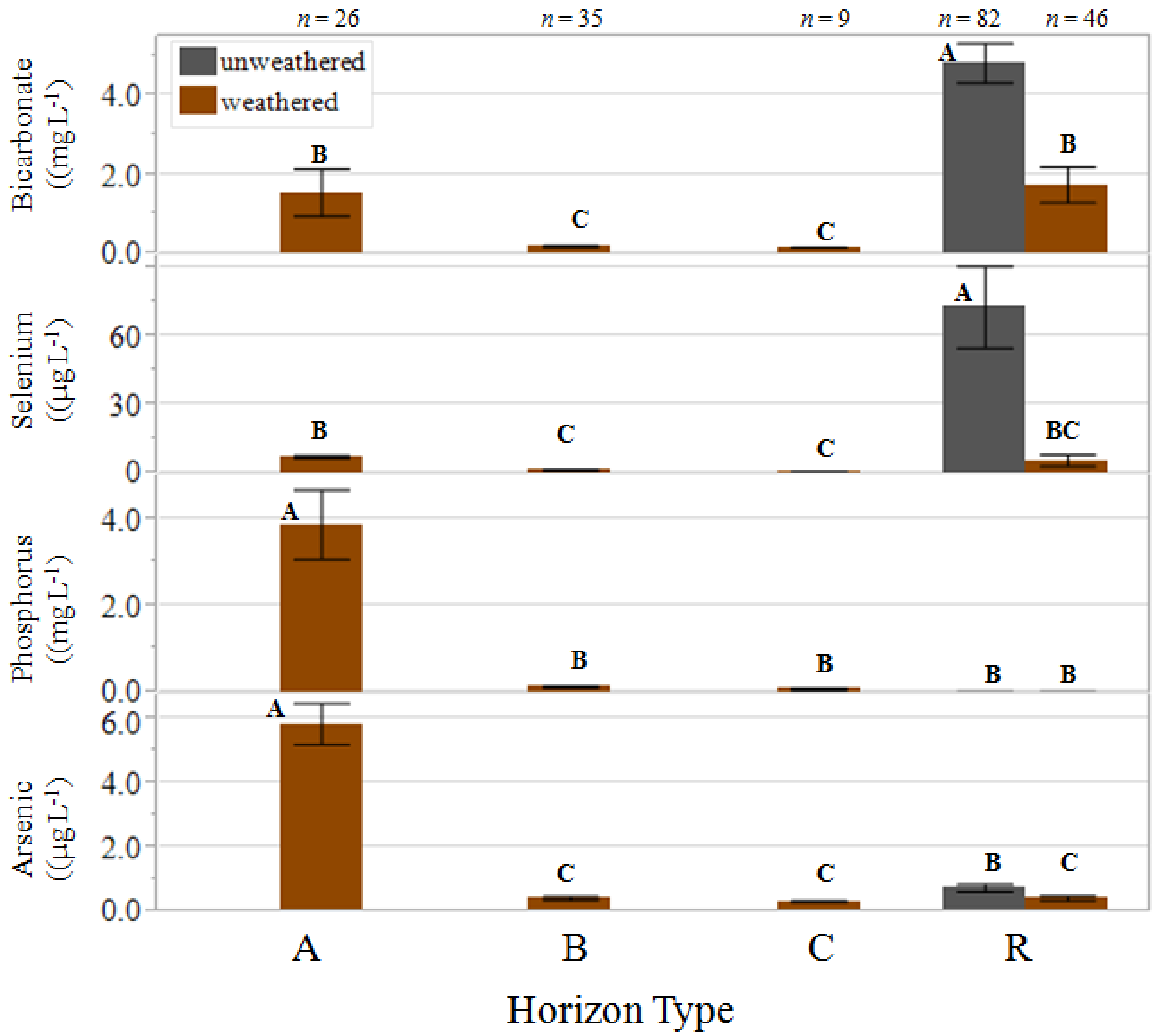

Figure. 4.10. Mean saturated paste As, P, and Se by horizon type for 198 soil and rock samples. The R layers (bedrock are also sorted into weathered and unweathered categories. Error bars represent one standard error above and below the mean. Capital letters indicate means significantly different at $\alpha = 0.05$ for each element.

Degree of Pre-Weathering

A confining layer retarding water movement downward created an abrupt transition between the weathered and unweathered zones at 30 out of 33 of the sites (Figs. 4.11, 4.12, 4.13). Presumably, water percolated freely downward through the surficial soil and sandstone layers at most sites, until reaching the first shale or mudstone layer. Water was found springing horizontally from the profile in perched water tables directly above the confining layers at several of the sites, suggesting that shales and mudstone layers are impeding water flow downward in the study area. Wunsch (1993) suggested that coal beds in the region act to "dewater the upper portion of the ridge by laterally transmitting water that discharges as springs or seeps". Results for the current study suggest that mudstone and shale layers may also have a similar effect, at least to the extent of perching a saturated zone above them and enhancing lateral flow regimes. The Wunsch study also suggested that significant infiltration of water occurs along breaks in slope along the ridges that have a high degree of fracturing. This was quite evident at most of the sites visited. Highly weathered and fractured shale and mudstone layers provided cracks as preferential flow paths for water and did not have the same confining effect; weathering generally extended through and below these fractured layers. Thus, the weathered surficial materials were separated from the deeper unweathered materials by an intact shale or mudstone confining layer at most of the sites.

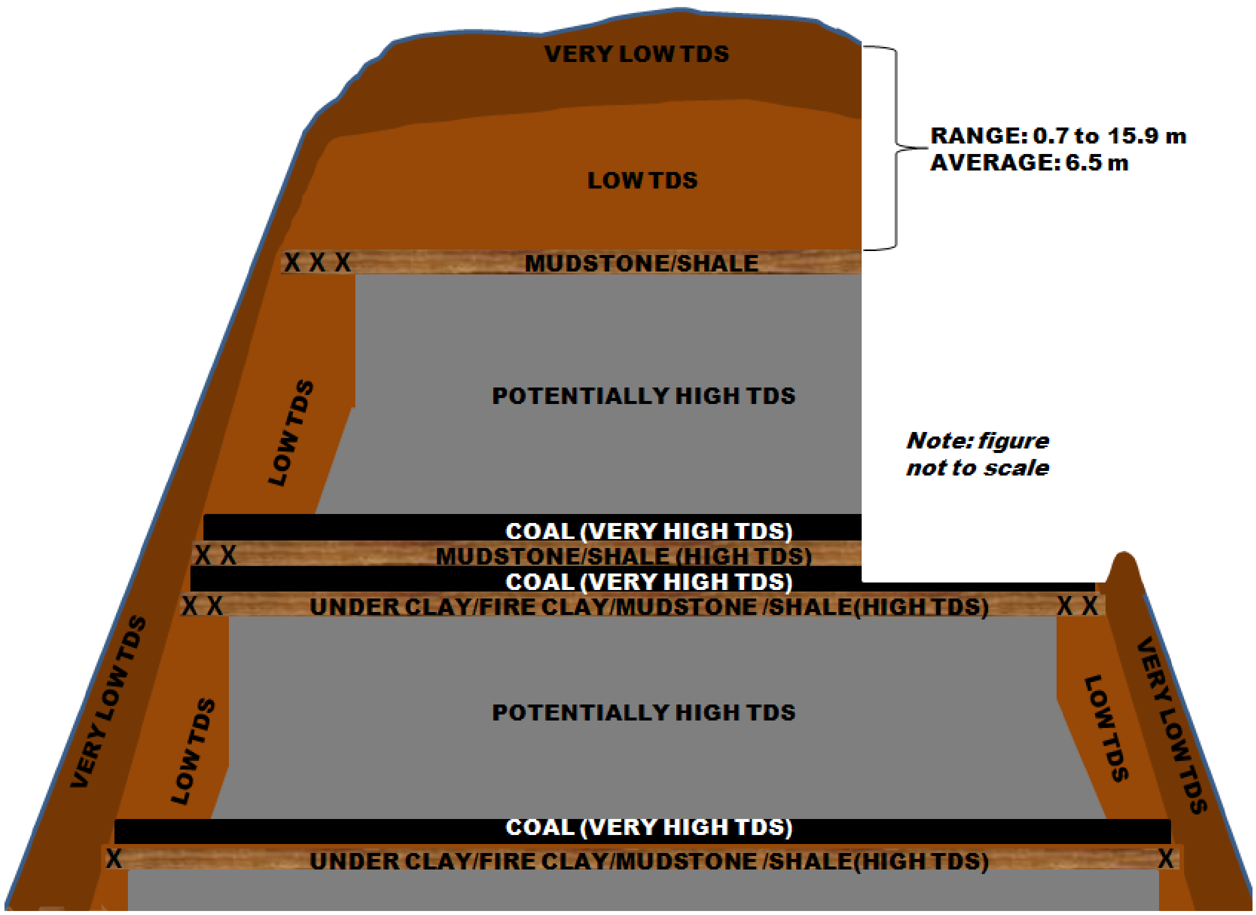

Figure 4.11. Layering of materials in a typical Appalachian coal surface mine. Relative TDS elution potentials are indicated as very low, low, high, or very high; however, a wide range in actual TDS leaching potentials among the deeper reduced rocks shown as "potentially high TDS" here. In general, intact shale and mudstone layers prevent the downward movement of water and oxygen, limiting the long-term weathering of deeper rocks. The capping of low-TDS surficial soil and weathered bedrocks ranged from 0.7 m - 15.9 m and averaged 6.5 m thick; areas lacking a near surface shale or mudstone layer or having a high degree of fracturing generally had a thicker capping of low-TDS material.

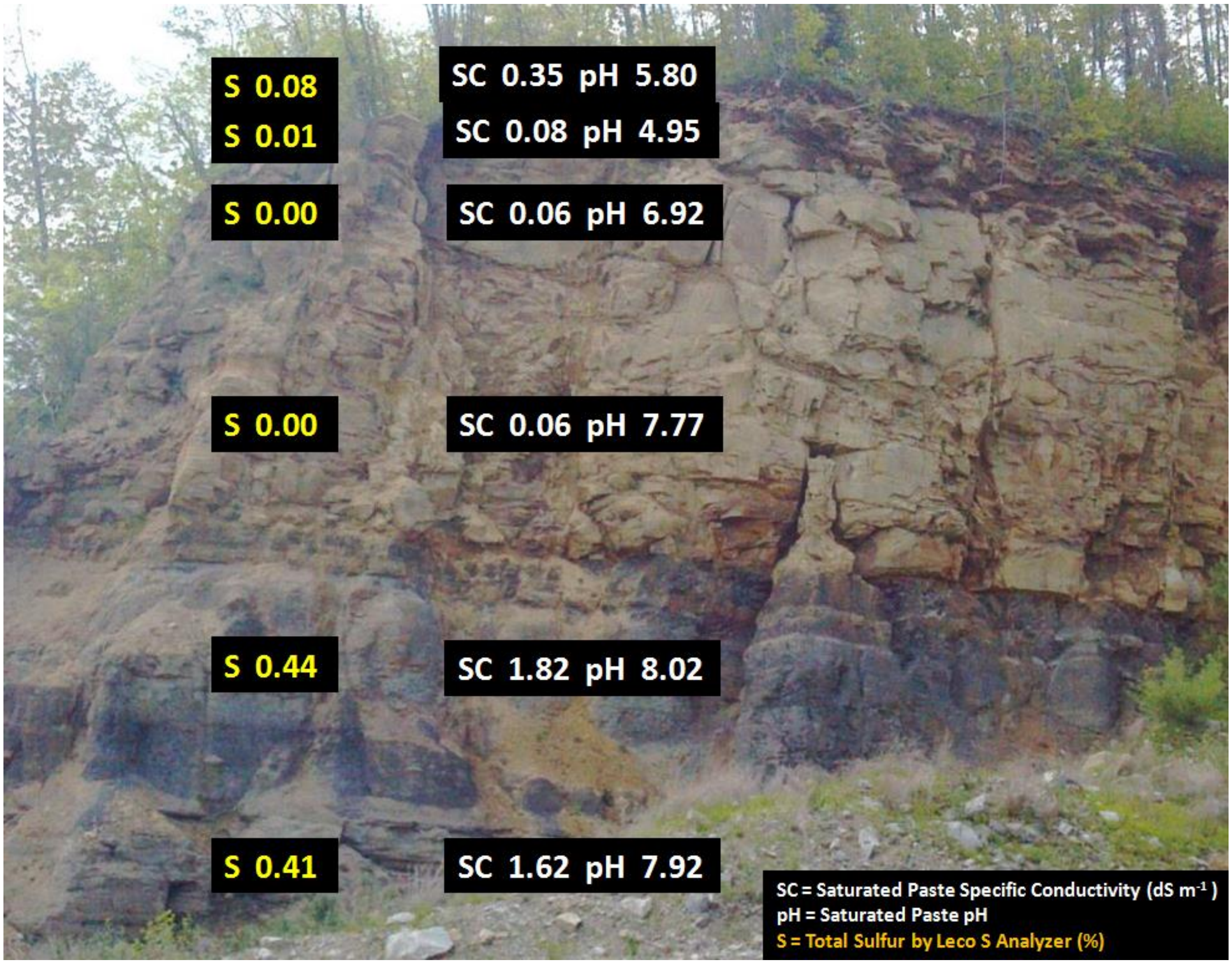

Figure 4.12. Site #2 located in Wise County, Virginia. Soil and bedrock layers from top to bottom were: 1) very dark gray topsoil, 2) dark yellowish-brown subsoil, 3) yellowish-brown weathered sandstone, 4) yellowish-brown weathered sandstone, 5) black, unweathered mudstone, 6) very dark gray, unweathered sandstone. Note the abrupt changes in pH, S and SC above and below the change in rock color.

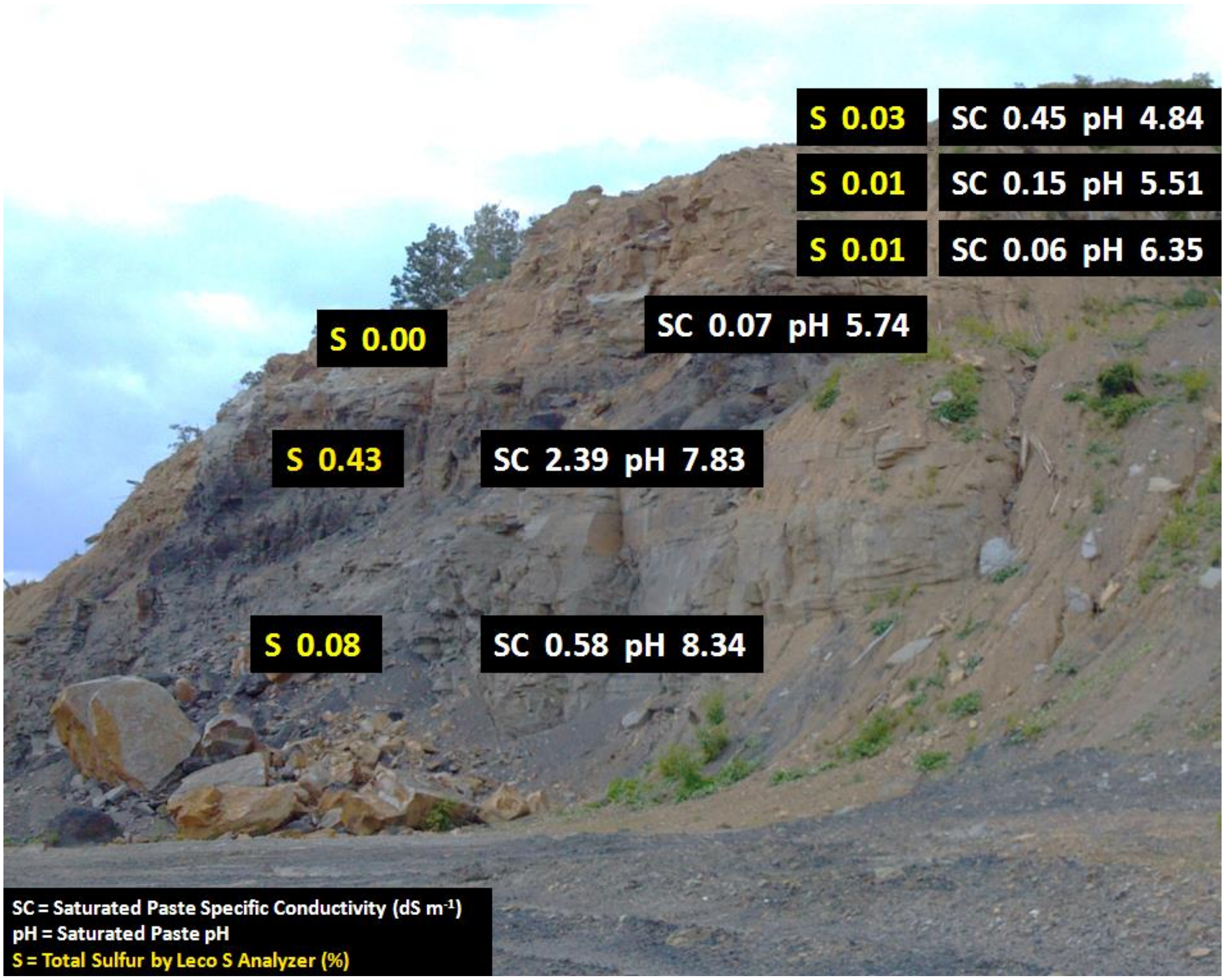

Figure 4.13. Site #3 located in Wise County, Virginia. Soil and bedrock layers from top to bottom were: 1) very dark grayish-brown topsoil, 2) yellowish-brown subsoil, 3) yellowish-brown, soft, weathered siltstone, 4) yellowish-brown, weathered sandstone, 5) black, unweathered mudstone, 6) black, unweathered mudstone. Brown weathered material on right is debris fallen down from upper soil layers. Sampled sequence was to the middle left of the photograph.

Massive sandstone strata dominated the near-surface geology at a few of the sites, however. Since these locations lacked shale or mudstone layers near the surface to block the flow of water and oxygen downward, the weathering boundary was much more diffuse and generally deeper below the surface. In these instances, large transition zones up to 5-10 m in thickness were found between the weathered and unweathered material, which often contained alternating distinct layers of weathered and unweathered material. Additionally, deep, isolated vertical cracks in the bedrock created pockets of weathered material deep into the unweathered strata at nearly all of the sites; this phenomenon was quite apparent in the field, but comprised a very small volume compared to the overall strata. While most of the observations for these isolated pockets were qualitative and lacked lab analysis, the weathered pockets were obviously distinctly different and largely unrepresentative of the overall surrounding strata. Sampling to predict TDS release should avoid these isolated, weathered pockets of bedrock to avoid misestimating TDS potential. Thus, sites lacking near-surface shale or mudstone layers had a larger transition zone between weathered and unweathered materials and some weathered material was found below the general weathering boundary in deep cracks at nearly all of the sites.

Samples collected from the surficial soils and sandstones, above any shale or mudstone confining layers, were designated as "weathered"; samples collected within or below this confining layer were designated as "unweathered". The weathered zones consisted of nearly flat to slightly sloping soil and sandstone layers, in addition to highly fractured shales, mudstones, and coals in a few instances. The weathered zones were full of visible evidence of water percolation throughout, such as Fe-oxide staining (reddish-brown), Mn-oxide staining (black), illuviated soil materials from higher in the profile, and yellowish brown colors from Fe-oxidation. In contrast, the unweathered zones contained alternating layers of mudstones, shales, and coals, in addition to sandstones. The unweathered zones showed signs of hydrologic isolation, such as well-preserved fossils and visible soluble salt accumulations. Colors in the unweathered zones tended to be grayish (average chroma 1.5) overall compared to the yellowish brown colors (average chroma 4.4) found in the weathered zone. So, a number of readily observable traits separated the weathered from unweathered samples.

Geochemical properties varied between weathered and unweathered samples as well. Saturated paste SC, sulfate, Mg, Ca, and Se were all significantly lower ($p < 0.001$) in weathered samples versus unweathered samples (Figs. 4.14 and 4.15), but As and CD-extractable Fe, Al, and Mn were significantly higher ($p < 0.02$) in weathered samples (Fig. 4.16). Weathered and unweathered samples averaged 203 µS cm^{-1} and 927 µS cm^{-1}, respectively, for SC. Sulfate averaged 550 mg L^{-1} in weathered samples and 31 mg L^{-1} in unweathered samples. The mean Mg concentration was 57 mg L^{-1} for unweathered samples and 8 mg L^{-1} for weathered samples. Calcium averaged 92 mg L^{-1} and 19 mg L^{-1} for unweathered and weathered samples, respectively. Selenium mean concentrations were 73 µg L^{-1} for unweathered samples and 4 µg L^{-1} for weathered samples. Conversely, As was significantly higher in weathered samples (1.6 µg L^{-1}) than unweathered samples (0.7 µg L^{-1}). CD-extractable Fe, Al, and Mn were also significantly higher ($p < 0.01$) in weathered samples compared to unweathered samples. So, while As and CD-extractable Fe, Al, and Mn were significantly higher in weathered samples, SC, sulfate, Mg, Ca, and Se were all significantly higher in unweathered samples.

Wunsch (1993) found groundwater from coal seams to have the lowest pH values and to be a Ca-Mg-HCO_3^- water type; fractured zones were Ca-HCO_3^- or Mg-sulfate water types; ridge interiors were Na-HCO_3^- water types, high in Fe, and highest in pH. Agouridis et al. (2012) showed weathered sandstone leachates to be lower in Ca, Mg, SC, and sulfate than unweathered sandstones. Daniels et al. (2016) showed weathered mine spoil leachates had both lower peak

(~750 µS cm^{-1}) and long-term "tail" (~150 µS cm^{-1}) SC than unweathered mine spoils (>1500 and 500 µS cm^{-1} for peak and tail). So, the current study reinforces previous results; weathering status is a strong indicator of both individual ionic concentrations and overall TDS.

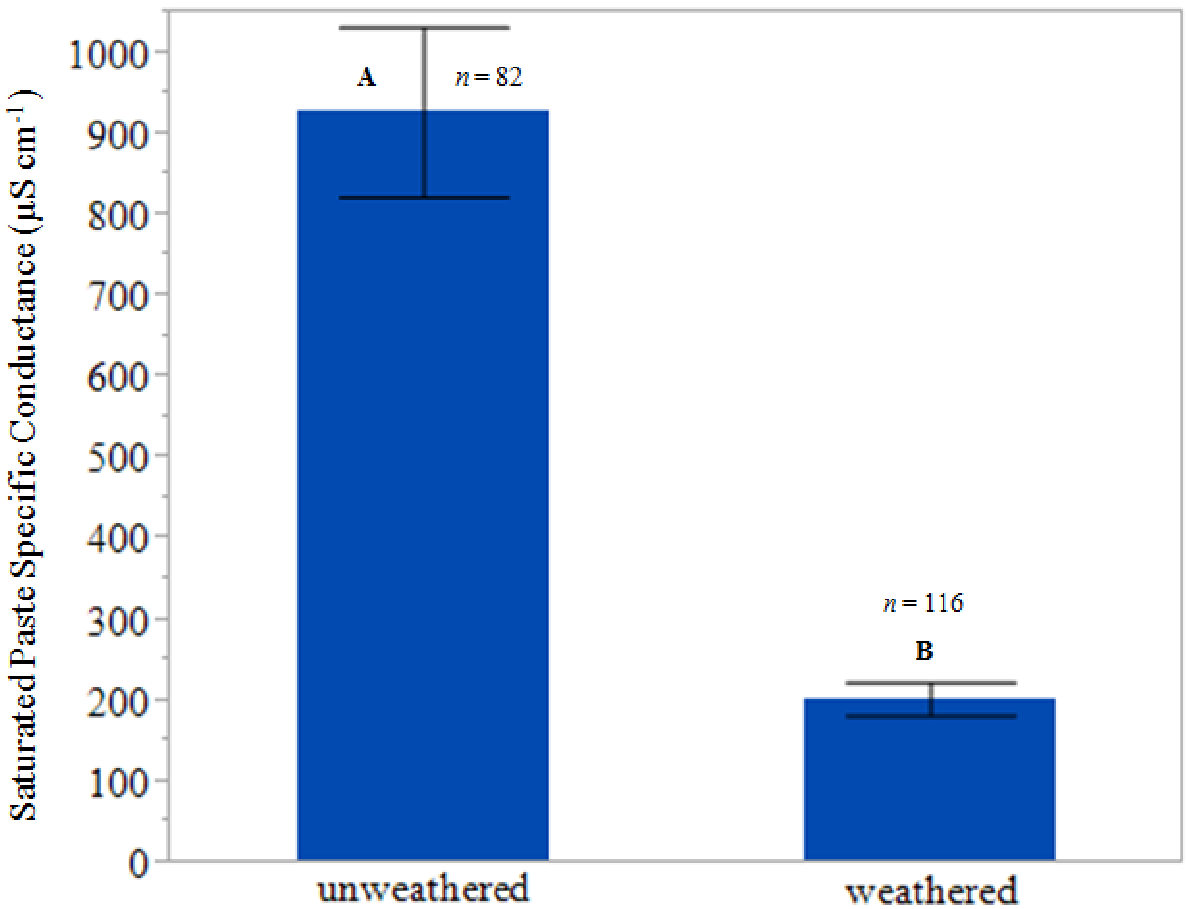

Figure. 4.14. Mean saturated paste SC (µS cm^{-1}) for 198 soil and rock samples sorted by sample origin. Samples orginating above the shallowest intact shale or mudstone layer present at each site were labled weathered. Samples collected within or below this transistional shale or mudstone layer were labeled unweathered. Error bars represent one standard error above and below the mean. Capital letters indicate means significantly different at $\alpha = 0.05$.

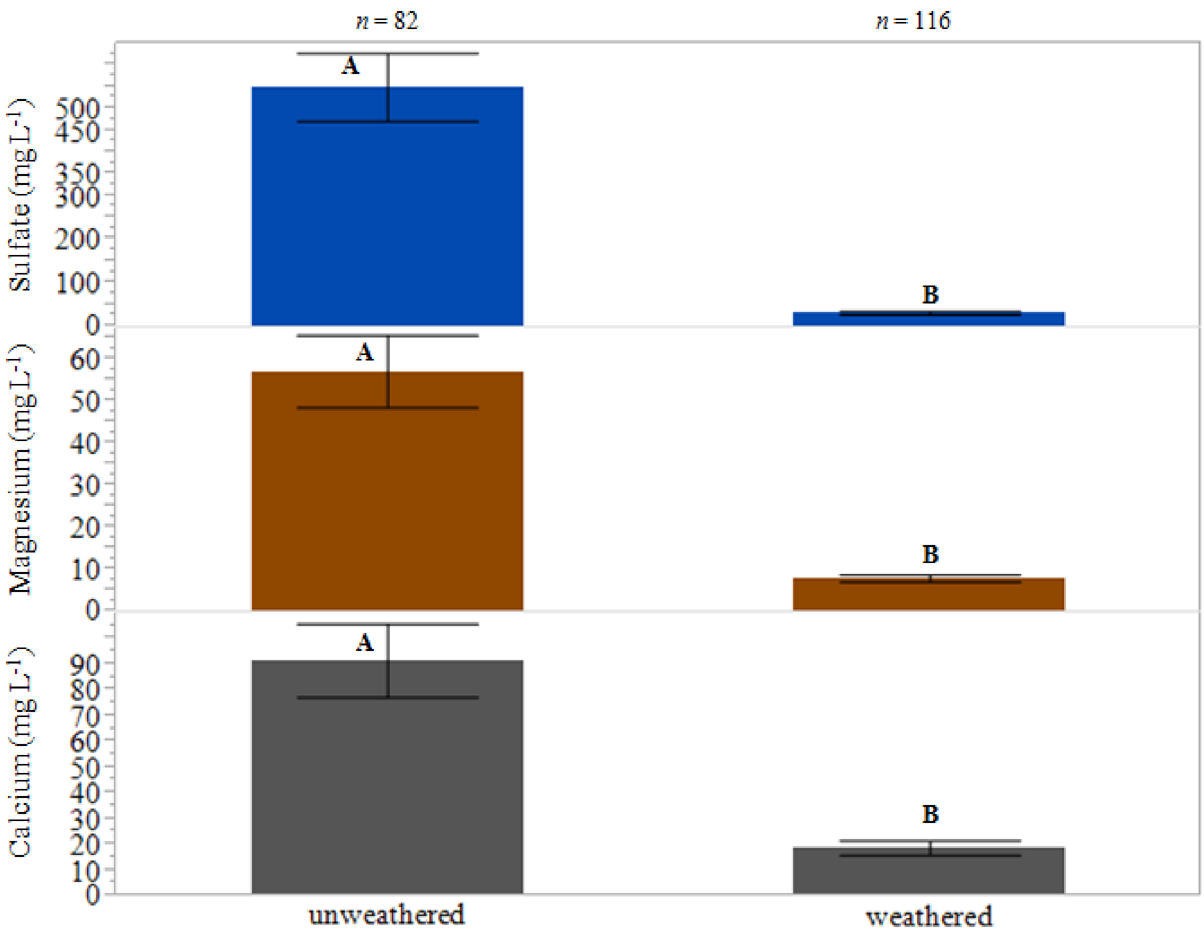

Figure 4.15. Mean saturated paste Ca, Mg, and sulfate for 198 soil and rock samples sorted by sample origin. Samples orginating above the shallowest intact shale or mudstone layer present at each site were labled weathered. Samples collected within or below this transistional shale or mudstone layer were labeled unweathered. Error bars represent one standard error above and below the mean. Capital letters indicate means significantly different at α = 0.05 for each element.

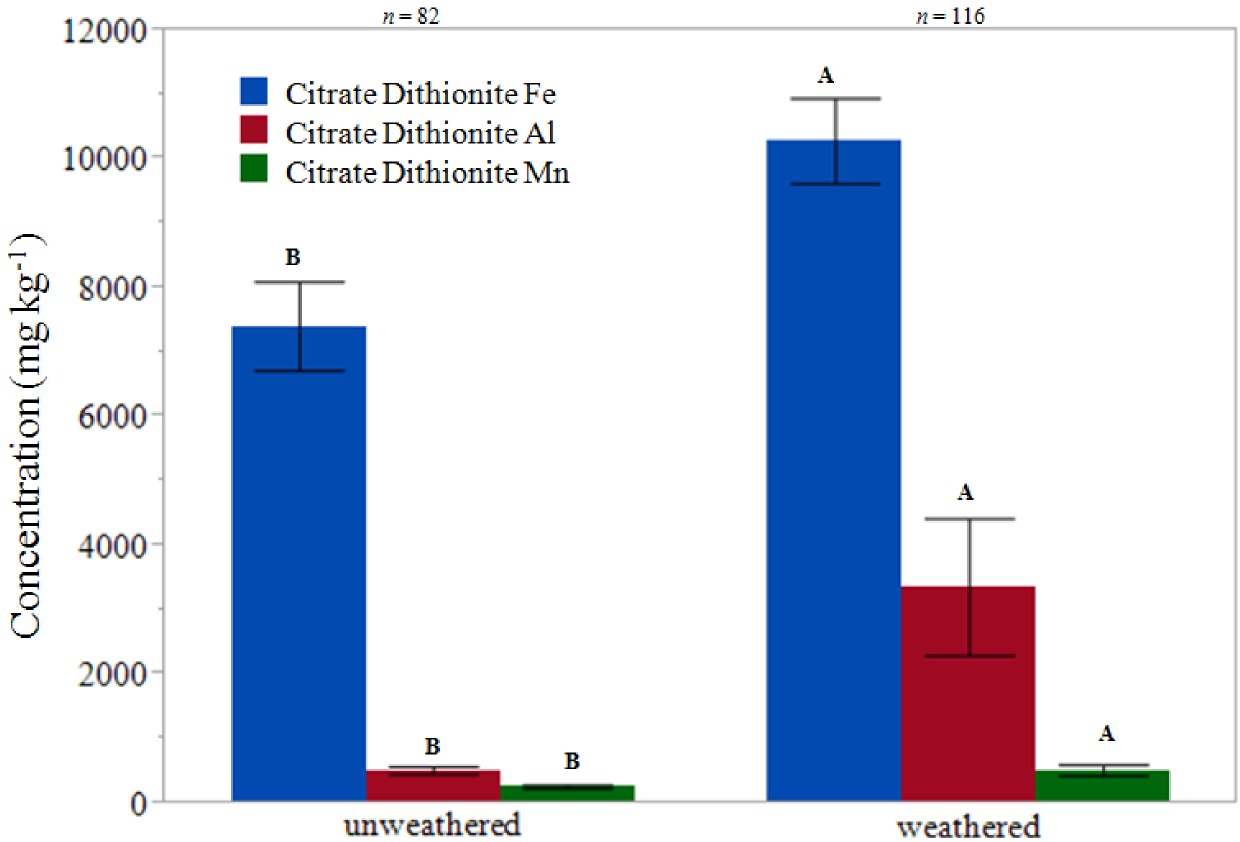

Figure. 4.16. Mean CD-extractable Al, Fe, and Mn for 198 soil and rock samples sorted by sample origin. Samples orginating above the shallowest intact shale or mudstone layer present at each site were labled weathered. Samples collected within or below this transistional shale or mudstone layer were labeled unweathered. Error bars represent one standard error above and below the mean. Capital letters indicate means significantly different at $\alpha = 0.05$.

Hydrochloric Acid Reaction Test

Very few materials reacted with HCl in the study area. In addition to the recorded HCl fizz test data, the HCl was used extensively to investigate samples and nearby rock layers. Anything of interest or out of the ordinary (e.g. siderite nodules, fossils, salt accumulations) noticed was subjected to the acid test, generally all resulting in no reaction. No samples collected were designated as limestones and only 7 of the 204 samples collected reacted at all for the HCl acid fizz test. In two of these cases, the HCl reactions were with inclusions within the rock strata, such as fossilized brachiopod shells, while the overall rock strata did not fizz. Pure carbonate strata are scarce in the study area (Howard, 1979; USGS 2012), so these results are unsurprising. Low sample numbers reacting with the acid limited statistical tests and no significant differences ($p = 0.07$) were detected in SC between HCl reaction levels, but there was a strong relationship (Fig. 4.17). Samples ranked as noneffervescent for HCl reaction, however, were significantly lower in CCE ($p = 0.02$) than samples ranked as slightly effervescent or strongly effervescent ; with averages of 5%, 7%, 12%, and 13%, for ranks noneffervescent, very slightly effervescent, slightly effervescent, and strongly effervescent, respectively. No samples were ranked violently effervescent. Thus, while the HCl acid fizz test was useful for predicting high CCE values, it proved to be a poor indicator of SC.

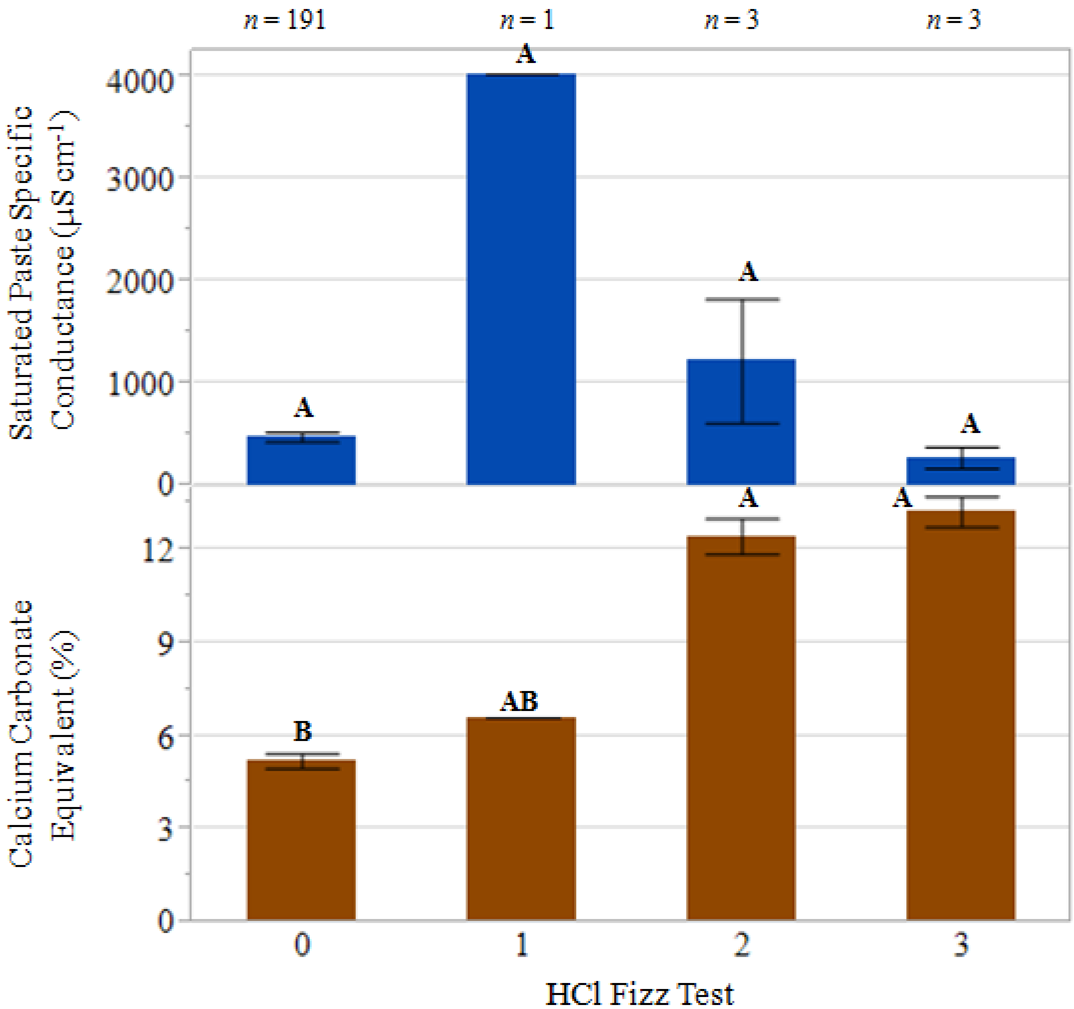

Figure 4.17. Saturated paste SC and CCE versus HCl fizz test reaction for 198 (for CCE n=106) soil and rock samples. Samples with no bubbles were labeled noneffervescent (0). Samples forming few bubbles were labeled very slightly effervescent (1). Samples forming numerous bubbles were labeled slightly effervescent (2). Samples forming a low foam or slight audible bubbles were labeled strongly effervescent (3) and samples reacting with thick foam or very audible bubbles were labeled as violently effervescent (4). Only 7 of 198 samples reacted to the acid and none of the samples reacted violently. Error bars represent one standard error above and below the mean. Capital letters indicate means significantly different at α = 0.05.

Hydrogen Peroxide Reaction Test

The H_2O_2 reaction test turned out to be very useful for distinguishing between not only overall TDS, but specific ion concentrations as well. Generally, samples with higher Ca, Mg, SC, sulfate, and total-S produced more heat and more violent reactions to the H_2O_2 (Figs. 4.18, 4.19). The mean SC for samples with reactions of no reaction, foam, heat, and violent was 315 µS cm^{-1}, 510 µS cm^{-1}, 676 µS cm^{-1}, and 889 µS cm^{-1}, respectively; samples with no reaction were significantly lower in SC than the other samples ($p < 0.04$). Similarly, sulfate concentrations were significantly lower ($p < 0.01$) in samples with no reaction or foam only. Sulfate averaged 145 mg L^{-1}, 64 mg L^{-1}, 371 mg L^{-1}, and 551 mg L^{-1}, for no reaction, foam, heat, and violent, respectively. Calcium varied from 30 mg L^{-1}, 64 mg L^{-1}, 57 mg L^{-1}, to 89 mg L^{-1} for samples with reactions of no reaction, foam, heat, and violent, respectively. Calcium was significantly lower ($p < 0.02$) in no reaction samples. Average values for Mg were 15 mg L^{-1} for no reaction, 22 mg L^{-1} for foam, 43 mg L^{-1} for heat, and 57 mg L^{-1} for violent. Total-S averaged 0.04% for no reaction, 0.07% for foam, 0.07% for heat, and 0.14% for violent (Fig. 4.20). Total-S was significantly lower ($p < 0.005$) in no reaction samples. Average Se values were significantly lower ($p < 0.001$) for no reaction (11 µg L^{-1}) and foam (7 µg L^{-1}) than heat (72 µg L^{-1}) and violent (67 µg L^{-1}) reactions. Arsenic, however, followed different trends than the other elements. Samples reacting to the H_2O_2 with foam (generally high-organic matter topsoils) produced the significantly highest As values ($p < 0.001$); averages were 0.5 µg L^{-1}, 5.9 µg L^{-1}, 0.9 µg L^{-1}, and 0.7 µg L^{-1} for no reaction, foam, heat, and violent reactions, respectively. So, while samples reacting to the H_2O_2 with foam only had high levels of As, samples with high levels of Ca, Mg, SC, Se, sulfate, and Total-S consistently produced more violent and exothermic reactions than other samples.

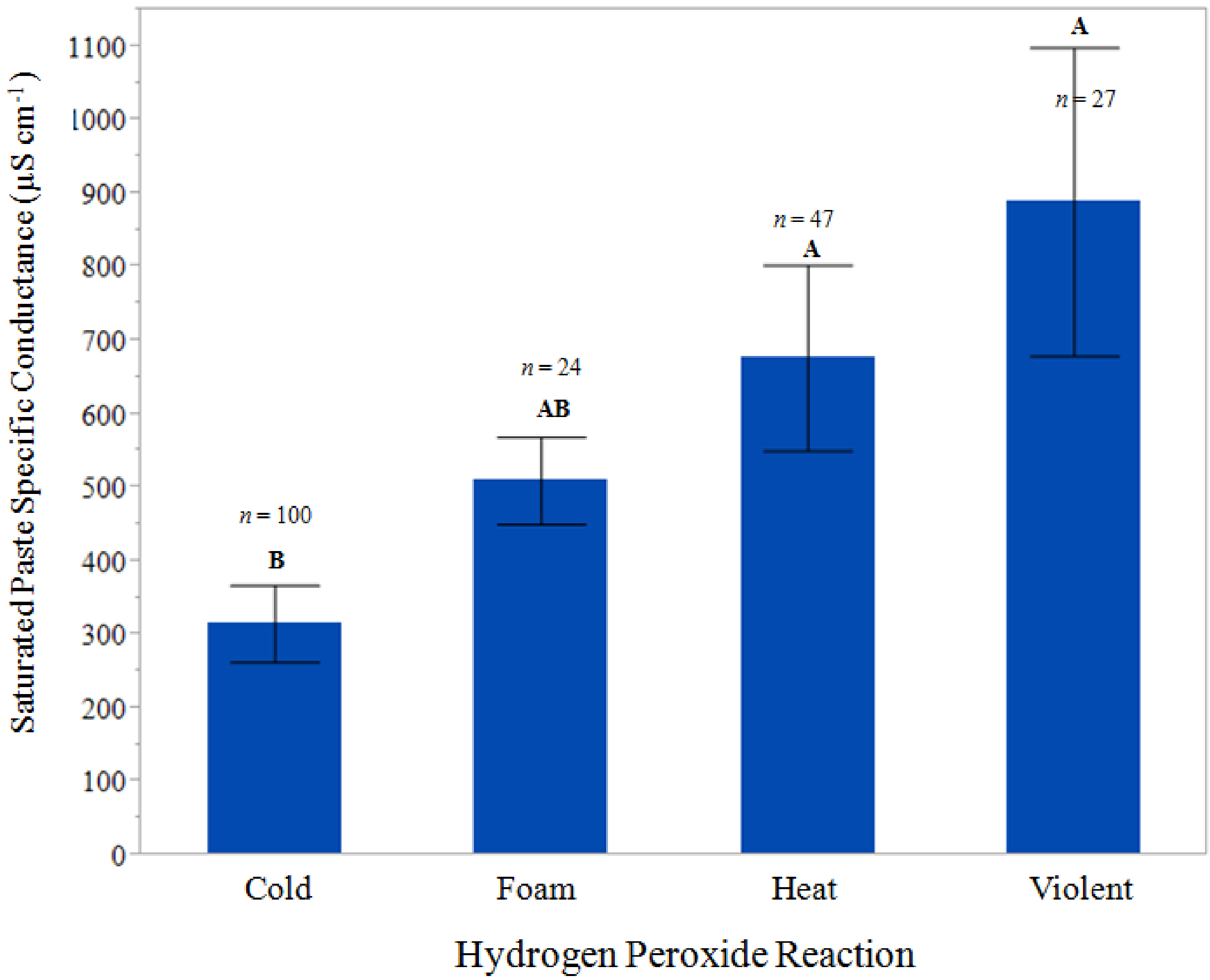

Figure 4.18. Saturated paste SC versus 30% H_2O_2 reaction for 198 soil and rock samples. Samples producing only bubbles and no heat were labeled "no reaction". Samples producing foam, but no heat were labeled "foam". Samples generating minor amounts of heat or steam were labeled "heat". Samples reacting vigorously, producing excess heat and/or a rolling boil were labeled as "violent". Error bars represent one standard error above and below the mean. Capital letters indicate means significantly different at $\alpha = 0.05$.

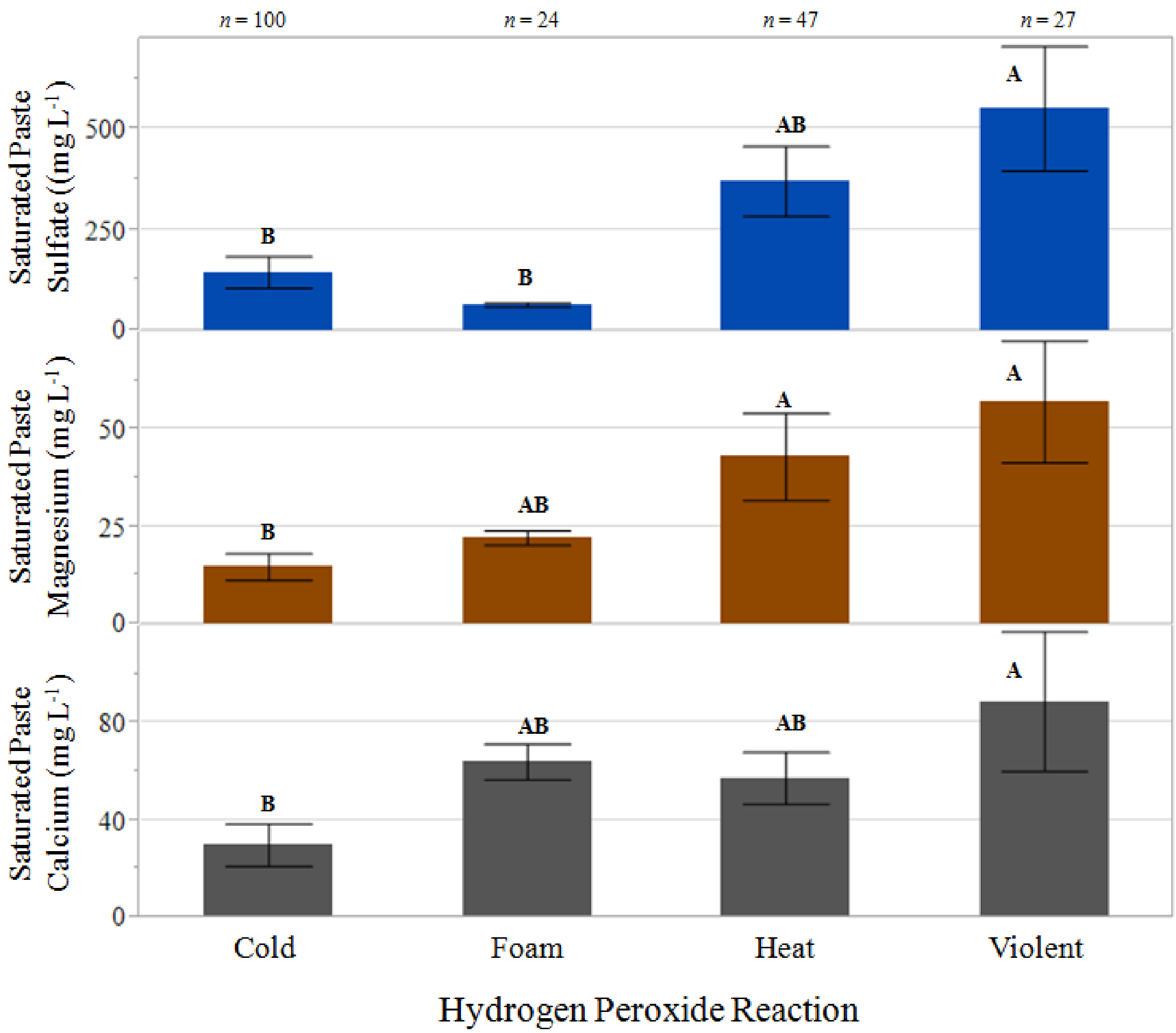

Figure. 4.19. Saturated paste Ca, Mg, and sulfate versus 30% H_2O_2 reaction for 198 soil and rock samples. Samples producing only bubbles and no heat were labeled "no reaction". Samples producing foam, but no heat were labeled "foam". Samples generating minor amounts of heat or steam were labeled "heat". Samples reacting vigorously, producing excess heat and/or a rolling boil were labeled as "violent". Error bars represent one standard error above and below the mean. Capital letters indicate means significantly different at $\alpha = 0.05$ for each element.

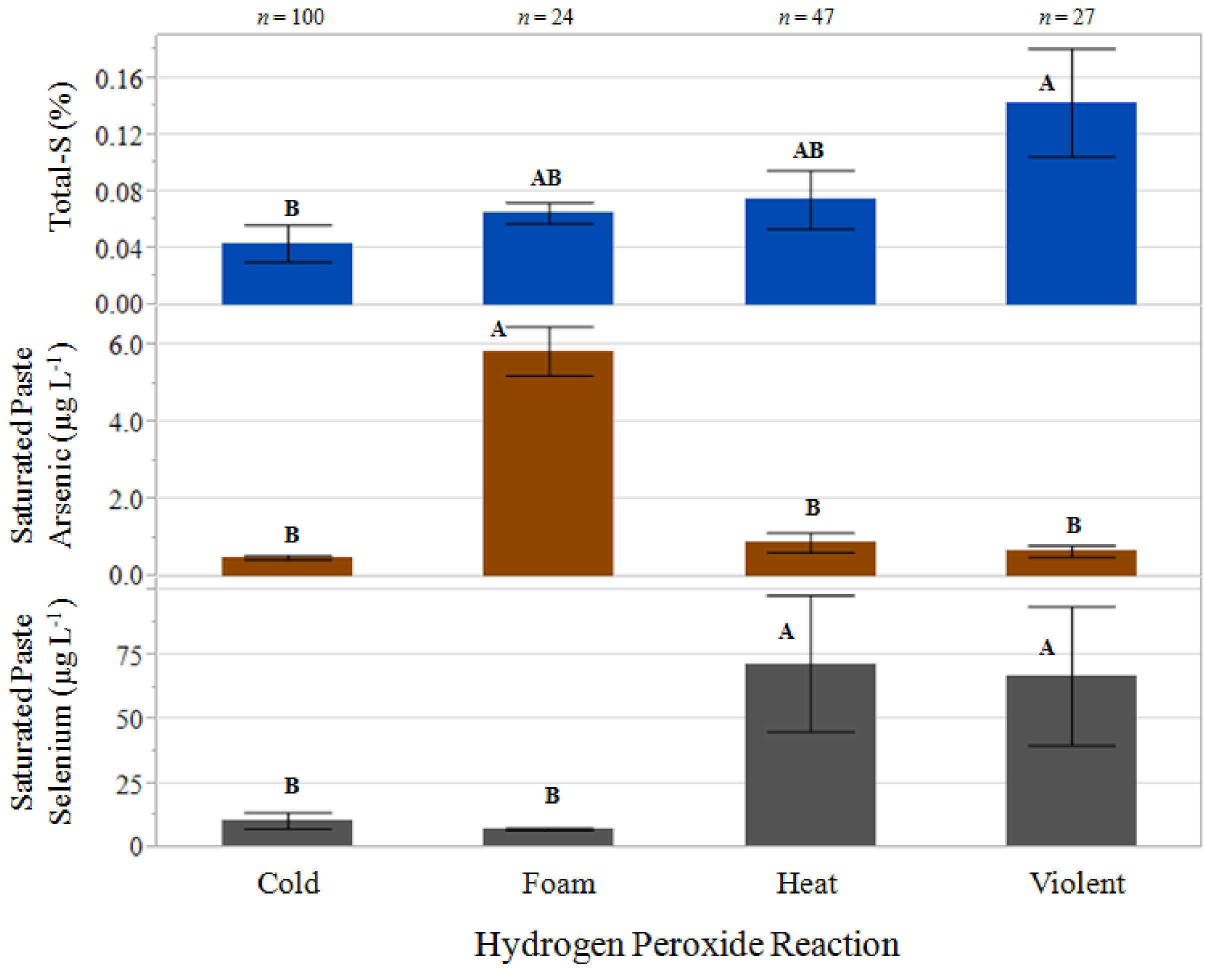

Figure. 4.20. Saturated paste As, Se, and total-S versus 30% H_2O_2 reaction for 198 soil and rock samples. Samples producing only bubbles and no heat were labeled "no reaction". Samples producing foam, but no heat were labeled "foam". Samples generating minor amounts of heat or steam were labeled "heat". Samples reacting vigorously, producing excess heat and/or a rolling boil were labeled as "violent". Error bars represent one standard error above and below the mean. Capital letters indicate means significantly different at $\alpha = 0.05$ for each element.

Conclusions

Many of the indicators tested turned out to be quite useful at predicting both specific ionic concentrations and overall SC. Munsell hue was insignificant, but value and chroma both had significant affects on Ca, Mg, SC, and sulfate. Low chroma, low value samples had significantly higher Ca, Mg, SC, and sulfate than high chroma, high value samples. Dark gray (4/1), very dark gray (3/1), and black (2/1) samples were significantly higher in Ca, Mg, SC, and sulfate than any other sample colors. Rock type also had a significant effect on saturated paste Ca, Mg, SC, sulfate, and Mg, and total-S. Overall SC and ion concentrations all generally decreased in the order of: coal > mudstone > shale > siltstone > sandstone > soil; however, Ca and Mg were highest in mudstones and shales. Sandstones were generally quartz rich subarkoses or sublitharenites as described in Chapter 3. Soil B horizon, C horizon, and weathered R layer samples were significantly lower in saturated paste HCO_3^-, Ca, Mg, SC, Se, and sulfate than samples from A horizons and unweathered R horizons; saturated paste As and P, however were highest in A horizons.

The transition between weathered and unweathered materials at most of the sites studied occurred abruptly at the fine-grained rock layer (i.e. mudstone or shale) nearest to the surface. The depth of weathering below the surface ranged from 0.7 m to 15.9 m across the sites and the average depth was 6.5 m. The weathered zones contained visible evidence of weathering, such as Fe- and Mn-oxide staining, transportation of soil materials downward, and generally yellowish brown colors from oxidation of Fe-bearing minerals; conversely, the unweathered zones showed signs of hydrologic isolation, like soluble salt accumulations, fossils, and low chroma (1-2), grayish colors. Calcium, Mg, SC, and sulfate were all significantly lower in weathered samples than unweathered samples, but As and CD-extractable Al, Fe, and Mn were all significantly higher in weathered samples. The HCl acid for the fizz test only reacted with 7 of the 204 samples, so it was of limited used for predicting TDS; however, samples reacting with the acid were significantly higher in CCE. Samples reacting to the H_2O_2 fizz test with heat or violent reaction had significantly higher levels of Ca, Mg, SC, Se, sulfate, and Total-S than samples not reacting or reacting with foam; meanwhile, samples producing foam had significantly higher levels of As than other samples.

These results generally confirm my initial hypotheses; a combination of one or more of the simple indicators presented here can be used to accurately predict overall TDS and specific ionic concentrations. Unweathered rocks, especially fine-grained rocks, rocks producing heat reactions with H_2O_2, and dark gray, very dark gray and black rocks should be considered high risk for TDS generation; the weathered rocks and soil occurring above should be considered low risk. This data reinforces the results of several previous TDS prediction studies with a much larger sample set and more detail on individual strata samples collected in situ pre-mining, rather than blasted spoils. In short, I recommend using a combination of weathering status, color, rock type, and reaction with H_2O_2 to produce the best prediction of TDS generation potential for a given spoil material.

References

American Petroleum Institute. 1998. The toxicity of common ions to freshwater and marine organisms. Document 0300–029. Washington, DC.

Agouridis, C. T., P. N. Angel, T. J. Taylor, C. D. Barton, R. C. Warner, X. Yu, and C. Wood. 2012. Water quality characteristics of discharge from reforested loose-dumped mine spoil in Eastern Kentucky. J. Environ. Qual. 41:454–468.

Bernhardt, E.S., and M. A. Palmer. 2011. The environmental costs of mountaintop mining valley fill operations for aquatic ecosystems of the Central Appalachians. Ann. N. Y. Acad. Sci. 1223, 39-57.

Bernhardt, E.S., Lutz, B.D., King, R.S., Fay, J.P., Carter, C.E., Helton, A.M., Campagna, D., and Amos, J. 2012. How many mountains can we mine? Assessing the regional degradation of central Appalachian rivers by surface coal mining. Environ. Sci. Technol. 46:8115-8122.

Borchers, J. W. and G. G. Wyrick. 1981. Application of stress-relief-fracturing concepts for monitoring the effects of surface mining on groundwater in Appalachian Plateau valleys. p. 443-449. *In* Proc., Nat. Symp. on Surface Mining Hydrology, Sedimentology, and Reclamation, Lexington, KY. 7-11 Dec. 1981. Univ. of Kentucky, Lexington, KY.

Burger, J., D. Graves, P. Angel, V. Davis and C. Zipper. 2005. The Forestry Reclamation Approach. App. Reg. Reforestation Init. (ARRI), Forest Reclamation Advisory No. 2. USDI Office of Surface Mining Reclamation and Enforcement, Pittsburgh. Available at http://arri.osmre.gov/FRA/Advisories/FRA_No.2.7-18-07.Revised.pdf

Daniels, W. L., C. E. Zipper, Z. W. Orndorff, J. Skousen, C. D. Barton, L. M. McDonald, and M. A. Beck. 2016. Predicting total dissolved solids release from Central Appalachian coal mine spoils. Environ. Poll. 216:371-379.

Griffith, M.B., S.B. Norton, L. C. Alexander, A. I. Pollard, and S. D. LeDuc. 2012. The effects of mountaintop mines and VFs on the physiochemical quality of stream ecosystems in the Central Appalachians: A review. Sci. Total Environ. 417-418: 1-12.

Goodfellow, W. L., L. W. Ausley, D. T. Burton, D. Denton, P. Dorn, D. Grothe, M. Heber, T. Norberg-King, and J. Rodgers. 2000. Major ion toxicity in effluents: A review with permitting recommendations. Env. Toxicol. Chem. 19: 175–182.

Hartman, K. J., M. D. Kaller, J. W. Howell, J. A. Sweka, 2005. How much do valley fills influence headwater streams? Hydrobiologia. 532: 91-102.

Howard, J.L. 1979. Physical, chemical, and mineralogical properties of mine spoil derived from the Wise Formation, Buchanan County. Virginia. M.S. Thesis, Va. Poly. Inst. & State Univ., Blacksburg, VA.

Kipp, J.A. and J.S. Dinger. 1987. Stress-relief fracture control of ground-water movement in the Appalachian Plateaus. p. 423-438 In: Proc, Fourth Annual Eastern Regional Ground Water Conference, Focus on Eastern Regional Ground Water Issues, July 14-16, 1987, Burlington, Vermont. The National Water Well Association. REPRINT 30, Series X1, 1991, KY Geological Survey, Lexington, KY.

Larsen, D. and R. Mann. 2005. Origin of high manganese concentrations in coal mine drainage, eastern Tennessee. J. Geochem. Explor. 86:143–163.

Lee, G., J.M. Bigham, and G. Faure. 2002. Removal of trace metals by coprecipitation with Fe, Al, and Mn from natural waters contaminated with acid mine drainage in the Ducktown Mining District, Tennessee. Appl. Geochem. 17(5):569−581.

Mack, B., J. Filbert, B. Gutta, P. Ziemkiewicz. 2013. Natural attenuation of TDS in mountaintop mines. p. 265-274 *In* Craynon, J.R. (Ed.), Environ. Considerations in Energy Prod. Society for Mining, Metallurgy, and Explor. Englewood, Colorado.

Mount, D. R., J. M. Gulley, J. R. Hockett, T. D. Garrison, and J. M. Evans. 1997. Statistical models to predict the toxicity of major ions to *Ceriodaphniadubia*, *Daphnia magna*, and fathead minnows (*Pimephalespromelas*). Environ. Toxicol. Chem. 16:2009-2019.

Odenheimer, J., J. Skousen, and L. McDonald. 2013. Predicting total dissolved solids release from overburden in Appalachian coal fields. pp. 255-264 In Craynon, J.R. (Ed.), Environmental Considerations in Energy Prod. Society for Mining, Metallurgy, and Exploration. Englewood, Colorado.

Odenheimer, J., J. Skousen, L.M. McDonald, D.J. Vesper, M. Mannix, and W. L. Daniels. 2014. Predicting release of total dissolved solids from overburden material using acid-base accounting parameters. Geochem. Explor. Env. A. 15: 131-137.

Orndorff, Z.W., W. L. Daniels, C.E. Zipper, M. Eick, and M. Beck. 2015. Column evaluation of Appalachian coal mine spoils' temporal leaching behavior. Environ. Poll. 204: 39-47.

Pond, G. J., M. E. Passmore, F. A. Borsuk, L. Reynolds, and C. J. Rose. 2008. Downstream effects of mountaintop coal mining: comparing biological conditions using family- and genus-level macroinvertebrate bioassessment tools. J. North Am. Benthol. Soc. 27:717–737.

Pond, G.J., M. E. Passmore, N.D. Pointon, J.K. Felbinger, C.A Walker, K.J. Krock, J.B. Fulton, W.L. Nash. 2014. Long-term impacts on macroinvertebrates downstream of reclaimed mountaintop mining valley fills in central Appalachia. Environ. Manag. 54: 919-933.

Schoeneberger, P.J., D.A. Wysocki, E.C. Benham, and Soil Survey Staff. 2012. Field book for describing and sampling soils, Version 3.0. Natural Resources Conservation Service, National Soil Survey Center, Lincoln, NE.

Skousen, J.G., A. Sexstone, P. F. Ziemkiewicz. 2000. Acid mine drainage control and treatment. p 131-168 *In* Barnhisel, R.I., et al. (Eds.), Reclamation of Drastically Disturbed Lands. Agronomy Mono. 621 No. 41. ASA-SSSA, Madison, WI, USA.

Skousen, J., J. Simmons, L.M. McDonald and P. Ziemkiewicz. 2002. Acid-base accounting to predict post-mining drainage quality on surface mines. J. Environ. Qual. 31:2034 - 2044.

Timpano, A. 2011. Levels of dissolved solids associated with aquatic life effects in headwater streams of Virginia's Central Appalachian coalfield region. M.S. Thesis, Va. Poly. Inst. & State Univ., Blacksburg, VA.

Toy, T.J. and W.L. Daniels. 1998. Reclamation of disturbed lands. P. 4078-4101 In R.A. Meyers (ed.). Encyclopedia of Environmental Analysis and Remediation. Wiley, New York.

USEPA (U.S. Environmental Protection Agency). 2005. Mountaintop mining/valley fills in Appalachia. Final programmatic environmental impact statement. U.S. Environmental Protection Agency, Region 3, Philadelphia, PA. Available at http://www.epa.gov/region3/mtntop/pdf/mtm-vf_fpeis_full-document.pdf.

USEPA (U.S. Environmental Protection Agency). 2011. The effects of mountaintop mines and valley fills on aquatic ecosystems of the Central Appalachian coalfields (2011 final). U.S. Environmental Protection Agency, Washington, DC. Available at http://cfpub.epa.gov/ncea/cfm/recordisplay.cfm?deid=225743

USGS (U.S. Geological Survey). 2012. Geologic maps of US states. Available at http://mrdata.usgs.gov/geology/state/.

Wunsch, D.R. 1993. Ground-water geochemistry and its relationship to the flow system at an unmined site in the eastern Kentucky coal field. Thesis series 5. Kentucky Geological Survey, Lexington, KY.

Chapter 5. Summary and Conclusions

This chapter provides an overall summary of the results of this research. The overall objective of this study was to develop a set of simple field and lab indicators that would assist field operators, regulators, consultants and researchers in the separation of low and high TDS generation potential mine spoils. Many of the simple indicators investigated were quite effective at distinguishing low from high TDS potential spoils and these results provide a valuable field guide to identifying and separating low and high TDS spoils. Below is an overall description of the various types of soils and geologic materials that were encountered throughout the study area and an associated summary of TDS prediction tools and their potential for field application.

Weathered Mantle

Soils

Weathered native soils in the Central Appalachians are a source of low SC mine spoil for use in reclamation. For this study, soils were differentiated from bedrock when they could no longer be dug through by hand with a shovel and were separated broadly into A (topsoil), B (subsoil), and C (soft, shovel diggable bedrock) horizons. Soil A horizons were significantly higher in SC than B and C horizons, but made up the lowest volume of material (generally < 15 cm thick) overall. Distinct C horizons were only found at a few of the sites and soils generally transitioned from B horizons directly into hard bedrock; few saprolitic materials were found at any of the study sites. On the other hand, B horizons were present at every site and nearly always were the lowest SC material available. The A horizons were generally brownish to blackish in color, while B and C horizons were generally yellowish brown. Thus, while A horizons are somewhat higher in SC than other soils layers, they are generally very thin and all combined soil layers in general are a good source of low SC material.

Brown, Weathered, Near-Surface Sandstones

Brown, weathered, near-surface sandstones, located in situ above any shale or mudstone layers, are also a source of low SC material. Increased exposure to groundwater flow and oxidation of sandstone strata near the surface results in a complex set of colorations in these layers from Fe and Mn staining, soil transportation downward, and the exposure of inclusions in the sandstones, such as lithic fragments. The dominant colors of these materials are yellowish brown, with many individual red, brown, and yellow colors (Figs. 5.1; 5.2). Weathered sandstones were found to be significantly lower in SC than any other rock strata studied. Both weathered and unweathered sandstones were generally quartz rich subarkoses or sublitharenites. Thus, brown, weathered sandstones found near the surface can reliably be used as a source of low SC reclamation material.

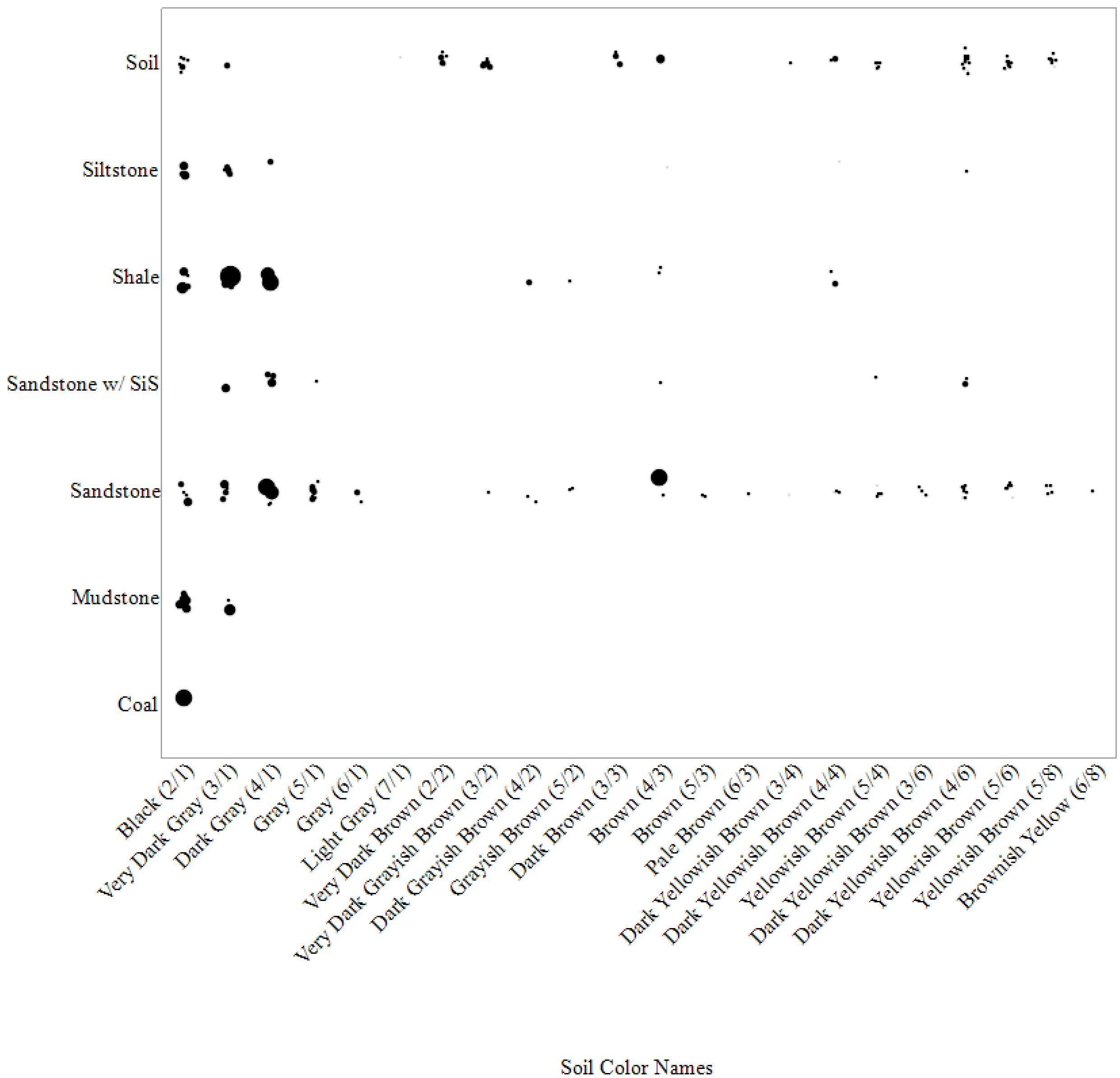

Figure 5.1. Effects of rock type and Munsell color (value / chroma) for all 204 samples, including outliers. The relative sizes of the bubbles represent relative saturated paste SC (i.e. small bubbles represent low SC samples and large bubbles represent high SC samples). The range of SC was from 23 µS cm^{-1} to 4,690 µS cm^{-1}. The mean and median SC were 503 µS cm^{-1} and 204 µS cm^{-1}, respectively. Black, very dark gray, and gray samples were generally higher in SC than other samples.

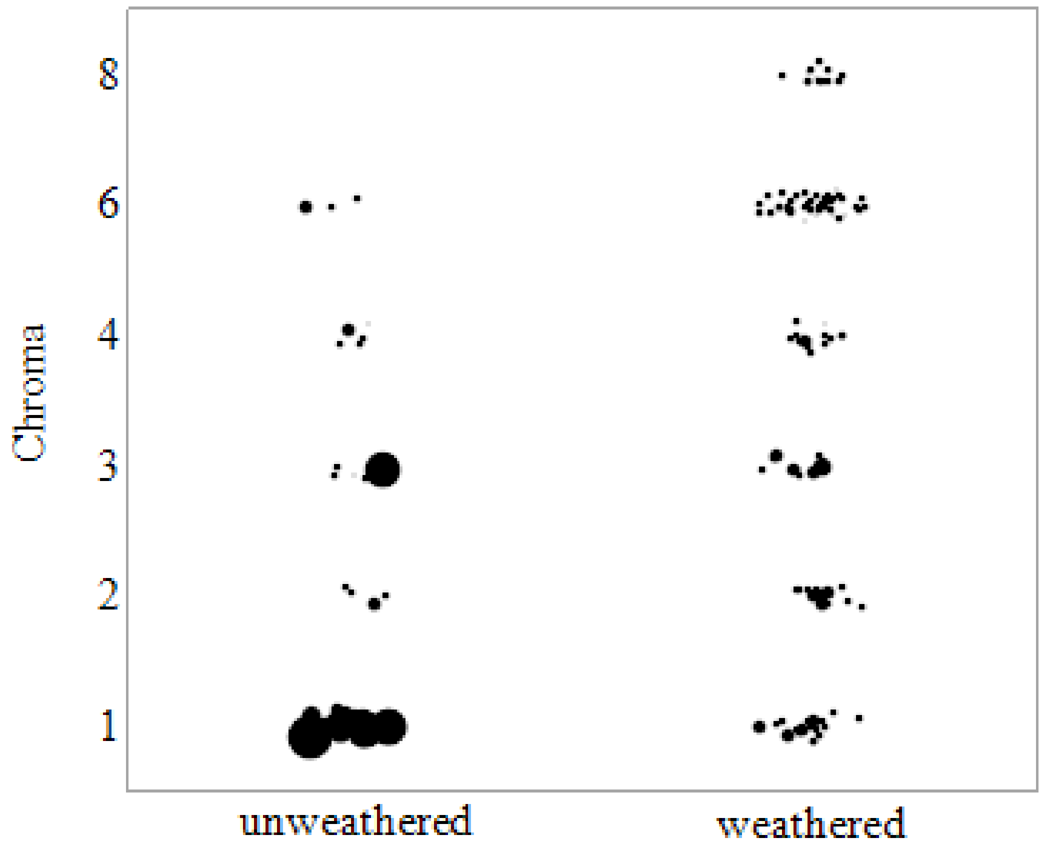

Figure 5.2. Effect of weathering status and Munsell chroma on saturated paste SC for all 204 samples, including outliers. The relative sizes of the bubbles represent relative saturated paste SC (i.e. small bubbles represent low SC samples and large bubbles represent high SC samples). The range of SC was from 23 µS cm^{-1} to 4,690 µS cm^{-1}. The mean and median SC were 503 µS cm^{-1} and 204 µS cm^{-1}, respectively. Unweathered samples with chroma 1 colors were generally higher in SC than other samples.

Underlying Materials

Gray, Unweathered Sandstones

Sandstones originating deeper below the surface, especially those below an intact shale or mudstone layer preventing downward water movement, were generally gray and potentially high in SC. Hydrologic isolation of these layers resulted in distinctly different properties than the sandstones above. Iron and Mn oxidation was minimal and most colors were uniformly grayish. Gray, unweathered sandstones were significantly higher in SC than weathered sandstones, but some gray, unweathered sandstones also produced low saturated paste SC values. The H_2O_2 reaction test discussed in Chapter 4 was effective at further differentiating between high and low SC for the unweathered sandstones (Fig. 5.3); many of the unweathered sandstones producing violent or heat reactions to the peroxide produced high SC while those that produced only bubbles or foam were mostly low in SC. The Virginia Tech Soil Testing Lab (VTSTL) plant available Mg rating was also effective at further differentiating between high and low TDS risk for unweathered bedrock strata (Fig. 5.4); nearly all of the unweathered samples that were high TDS risk had a Mg rating of very high (VH). As mentioned above, both weathered and unweathered sandstones were generally quartz rich subarkoses or sublitharenites. Thus, gray, unweathered sandstones in the study area are generally higher in SC than brown, weathered sandstones; however, some unweathered sandstones do produce low SC.

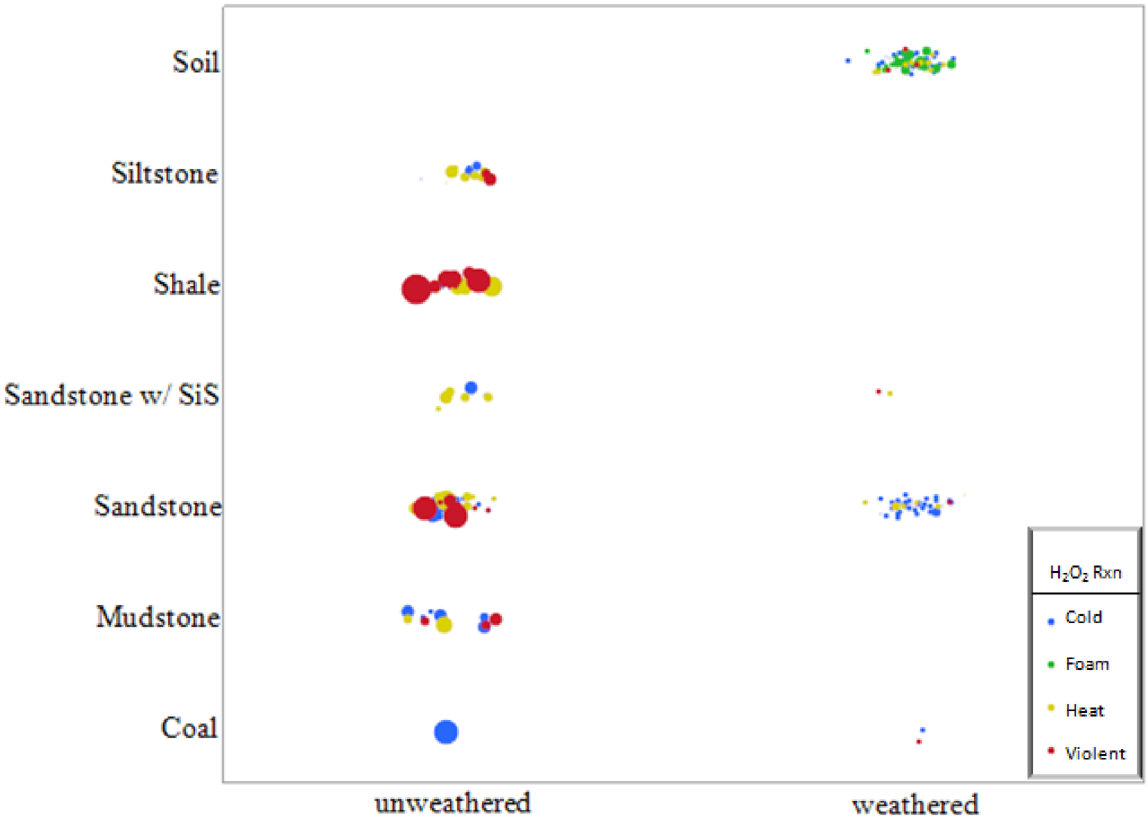

Figure 5.3. Effect of rock type, weathering status, and H_2O_2 reaction on saturated paste SC for all 204 samples, including outliers. The relative sizes of the bubbles represent relative saturated paste SC (i.e. small bubbles represent low SC samples and large bubbles represent high SC samples). The range of SC was from 23 µS cm^{-1} to 4,690 µS cm^{-1}. The mean and median SC were 503 µS cm^{-1} and 204 µS cm^{-1}, respectively. 30% H_2O_2 reaction indicated by color; blue= cold, green = foam, yellow = heat, and red = violent. Unweathered samples reacting with heat or violently to the H_2O_2 were generally higher in SC than other unweathered samples.

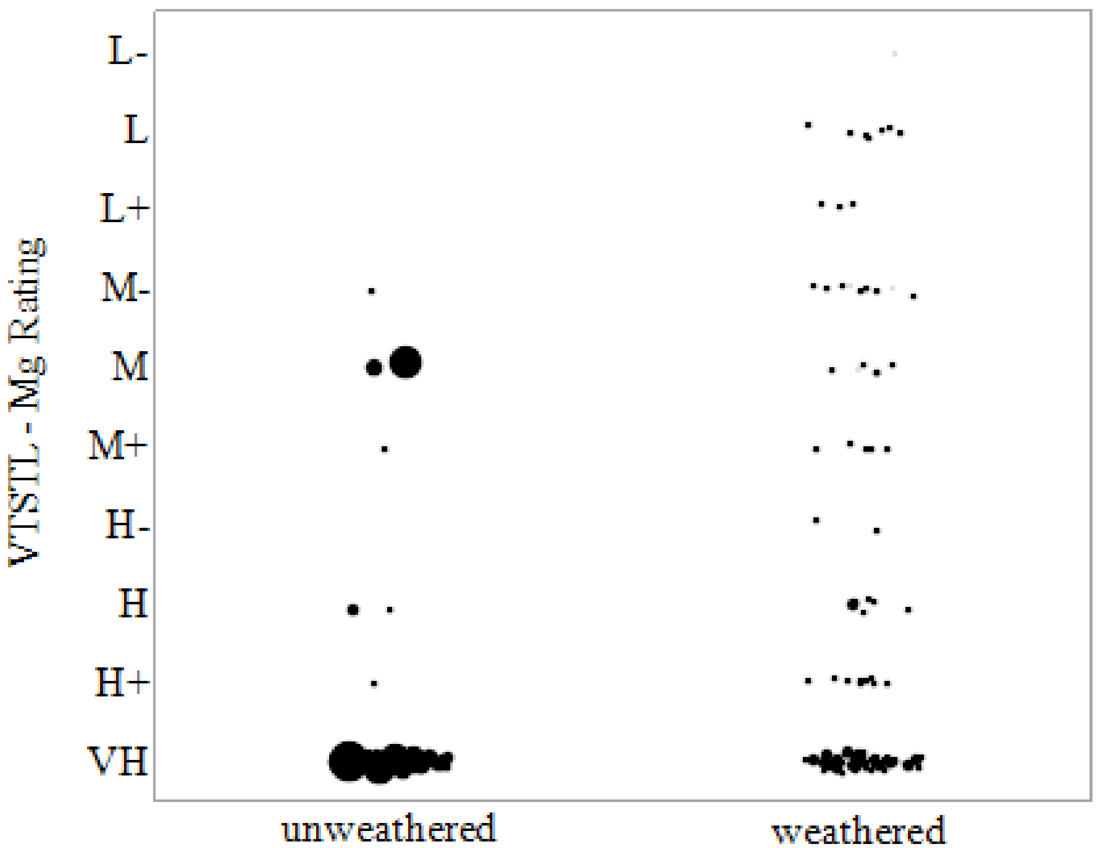

Figure 5.4. Effect of weathering status and Virginia Tech Soil Testing Lab (VTSTL) Mg rating on saturated paste SC for all 204 samples, including outliers. The relative sizes of the bubbles represent relative saturated paste SC (i.e. small bubbles represent low SC samples and large bubbles represent high SC samples). The range of SC was from 23 µS cm^{-1} to 4,690 µS cm^{-1}. The mean and median SC were 503 µS cm^{-1} and 204 µS cm^{-1}, respectively. VTSTL Mg ratings: L = low, M = medium, H = high, and VH = very high. Unweathered samples rated as very high (VH) for Mg were generally higher in SC than other unweathered samples.

Shales, Siltstones, and Mudstones

Fine-grained rocks produced significantly higher SC levels than sandstones and generally followed the sequence of mudstone > shale > siltstone. Mudstones were either very dark gray or black and significantly higher SC than any of the other rock types (except coal and associated materials). Siltstones were similar in color, often being black, very dark gray, or dark gray, but were moderate in SC. Shales ranged in color and SC, but generally brownish shales were low in SC and black, very dark gray, and dark gray shales were moderate to very high in SC. Fractured, near-surface, fine-grained layers that would have been deemed "weathered", per the convention for sandstones discussed above, had generally weathered to the extent that they were able to be dug by shovel. Therefore, these materials were included as "soil" samples and not reported as siltstone, mudstone, or shale. These degraded layers formed the only saprolitic C horizons found in the study area and were generally lower in SC than similar rock types in an unweathered state. Thus, brown shales and saprolites are generally low in SC, but most other fine-grained rocks are moderate to high in SC.

Coals, Fireclays, Underclays, Flint Clays, and Other Coal Associated Materials

Coal beds commonly occurred in the study area in conjunction with other thin strata, described by many local names, such as fireclay, underclay, flint clay, mudrock, mudstone, or black shale. Coal and all of these associated materials are generally very high SC and should be considered "hot" with respect to SC. The coal associated materials are all dark in color, commonly contain plant fossils, and occur directly above, between, or below coal beds. These layers are often small in volume compared to the total overburden removed, so extra effort focused towards identifying and isolating these layers will be particularly rewarding in the effort to reduce overall mine site

TDS elution. In short, coal, fireclays, flint clays, underclays, and associated materials are all very high SC and should be handled separately and isolated from surface or subsurface flow whenever possible.

Conclusions

The central Appalachian mine spoils studied were found to vary significantly in geochemical properties and several of the predictors for TDS evaluated in this study turned out to be quite useful, such as chroma, color, weathering status, VTSTL Mg rating, rock type, and H_2O_2 reaction. Significant differences in both overall TDS risk and in individual ionic concentrations were detected between individual samples, but no differences were found between sites. Overall saturated paste extract solutions were dominated by sulfate, but Ca and Mg were also significant contributors. Yellowish-brown sandstones and soil materials were low in saturated paste SC and high in CD-extractable Al, Fe, and Mn, compared to the underlying grayish to black sandstones, shales, and mudstones, which were higher in saturated paste SC and lower in CD-extractable Al, Fe, and Mn. Selenium was significantly lower in soil and weathered bedrock than unweathered bedrock. Soil A horizons were significantly higher in As than B horizons, C horizons, or bedrock layers. Magnesium, SC, Se, and sulfate were all significantly higher in samples that reacted with heat or violently to H_2O_2.

None of the predictors studied here were an absolute indicator of SC production risk by themselves, but several different combinations of indicators proved quite effective at separating low and high SC spoils. Weathering status and chroma make a simple, but effective combination. Weathering status, rock type, and H_2O_2 reaction also make a reliable combination and improve overall discrimination ability for both SC and Se risk. Weathering status and the VTSTL Mg rating make an even better combination for predicting overall TDS risk, but this would require shipping samples to a soil testing lab. When weathering status is unknown, color and rock type alone make a suitable combination for prediction TDS risk.

Handling techniques similar to those used with acid forming materials are recommended to hydrologically isolate especially high TDS risk spoils and these include gray to black mudstones and shales, coals, and coal associated shales, mudstones, and clays directly associated with coal seams. Yellowish-brown surficial soil and sandstone layers are recommended as a source of low TDS fill for use in areas with significant contact with rainwater or groundwater. Harder, low TDS risk sandstones are recommended (when available) for rock drains and other direct water contact applications.

In summary, there were relatively few high TDS risk materials in my sample set and these originated from strata that were thin in comparison to the overall amount of overburden removed; the field indicators described here were effective at distinguishing those strata. Identification and special handling of high TDS risk strata should be an effective means of reducing overall mine site TDS elution. These results provide a guide for identifying low and high TDS strata pre-mining, which can allow operators to effectively manage materials for TDS risk.

Appendix A. Weathering sequence field descriptions.

Site ID	Sample ID	Horizon Name	Depth (meters)	Rock Type	Coarse Fragment Type	Weathering Status	Value	Chroma	HCl Reaction	H_2O_2 Reaction
1	**1**	A+E	0.3	Soil	Soil <1% Rocks	weathered	2	1	0	foam
1	**2**	Bt	1.0	Soil	Sandstone	weathered	5	6	0	cold
1	**3**	Bt	1.5	Soil	Siltstone	weathered	5	6	0	heat
1	**4**	Bt	2.4	Soil	Soil <1% Rocks	weathered	5	8	0	cold
1	**5**	Bt	2.9	Soil	Soil <1% Rocks	weathered	7	1	0	cold
1	**6**	C	3.1	Soil	Coal	weathered	2	1	0	violent
1	**7**	C	3.4	Soil	Coal	weathered	2	1	0	violent
1	**8**	Cr	3.7	Soil	Soil <1% Rocks	weathered	5	4	0	cold
1	**9**	Cr	4.9	Soil	Soil <1% Rocks	weathered	5	6	0	cold
1	**10**	R1	6.1	Sandstone	Sandstone	weathered	4	2	3	heat
1	**11**	R2	10.1	Sandstone	Sandstone	weathered	4	1	3	cold
1	**12**	R3	11.9	Sandstone	Sandstone	weathered	5	1	0	cold
1	**13**	R4	13.7	Sandstone	Sandstone	weathered	5	6	0	heat
1	**14**	R5	15.9	Sandstone	Sandstone	weathered	4	2	0	cold
1	**15**	R6	16.8	Shale	Shale	unweathered	3	1	0	heat
1	**16**	R7	21.6	Sandstone	Sandstone	unweathered	4	1	0	heat
1	**17**	R8	30.8	Sandstone	Sandstone	unweathered	3	1	0	heat
1	**18**	R9	39.9	Sandstone w/ SiS	Sandstone w/ SiS	unweathered	4	1	3	heat
1	**19**	R10	69.2	Shale	Shale	unweathered	3	1	2	heat
1	**20**	R11	69.2	Sandstone w/ SiS	Sandstone w/ SiS	unweathered	4	1	2	heat
2a	**1**	A	0.0	Soil	Sandstone	weathered	3	1	0	foam
2a	**2**	AB	0.2	Soil	Sandstone	weathered	4	3	0	heat
2a	**3**	Bw1	0.5	Soil	Sandstone	weathered	4	6	0	heat
2a	**4**	Bw2	0.7	Soil	Soil <1% Rocks	weathered	4	6	0	heat
2a	**5**	R1	6.0	Sandstone	Sandstone	weathered	5	6	0	heat
2a	**6**	R2	14.0	Sandstone	Sandstone	weathered	5	4	0	cold
2a	**7**	R3	19.0	Mudstone	Mudstone	unweathered	2	1	0	cold

Site ID	Sample ID	Horizon Name	Depth (meters)	Rock Type	Coarse Fragment Type	Weathering Status	Value	Chroma	HCl Reaction	H_2O_2 Reaction
2a	**8**	R4	19.0	Sandstone	Sandstone	unweathered	3	1	0	cold
2b	**1**	A	0.1	Soil	Sandstone	weathered	3	1	0	foam
2b	**2**	Bw1	1.0	Soil	Sandstone	weathered	5	8	0	cold
2b	**3**	Bw2	1.5	Soil	Sandstone	weathered	5	8	0	heat
2b	**4**	R1	6.0	Sandstone	Sandstone	weathered	5	6	0	violent
2b	**5**	R2	14.0	Sandstone	Sandstone	weathered	5	6	0	cold
2b	**6**	R3	19.0	Mudstone	Mudstone	unweathered	2	1	0	cold
2b	**7**	R4	19.0	Sandstone	Sandstone	unweathered	4	1	0	cold
2c	**1**	A	0.1	Soil	Sandstone	weathered	3	1	0	foam
2c	**2**	Bw	0.8	Soil	Sandstone	weathered	5	8	0	cold
2c	**3**	R1	1.8	Sandstone	Sandstone	weathered	6	6	0	cold
2c	**4**	R2	2.8	Sandstone	Sandstone	weathered	4	4	0	cold
2c	**5**	R3	6.0	Sandstone w/ SiS	Sandstone w/ SiS	weathered	4	3	0	heat
2c	**6**	R4	7.0	Mudstone	Mudstone	unweathered	2	1	0	violent
2c	**7**	R5	8.0	Mudstone	Mudstone	unweathered	2	1	2	violent
2c	**8**	R6	8.0	Siltstone	Siltstone	unweathered	3	1	0	heat
3	**1**	A	0.1	Soil	Soil <1% Rocks	weathered	3	2	0	foam
3	**2**	Bt	0.4	Soil	Sandstone	weathered	5	6	0	cold
3	**3**	BC	0.7	Soil	Siltstone	weathered	4	6	0	cold
3	**4**	Cr	1.7	Soil	Siltstone	weathered	5	4	0	cold
3	**5**	R1	12.9	Sandstone	Sandstone	weathered	5	8	0	cold
3	**6**	R2	19.0	Mudstone	Mudstone	unweathered	2	1	0	cold
3	**7**	R3	23.0	Mudstone	Mudstone	unweathered	2	1	0	cold
4a	**1**	A	0.0	Soil	Siltstone	weathered	2	2	0	foam
4a	**2**	Bw	1.5	Soil	Siltstone	weathered	5	6	0	cold
4a	**3**	R1	3.5	Sandstone	Sandstone	weathered	2	1	0	heat
4a	**4**	R2	3.9	Coal	Coal	weathered	2	1	0	violent
4a	**5**	R3	3.9	Shale	Shale	unweathered	2	1	0	violent

Site ID	Sample ID	Horizon Name	Depth (meters)	Rock Type	Coarse Fragment Type	Weathering Status	Value	Chroma	HCl Reaction	H_2O_2 Reaction
4b	**1**	A	0.0	Soil	Soil <1% Rocks	weathered	2	1	0	heat
4b	**2**	Bw	1.3	Soil	Siltstone	weathered	5	6	0	cold
4b	**3**	R1	3.3	Sandstone	Sandstone	weathered	4	6	0	cold
4b	**4**	R2	3.8	Sandstone	Sandstone	weathered	4	6	0	cold
4b	**5**	R3	3.8	Siltstone	Siltstone	unweathered	3	1	0	cold
4c	**1**	A	0.0	Soil	Sandstone	weathered	2	1	0	foam
4c	**2**	Bw	1.4	Soil	Sandstone	weathered	5	6	0	cold
4c	**3**	R1	9.0	Sandstone	Sandstone	weathered	4	6	0	cold
4c	**4**	R2	9.8	Shale	Shale	unweathered	3	1	0	heat
4c	**5**	R3	9.8	Sandstone	Sandstone	unweathered	2	1	0	cold
5	**1**	Bw	0.4	Soil	Siltstone	weathered	4	6	0	heat
5	**2**	C1	0.5	Soil	Coal	weathered	3	2	0	violent
5	**3**	C2	1.5	Soil	Coal	weathered	5	8	0	heat
5	**4**	C3	3.0	Soil	Soil <1% Rocks	weathered	5	8	0	cold
5	**5**	R1	4.5	Mudstone	Mudstone	unweathered	3	1	0	heat
5	**6**	R2	7.5	Siltstone	Siltstone	unweathered	3	1	0	cold
6	**1**	Bw	2.0	Soil	Sandstone w/ SiS	weathered	4	6	0	cold
6	**2**	R1	3.0	Sandstone	Sandstone	weathered	5	8	0	cold
6	**3**	R2	5.0	Sandstone	Sandstone	weathered	3	2	0	cold
6	**4**	R3	10.0	Sandstone	Sandstone	weathered	6	1	0	cold
6	**6**	R4	17.5	Sandstone	Sandstone	unweathered	5	1	0	cold
7	**1**	A	0.1	Soil	Sandstone	weathered	2	1	0	foam
7	**2**	Bw	0.3	Soil	Sandstone	weathered	5	6	0	cold
7	**3**	R1	1.0	Sandstone	Sandstone	weathered	5	8	0	cold
7	**4**	R2	1.8	Coal	Coal	weathered	2	1	0	cold
7	**5**	R3	3.3	Siltstone	Siltstone	unweathered	4	6	0	heat
7	**6**	R4	7.0	Sandstone	Sandstone	unweathered	5	1	0	cold
8	**1**	A	0.2	Soil	Soil <1% Rocks	weathered	3	2	0	foam

Site ID	Sample ID	Horizon Name	Depth (meters)	Rock Type	Coarse Fragment Type	Weathering Status	Value	Chroma	HCl Reaction	H_2O_2 Reaction
8	**2**	Bt	0.8	Soil	Soil <1% Rocks	weathered	4	6	0	heat
8	**3**	BC	1.3	Soil	Sandstone	weathered	5	6	0	cold
8	**4**	R1	3.0	Sandstone	Sandstone	weathered	2	1	0	cold
8	**5**	R2	4.5	Mudstone	Mudstone	unweathered	3	1	0	cold
8	**6**	R3	7.5	Sandstone	Sandstone	unweathered	2	1	0	cold
9	**2**	R1	10.0	Sandstone	Sandstone	weathered	4	6	0	cold
9	**3**	R2	20.0	Sandstone	Sandstone	weathered	6	1	0	cold
10	**1**	A	0.1	Soil	Sandstone	weathered	3	2	0	foam
10	**2**	Bt	1.1	Soil	Sandstone	weathered	5	8	0	cold
10	**3**	Cr	2.1	Soil	Sandstone	weathered	4	6	0	cold
10	**4**	R1	3.6	Sandstone	Sandstone	weathered	5	6	0	cold
10	**5**	R2	5.0	Shale	Shale	unweathered	4	4	0	cold
10	**6**	R3	5.0	Coal	Coal	unweathered	2	1	0	cold
11	**1**	A	0.1	Soil	Sandstone	weathered	2	2	0	foam
11	**2**	Bt	1.1	Soil	Sandstone	weathered	5	8	0	cold
11	**3**	R1	2.5	Sandstone	Sandstone	weathered	6	3	0	cold
11	**4**	R2	2.5	Shale	Shale	unweathered	5	2	0	cold
12	**1**	A	0.1	Soil	Sandstone	weathered	3	2	0	foam
12	**2**	Bw	0.8	Soil	Sandstone	weathered	4	6	0	heat
12	**3**	R1	6.8	Sandstone	Sandstone	weathered	5	4	0	cold
12	**5**	R3	7.0	Sandstone	Sandstone	unweathered	5	2	0	cold
13	**1**	A+E	0.1	Soil	Sandstone	weathered	2	2	0	foam
13	**2**	Bw	0.7	Soil	Sandstone	weathered	5	8	0	cold
13	**3**	R1	20.7	Sandstone w/ SiS	Sandstone w/ SiS	unweathered	4	6	0	heat
13	**4**	R2	20.7	Sandstone	Sandstone	unweathered	5	1	0	cold
14	**1**	A	0.1	Soil	Sandstone	weathered	2	2	0	foam
14	**2**	B	1.5	Soil	Sandstone	weathered	5	6	0	cold
14	**4**	R1	4.5	Sandstone	Sandstone	weathered	5	4	0	cold

Site ID	Sample ID	Horizon Name	Depth (meters)	Rock Type	Coarse Fragment Type	Weathering Status	Value	Chroma	HCl Reaction	H_2O_2 Reaction
14	**5**	R2	11.5	Sandstone	Sandstone	weathered	5	3	0	cold
14	**6**	R3	14.0	Mudstone	Mudstone	unweathered	2	1	0	heat
14	**7**	R4	16.5	Sandstone	Sandstone	unweathered	3	1	0	heat
15	**1**	A	0.1	Soil	Sandstone	weathered	2	1	0	foam
15	**2**	B	1.0	Soil	Sandstone	weathered	4	6	0	cold
15	**3**	R1	3.0	Sandstone	Sandstone	weathered	3	4	0	cold
15	**4**	R2	4.0	Shale	Shale	unweathered	2	1	0	violent
15	**5**	R3	6.0	Shale	Shale	unweathered	4	4	0	cold
15	**7**	R5	45.0	Sandstone	Sandstone	unweathered	5	1	0	cold
16	**1**	A	0.1	Soil	Sandstone	weathered	2	2	0	foam
16	**2**	B	0.8	Soil	Sandstone	weathered	4	4	0	cold
16	**3**	R1	6.0	Sandstone	Sandstone	weathered	4	4	0	violent
16	**5**	R3	8.5	Shale	Shale	unweathered	4	3	0	cold
16	**6**	R4	14.5	Sandstone	Sandstone	unweathered	5	2	0	cold
17	**3**	R1	3.8	Sandstone	Sandstone	weathered	5	6	0	violent
17	**4**	R2	5.9	Sandstone	Sandstone	weathered	5	4	0	cold
17	**5**	R3	6.2	Sandstone	Sandstone	weathered	5	1	0	heat
17	**6**	R4	7.9	Sandstone w/ SiS	Sandstone w/ SiS	weathered	4	6	0	violent
17	**7**	R5	8.8	Sandstone	Sandstone	weathered	5	1	0	cold
17	**9**	R7	9.3	Shale	Shale	unweathered	3	1	0	heat
17	**10**	R8	9.6	Sandstone w/ SiS	Sandstone w/ SiS	unweathered	4	1	0	cold
17	**11**	R9	22.7	Sandstone w/ SiS	Sandstone w/ SiS	unweathered	5	4	0	cold
17	**12**	R10	23.5	Sandstone	Sandstone	unweathered	4	1	0	cold
17	**13**	R11	24.1	Sandstone	Sandstone	unweathered	5	3	0	cold
17	**14**	R12	26.2	Sandstone	Sandstone	unweathered	4	1	0	cold
17	**15**	R13	30.5	Sandstone w/ SiS	Sandstone w/ SiS	unweathered	3	1	0	heat
18	**3**	R1	6.2	Sandstone	Sandstone	unweathered	4	1	0	heat
18	**4**	R2	6.6	Shale	Shale	unweathered	4	1	0	heat

Site ID	Sample ID	Horizon Name	Depth (meters)	Rock Type	Coarse Fragment Type	Weathering Status	Value	Chroma	HCl Reaction	H_2O_2 Reaction
18	**5**	R3	6.9	Sandstone	Sandstone	unweathered	4	3	0	violent
18	**6**	R4	8.2	Sandstone	Sandstone	unweathered	4	1	0	violent
18	**7**	R5	8.5	Sandstone	Sandstone	unweathered	4	4	0	violent
18	**8**	R6	9.4	Sandstone	Sandstone	unweathered	4	1	0	heat
18	**9**	R7	9.6	Sandstone	Sandstone	unweathered	4	1	0	heat
18	**10**	R8	15.2	Shale	Shale	unweathered	4	1	1	violent
18	**11**	R9	15.8	Shale	Shale	unweathered	3	1	0	violent
18	**12**	R10	16.5	Sandstone	Sandstone	unweathered	4	1	0	violent
19	**3**	R1	7.9	Shale	Shale	unweathered	4	3	0	violent
19	**4**	R2	9.1	Shale	Shale	unweathered	4	2	0	violent
19	**5**	R3	12.2	Shale	Shale	unweathered	3	1	0	heat
19	**6**	R4	15.2	Shale	Shale	unweathered	3	1	0	violent
19	**7**	R5	18.3	Shale	Shale	unweathered	2	1	0	violent
20	**3**	R1	8.2	Shale	Shale	unweathered	4	1	0	violent
20	**4**	R2	8.5	Sandstone	Sandstone	unweathered	4	3	0	violent
20	**5**	R3	10.2	Sandstone	Sandstone	unweathered	5	1	0	violent
20	**6**	R4	12.2	Sandstone	Sandstone	unweathered	4	6	0	violent
21a	**1**	A	0.1	Soil	Soil <1% Rocks	weathered	3	3	0	foam
21a	**2**	Bw	1.2	Soil	Soil <1% Rocks	weathered	4	6	0	cold
21a	**3**	R1	5.8	Sandstone	Sandstone	weathered	4	6	0	cold
21a	**4**	R2	8.8	Siltstone	Siltstone	unweathered	2	1	0	violent
21a	**5**	R3	16.8	Siltstone	Siltstone	unweathered	2	1	0	heat
21a	**6**	R4	24.4	Sandstone	Sandstone	unweathered	4	1	0	cold
21a	**7**	R5	5.8	Mudstone	Mudstone	unweathered	2	1	0	cold
21b	**1**	A	0.1	Soil	Soil <1% Rocks	weathered	3	2	0	foam
21b	**2**	Bw	1.2	Soil	Soil <1% Rocks	weathered	4	6	0	cold
21b	**3**	R1	6.7	Sandstone	Sandstone	weathered	5	8	0	cold
21b	**4**	R2	12.2	Siltstone	Siltstone	unweathered	2	1	0	heat

Site ID	Sample ID	Horizon Name	Depth (meters)	Rock Type	Coarse Fragment Type	Weathering Status	Value	Chroma	HCl Reaction	H_2O_2 Reaction
21b	**5**	R3	12.2	Sandstone	Sandstone	unweathered	4	1	0	cold
21c	**1**	A	0.1	Soil	Soil <1% Rocks	weathered	3	3	0	foam
21c	**2**	Bw	1.2	Soil	Soil <1% Rocks	weathered	5	4	0	cold
21c	**3**	R1	6.7	Sandstone	Sandstone	weathered	4	6	0	cold
21c	**4**	R2	12.2	Siltstone	Siltstone	unweathered	2	1	0	heat
21c	**5**	R3	12.2	Sandstone	Sandstone	unweathered	3	1	0	heat
22a	**1**	A	0.3	Soil	Soil <1% Rocks	weathered	4	3	0	foam
22a	**2**	Bt	1.3	Soil	Soil <1% Rocks	weathered	5	4	0	cold
22a	**3**	R1	4.9	Sandstone	Sandstone	weathered	3	6	0	cold
22a	**4**	R2	10.7	Siltstone	Siltstone	unweathered	3	1	0	cold
22a	**5**	R3	30.5	Sandstone	Sandstone	unweathered	4	1	0	cold
22b	**1**	A	0.3	Soil	Soil <1% Rocks	weathered	4	3	0	foam
22b	**2**	Bt	1.3	Soil	Soil <1% Rocks	weathered	4	6	0	cold
22b	**3**	R1	4.9	Sandstone	Sandstone	weathered	3	6	0	cold
22b	**4**	R2	10.7	Siltstone	Siltstone	unweathered	3	1	0	heat
22b	**5**	R3	30.5	Sandstone	Sandstone	unweathered	4	1	0	cold
22c	**1**	A	0.3	Soil	Soil <1% Rocks	weathered	4	4	0	foam
22c	**2**	Bt	1.3	Soil	Soil <1% Rocks	weathered	5	4	0	cold
22c	**3**	R1	4.9	Sandstone	Sandstone	weathered	3	6	0	cold
22c	**4**	R2	10.7	Siltstone	Siltstone	unweathered	2	1	0	heat
22c	**5**	R3	30.5	Sandstone	Sandstone	unweathered	4	1	0	violent
23	**1**	A	0.1	Soil	Sandstone	weathered	3	4	0	foam
23	**2**	Bt	0.9	Soil	Sandstone	weathered	5	8	0	cold
23	**4**	R1	8.2	Sandstone	Sandstone	weathered	5	6	0	heat
23	**5**	R2	9.1	Siltstone	Siltstone	unweathered	4	4	0	cold
23	**6**	R3	15.2	Sandstone	Sandstone	unweathered	5	1	0	heat
23	**7**	R4	15.2	Mudstone	Mudstone	unweathered	2	1	0	violent
24	**1**	A	0.2	Soil	Sandstone	weathered	3	3	0	foam

Site ID	Sample ID	Horizon Name	Depth (meters)	Rock Type	Coarse Fragment Type	Weathering Status	Value	Chroma	HCl Reaction	H_2O_2 Reaction
24	**2**	Bw	1.5	Soil	Siltstone	weathered	5	6	0	cold
24	**3**	R1	3.0	Siltstone	Siltstone	unweathered	4	3	0	heat
24	**4**	R2	9.1	Shale	Shale	unweathered	2	1	0	heat
24	**5**	R3	16.8	Siltstone	Siltstone	unweathered	4	1	0	violent
24	**6**	R4	16.8	Shale	Shale	unweathered	2	1	0	violent
25	**2**	Bt	1.2	Soil	Sandstone	weathered	5	8	0	cold
25	**3**	R1	6.7	Sandstone	Sandstone	weathered	4	6	0	cold
25	**4**	R2	9.1	Sandstone w/ SiS	Sandstone w/ SiS	unweathered	5	1	0	heat
25	**5**	R3	30.5	Sandstone	Sandstone	unweathered	5	1	0	heat

Appendix B. Geochemistry results.

Site	ID	Paste SC (μS cm^{-1})	Paste pH	1:1 SC (dS m^{-1})	1:1 pH	1:1 Peroxide pH	1:1 Peroxide SC (dS m^{-1})	Total S (%)	CCE (%)	CD - Fe (mg kg^{-1})	CD - Al (mg kg^{-1})	CD - Mn (mg kg^{-1})
1	**1**	279	4.10	0.12	4.15	4.05	0.27	0.16	1.95	2155.0	10058.2	2642.8
1	**2**	62	4.70	0.02	4.76	4.63	0.10	0.01	2.75	5261.7	10948.7	250.7
1	**3**	51	4.88	0.01	4.92	5.05	0.13	0.02	3.9	31820.0	23373.3	8358.2
1	**4**	40	4.91	0.00	4.94	4.65	0.08	0.01	4.9	6905.0	8892.0	1417.3
1	**5**	45	4.97	0.00	4.87	4.57	0.09	0.00	4.63	3103.3	5838.7	55.7
1	**6**	63	4.73	0.03	4.73	3.98	0.01	0.28	-2.15	6720.0	84073.5	37.3
1	**7**	68	4.63	0.03	4.64	3.72	0.02	0.28	-7.7	5426.7	89493.8	24.2
1	**8**	53	4.93	0.03	4.85	4.46	0.08	0.01	5.67	2931.7	6197.3	98.4
1	**9**	104	4.82	0.06	4.75	4.40	0.11	0.01	5.6	6323.3	8371.7	225.8
1	**10**	192	8.45	0.08	8.79	7.98	0.19	0.00	14.14	4478.3	2195.7	2483.8
1	**11**	144	8.26	0.07	9.02	7.92	0.16	0.00	13.1	4495.0	2023.7	1606.3
1	**12**	183	8.21	0.08	9.10	7.02	0.19	0.01	6.25	362.0	253.5	242.2
1	**13**	124	8.31	0.05	9.02	7.64	0.16	0.00	6.1	2613.3	1644.8	1041.3
1	**14**	204	7.56	0.07	7.51	7.03	0.19	0.01	7.3	1941.7	1193.2	731.8
1	**15**	796	8.08	0.45	7.87	7.50	0.67	0.09	13.25	3358.3	1254.0	1256.7
1	**16**	445	8.07	0.14	8.65	6.63	0.31	0.04	9.25	2143.3	588.0	672.5
1	**17**	643	8.94	0.13	8.74	6.32	0.32	0.09	9.75	2163.3	509.2	762.7
1	**18**	483	8.40	0.14	9.11	7.12	0.35	0.06	12.45	2136.7	654.3	789.0
1	**19**	640	8.28	0.22	9.09	7.56	0.31	0.47	13.45	1482.3	2409.3	1010.2
1	**20**	589	8.50	0.19	9.18	7.56	0.36	0.20	11.45	1498.5	2330.3	654.0
2a	**1**	345	5.80	0.43	5.40	5.40	0.43	0.08	6.5	13336.7	2203.8	687.7
2a	**2**	153	5.00	0.01	5.11	5.04	0.19	0.02	6.3	6305.0	2773.2	293.8
2a	**3**	84	4.95	0.02	5.04	4.97	0.14	0.01	6.3	21225.0	2394.2	298.5
2a	**4**	57	5.02	0.08	5.08	5.10	0.11	0.01	3.4	16118.3	1489.3	371.0
2a	**5**	60	6.92	0.05	5.28	5.27	0.14	0.00	3.76	6991.7	666.2	247.0
2a	**6**	60	7.77	0.18	6.46	6.38	0.02	0.00	4.8	4738.3	306.8	60.2
2a	**7**	1820	8.02	0.54	7.75	7.52	0.82	0.44	7.35	3923.3	271.8	249.3

Site	ID	Paste SC (μS cm^{-1})	Paste pH	1:1 SC (dS m^{-1})	1:1 pH	1:1 Peroxide pH	1:1 Peroxide SC (dS m^{-1})	Total S (%)	CCE (%)	CD - Fe (mg kg^{-1})	CD - Al (mg kg^{-1})	CD - Mn (mg kg^{-1})
2a	**8**	1620	7.92	0.29	8.48	6.90	0.56	0.41	7.3	8463.3	296.8	240.2
2b	**1**	329	5.29	0.14	5.54	5.19	0.37	0.07	4.9	8773.3	1803.5	416.8
2b	**2**	52	5.09	0.04	4.96	4.87	0.11	0.01	4.89	8811.7	1293.7	211.2
2b	**3**	60	4.90	0.04	5.07	4.88	0.13	0.01	5.86	22838.3	2378.3	378.0
2b	**4**	50	7.50	0.02	5.52	6.29	0.12	0.00	3.93	30361.7	1573.0	1121.3
2b	**5**	220	7.05	0.07	6.23	6.69	0.22	0.00	3.8	8428.3	464.5	500.2
2b	**6**	2420	8.00	0.44	7.80	7.61	0.75	0.58	8.5	5041.7	374.0	345.5
2b	**7**	2290	7.83	0.39	7.47	6.40	0.81	0.75	N/A	6291.7	268.7	309.5
2c	**1**	1049	4.89	0.50	4.89	4.89	0.07	0.10	2.6	7338.3	2055.7	570.2
2c	**2**	86	4.66	0.04	4.88	4.69	0.15	0.01	3.5	13213.3	1913.5	89.8
2c	**3**	100	6.63	0.03	5.35	5.13	0.13	0.00	4.62	4645.0	502.3	111.3
2c	**4**	80	7.19	0.03	5.46	5.49	0.12	0.00	4.85	12086.7	872.8	291.7
2c	**5**	160	8.18	0.02	6.48	5.86	0.12	0.00	5.9	17378.3	1235.7	344.3
2c	**6**	1000	7.85	0.32	7.36	7.56	0.31	0.10	5.5	21870.0	1253.7	1217.8
2c	**7**	2430	8.03	0.53	8.08	7.60	0.83	0.51	12.4	6163.3	564.0	626.8
2c	**8**	800	8.16	0.17	8.14	7.24	0.34	0.07	8.6	9580.0	344.5	418.0
3	**1**	450	4.84	0.03	4.93	4.76	0.24	0.03	3.5	7661.7	1937.5	194.7
3	**2**	150	5.51	0.02	4.97	4.93	0.13	0.01	4	10763.3	2119.2	91.5
3	**3**	110	5.52	0.01	4.75	4.54	0.12	0.01	4.1	13858.3	1987.8	102.2
3	**4**	60	6.35	0.03	5.29	5.20	0.09	0.01	4.3	30913.3	2487.7	460.5
3	**5**	70	5.74	0.04	5.31	5.42	0.12	0.00	4.95	4681.7	570.5	145.5
3	**6**	2390	7.83	0.48	7.35	6.78	0.75	0.43	8.31	6198.3	413.0	295.0
3	**7**	580	8.34	0.17	8.60	7.63	0.26	0.08	9.44	5621.7	845.2	208.5
4a	**1**	250	4.52	0.13	4.60	4.39	0.33	0.07	5.55	12410.0	1423.3	615.3
4a	**2**	110	5.64	0.02	5.48	5.10	0.10	0.01	6.6	27810.0	1951.3	423.2
4a	**3**	220	7.92	0.04	7.23	7.17	0.17	0.00	7.8	11350.0	411.8	421.7
4a	**4**	250	4.38	0.10	4.54	3.36	0.73	0.76	N/A	15430.0	2815.2	31.7
4a	**5**	1413		0.46	4.50	4.10	0.46	0.02	6.55	4981.7	466.8	77.3

Site	ID	Paste SC ($\mu S\ cm^{-1}$)	Paste pH	1:1 SC ($dS\ m^{-1}$)	1:1 pH	1:1 Peroxide pH	1:1 Peroxide SC ($dS\ m^{-1}$)	Total S (%)	CCE (%)	CD - Fe ($mg\ kg^{-1}$)	CD - Al ($mg\ kg^{-1}$)	CD - Mn ($mg\ kg^{-1}$)
4b	**1**	340	4.93	0.09	4.92	5.00	0.37	0.14	3.2	6980.0	1424.3	1634.8
4b	**2**	140	4.82	0.04	4.64	4.56	0.10	0.02	6.9	29466.7	1484.8	22.5
4b	**3**	130	5.86	0.03	5.87	5.55	0.13	0.01	5.1	24160.0	1096.2	642.0
4b	**4**	100	6.48	0.02	6.43	6.51	0.13	0.01	5	23845.0	1020.3	514.0
4b	**5**	920	4.42	0.26	4.66	4.65	0.40	0.06	4.6	20926.7	1208.8	563.0
4c	**1**	280	4.54	0.18	4.58	4.45	0.32	0.08	N/A	6366.7	1561.0	653.2
4c	**2**	120	5.08	0.02	4.94	4.61	0.12	0.01	N/A	8771.7	1326.2	132.8
4c	**3**	80	6.44	0.02	6.19	5.88	0.11	0.00	2.8	16093.3	676.7	89.7
4c	**4**	660	7.04	0.19	6.91	6.42	0.34	0.06	3.7	576.7	369.0	4.2
4c	**5**	1050	7.94	0.19	8.59	7.15	0.42	0.01	3.85	2225.0	44.5	54.7
5	**1**	140	4.95	0.03	5.03	4.84	0.16	0.01	5.02	14015.0	1615.0	610.5
5	**2**	150	4.94	0.05	5.10	4.08	0.20	0.14	3.5	13481.7	2077.2	234.0
5	**3**	200	5.15	0.05	5.26	4.46	0.17	0.04	4.15	14273.3	1424.7	182.5
5	**4**	130	5.33	0.07	4.91	4.48	0.16	0.01	N/A	16896.7	1574.3	92.3
5	**5**	2750	6.87	0.45	6.61	6.49	0.83	0.08	N/A	10575.0	426.0	297.5
5	**6**	650	7.99	0.47	7.80	7.50	0.55	0.01	N/A	3981.7	197.8	120.2
6	**1**	89	5.13	0.03	5.50	4.93	0.14	0.01	N/A	16765.0	1835.7	236.5
6	**2**	180	5.88	0.04	5.57	6.39	0.18	0.00	N/A	2423.3	212.5	146.8
6	**3**	170	7.93	0.04	8.21	7.00	0.17	0.00	N/A	2318.3	80.2	58.8
6	**4**	570	7.82	0.14	8.44	6.91	0.27	0.01	N/A	2980.0	70.5	74.3
6	**6**	720	7.81	0.55	7.60	7.45	0.70	N/A	N/A	N/A	N/A	N/A
7	**1**	190	4.26	0.04	4.58	4.04	0.21	0.04	N/A	3373.3	940.3	67.5
7	**2**	130	4.51	0.03	4.80	4.25	0.16	0.01	N/A	3481.7	1047.5	8.2
7	**3**	120	5.06	0.04	5.08	5.95	0.13	0.00	N/A	3795.0	329.3	151.8
7	**4**	130	4.53	0.02	4.44	3.20	0.02	0.56	N/A	6213.3	7360.5	4.3
7	**5**	100	7.34	0.01	7.49	7.37	0.14	0.00	N/A	19325.0	859.7	443.3
7	**6**	300	7.88	0.05	8.27	7.19	0.20	0.00	N/A	4031.7	86.0	104.0
8	**1**	594	4.95	0.15	5.22	4.25	0.64	0.03	N/A	9360.0	773.3	220.5

Site	ID	Paste SC ($\mu S\ cm^{-1}$)	Paste pH	1:1 SC ($dS\ m^{-1}$)	1:1 pH	1:1 Peroxide pH	1:1 Peroxide SC ($dS\ m^{-1}$)	Total S (%)	CCE (%)	CD - Fe ($mg\ kg^{-1}$)	CD - Al ($mg\ kg^{-1}$)	CD - Mn ($mg\ kg^{-1}$)
8	**2**	230	5.42	0.05	5.80	5.43	0.15	0.01	N/A	11338.3	724.5	404.0
8	**3**	135	5.17	0.03	5.71	5.26	0.14	0.00	N/A	9658.3	715.2	148.8
8	**4**	90	6.43	0.02	6.44	5.55	0.14	0.00	N/A	4955.0	216.7	17.0
8	**5**	380	8.16	0.10	8.35	7.67	0.24	0.03	N/A	13010.0	392.7	365.3
8	**6**	1440	7.87	0.24	8.22	7.35	0.61	0.03	N/A	11080.0	143.5	233.5
9	**2**	40	6.87	0.01	6.65	6.11	0.10	0.00	N/A	9860.0	391.7	169.7
9	**3**	210	8.02	0.06	8.90	6.90	0.18	0.03	N/A	1921.7	36.2	73.8
10	**1**	200	4.44	0.08	4.66	4.29	0.18	0.03	N/A	3915.0	1617.3	229.7
10	**2**	49	4.94	0.02	5.08	4.90	0.11	0.01	N/A	7390.0	1054.0	36.3
10	**3**	49	5.15	0.03	5.02	4.76	0.11	0.00	N/A	6686.7	721.0	30.0
10	**4**	80	6.11	0.03	5.35	5.26	0.13	0.00	N/A	3065.0	294.3	78.5
10	**5**	250	4.82	0.08	4.61	4.54	0.23	0.02	N/A	23663.3	1092.5	516.3
10	**6**	6440	2.29	3.10	2.55	2.22	5.72	1.59	N/A	18603.3	851.0	54.3
11	**1**	250	5.16	0.16	5.17	5.27	0.29	0.06	N/A	8396.7	1739.7	1181.3
11	**2**	44	5.16	0.03	5.01	4.79	0.10	0.01	N/A	20161.7	2022.3	78.5
11	**3**	100	6.42	0.03	6.29	5.88	0.14	0.00	N/A	1208.3	142.2	30.8
11	**4**	70	5.50	0.04	4.54	4.26	0.10	0.01	N/A	6546.7	1274.0	4.3
12	**1**	621	6.85	0.29	6.37	6.32	0.51	0.07	N/A	7168.3	1555.2	663.7
12	**2**	177	6.69	0.04	6.87	6.40	0.18	0.01	N/A	5801.7	1348.8	336.2
12	**3**	100	5.05	0.03	5.57	5.10	0.13	0.00	N/A	2053.3	183.5	14.0
12	**5**	130	6.65	0.04	7.04	5.60	0.17	0.01	N/A	248.3	24.7	6.5
13	**1**	344	4.55	0.25	4.55	4.53	0.08	0.14	N/A	7393.3	2664.8	1102.3
13	**2**	52	4.73	0.03	4.83	4.71	0.11	0.01	N/A	9476.7	1335.0	30.3
13	**3**	990	6.49	0.36	6.61	7.25	0.46	0.01	N/A	20563.3	433.5	1075.2
13	**4**	573	7.83	0.16	8.86	7.08	0.32	0.02	N/A	3846.7	75.8	118.2
14	**1**	540	5.18	0.27	5.3	5.69	0.27	0.09	5.35	7041.7	2911.8	2909.5
14	**2**	185	4.18	0.07	4.26	4.36	0.12	0.01	4.9	11798.3	1677.7	345.7
14	**4**	43	6.11	0.02	5.42	5.15	0.13	0.00	3.01	3301.7	586.2	21.2

Site	ID	Paste SC (μS cm^{-1})	Paste pH	1:1 SC (dS m^{-1})	1:1 pH	1:1 Peroxide pH	1:1 Peroxide SC (dS m^{-1})	Total S (%)	CCE (%)	CD - Fe (mg kg^{-1})	CD - Al (mg kg^{-1})	CD - Mn (mg kg^{-1})
14	**5**	78	6.79	0.2	7.49	6.81	0.15	0.00	5.84	4496.7	209.2	90.0
14	**6**	618	7.16	0.12	7.56	7.22	0.26	0.03	4.6	3523.3	374.2	157.5
14	**7**	828	7.42	0.11	7.89	6.67	0.27	0.06	7.4	12150.0	221.5	430.0
15	**1**	501	3.97	0.13	4.25	3.75	0.22	0.06	4.5	6995.0	1647.5	165.8
15	**2**	224	4.03	0.02	4.25	5.86	0.01	0.02	6.6	8335.0	1514.2	40.7
15	**3**	30	7.56	0.01	5.78	4.96	0.01	0.00	3.2	7956.7	642.7	330.0
15	**4**	28	7.61	0.01	6.88	5.64	0.08	0.00	3.6	6580.0	936.2	57.3
15	**5**	828	7.42	0.01	7.01	6.53	0.13	0.00	7.45	15686.7	1016.0	297.7
15	**7**	251	7.89	0.06	8.64	7.07	0.18	0.01	5.8	4506.7	145.3	79.0
16	**1**	520	6.36	0.09	6.2	6.26	0.18	0.04	3.95	11525.0	1792.2	779.8
16	**2**	170	4.88	0.1	4.95	5.08	0.1	0.01	2.9	13698.3	2049.3	688.0
16	**3**	34	7.62	0.01	7.63	7.27	0.13	0.00	5.25	15591.7	849.8	716.2
16	**5**	90	5.9	0.03	5.68	5.01	0.1	0.00	6.5	8596.7	863.8	34.5
16	**6**	270	7.56	0.1	9.04	7.28	0.17	0.00	4.6	7493.3	189.7	112.3
17	**3**	69	6.73	0.01	7.48	6.72	0.12	0.00	3.5	20756.7	966.2	1516.7
17	**4**	72	6.56	0.02	6.98	6.01	0.12	0.00	4.4	6501.7	475.5	62.5
17	**5**	471	7.07	0.15	7.07	5.84	0.29	0.03	4.75	401.7	68.3	7.0
17	**6**	54	7.08	0.02	6.71	5.9	0.15	0.00	3.67	11670.0	698.8	150.5
17	**7**	457	6.26	0.15	6.23	5.67	0.25	0.02	4.7	1404.8	101.5	7.2
17	**9**	2330	5.09	0.65	5.52	4.64	0.81	0.05	6.36	1155.0	228.2	10.3
17	**10**	2380	5.12	0.43	5.68	4.12	0.79	0.06	6.1	2193.3	162.8	23.5
17	**11**	114	7.04	0.02	7.83	7.2	0.14	0.00	4.45	10436.7	462.5	212.3
17	**12**	347	7.98	0.07	9.04	7.06	0.23	0.01	6.71	2996.7	105.5	73.5
17	**13**	147	7.94	0.06	8.68	7.51	0.15	0.00	5	13980.0	638.3	359.3
17	**14**	259	7.97	0.08	9.19	7.08	0.22	0.01	7.35	2241.7	68.8	73.8
17	**15**	1708	7.62	0.28	8.25	6.27	0.69	0.15	4.1	6525.0	158.2	187.3
18	**3**	4680	5.68	1.08	6.42	4.85	0.8	0.17	2.84	4981.7	355.3	91.8
18	**4**	4970	6.46	0.63	6.94	4.78	1.39	0.22	3.5	6236.7	266.8	170.7

Site	ID	Paste SC ($\mu S\ cm^{-1}$)	Paste pH	1:1 SC ($dS\ m^{-1}$)	1:1 pH	1:1 Peroxide pH	1:1 Peroxide SC ($dS\ m^{-1}$)	Total S (%)	CCE (%)	CD - Fe ($mg\ kg^{-1}$)	CD - Al ($mg\ kg^{-1}$)	CD - Mn ($mg\ kg^{-1}$)
18	**5**	7660	4.91	0.82	5.43	5.15	0.97	0.22	5.5	28276.7	1243.3	827.0
18	**6**	2370	7.43	0.63	7.5	6.19	0.88	0.14	2.5	4426.7	68.7	121.5
18	**7**	254	6.79	0.06	6.83	7.38	0.16	0.00	3.5	19408.3	657.7	425.8
18	**8**	996	7.87	0.21	8.44	6.81	0.39	0.10	6.2	3045.0	62.5	104.0
18	**9**	1796	6.13	0.13	6.58	6.25	0.3	0.03	5.9	23358.3	1153.2	292.3
18	**10**	4030	7.68	1.03	6.62	6.36	1.08	0.14	6.6	4466.7	437.5	173.3
18	**11**	16550	3.41	4.47	3.65	2.78	4.15	1.12	3.05	7820.0	1276.5	56.2
18	**12**	8280	4.83	2.32	5.59	2.97	3.28	0.69	3.7	9721.7	555.8	219.5
19	**3**	186	7.58	0.03	7.99	7.28	0.16	0.00	N/A	19498.3	1565.7	516.8
19	**4**	744	7.73	0.07	8.32	7.54	0.22	0.04	6.6	13806.7	933.2	237.7
19	**5**	1438	8.02	0.2	8.71	7.74	0.44	0.11	9.1	7291.7	339.2	266.7
19	**6**	1957	7.85	0.5	8.4	6.35	0.58	0.18	6.6	8075.0	407.2	278.7
19	**7**	3190	7.87	0.56	8.34	7.39	0.57	0.44	7.7	5020.0	444.2	201.0
20	**3**	7070	4.18	1.87	4.41	3.66	1.8	0.30	5.36	11458.3	579.7	172.7
20	**4**	305	7.45	0.1	8.19	7.15	0.17	0.00	5.65	16291.7	645.2	436.2
20	**5**	1109	7.32	0.2	8.21	7.05	0.42	0.09	7.04	3363.3	73.5	119.2
20	**6**	232	7.84	0.1	8.63	7.79	0.18	0.00	8.15	16018.3	620.5	460.8
21a	**1**	585	6.58	0.24	5.35	6.13	0.31	0.0603	N/A	6718.3	1371.2	1155.3
21a	**2**	69	5.17	0.02	4.65	4.56	0.05	0.004	N/A	16546.7	1579.5	123.3
21a	**3**	154	4.87	0.02	4.63	4.65	0.1	0.0101	N/A	11803.3	976.0	249.7
21a	**4**	1936	5.07	0.35	4.84	3.63	0.11	0.194	N/A	3598.3	221.0	77.5
21a	**5**	335	8.14	0.07	9.21	7.36	0.05	0.027	N/A	8878.3	122.2	244.8
21a	**6**	225	8.57	0.09	9.39	7.45	0.34	0	N/A	3756.7	48.5	110.5
21a	**7**	450	8.31	0.08	7.89	6.87	0.14	0.011	N/A	1051.7	154.7	12.8
21b	**1**	508	5.98	0.26	5.56	6.22	0.24	0.015	N/A	6245.0	1228.3	928.3
21b	**2**	74	5.04	0.01	4.99	4.5	0.07	0.005	N/A	12805.0	1252.2	173.8
21b	**3**	55	6.7	0.01	6.65	6.47	0.1	0.002	N/A	3555.0	291.2	127.2
21b	**4**	862	5.95	0.09	5.7	5.16	0.11	0.045	N/A	4573.3	252.2	73.7

Site	ID	Paste SC ($\mu S\ cm^{-1}$)	Paste pH	1:1 SC ($dS\ m^{-1}$)	1:1 pH	1:1 Peroxide pH	1:1 Peroxide SC ($dS\ m^{-1}$)	Total S (%)	CCE (%)	CD - Fe ($mg\ kg^{-1}$)	CD - Al ($mg\ kg^{-1}$)	CD - Mn ($mg\ kg^{-1}$)
21b	**5**	218	8.18	0.06	9.27	7.22	0.02	0.007	N/A	3673.3	51.5	74.5
21c	**1**	766	7.28	0.23	6.24	6.81	0.17	0.015	N/A	5626.7	1160.0	558.0
21c	**2**	82	5.28	0.02	5.16	5.14	0.07	0.002	N/A	11376.7	1029.2	348.5
21c	**3**	57	7.08	0.01	6.62	6.73	0.06	0.184	N/A	4196.7	270.5	100.2
21c	**4**	1943	6.57	0.29	6.6	5.92	0.02	0.0875	N/A	6153.3	137.8	205.2
21c	**5**	345	8.27	0.12	9.1	7.38	0.27	0.0156	N/A	5113.3	69.5	123.0
22a	**1**	551	7.46	0.55	6.42	7.62	0.003	0.0878	N/A	3383.3	657.3	256.5
22a	**2**	212	5.97	0.04	5.45	5.3	0.1	0.0089	N/A	15978.3	2488.2	474.2
22a	**3**	88	6.64	0.02	5.77	6.03	0.1	0.0009	N/A	22620.0	670.7	500.8
22a	**4**	158	6.78	0.16	6.35	5.98	0.19	0.0835	N/A	10121.7	518.7	217.0
22a	**5**	155	8.22	0.08	9.27	7.09	0.19	0.0869	N/A	3135.0	44.8	53.3
22b	**1**	1303	7.3	0.55	6.36	7.07	0.12	0.1063	N/A	13013.3	2650.0	1570.2
22b	**2**	137	5.42	0.04	5.45	5.04	0.11	0.0088	N/A	14553.3	2222.5	449.2
22b	**3**	62	7.75	0.02	6.81	6.83	0.11	0.0006	N/A	9051.7	401.5	240.3
22b	**4**	484	8	0.16	7.87	7.35	0.25	0.083	N/A	1221.7	339.2	21.8
22b	**5**	173	8.33	0.08	9.23	7.44	0.23	0.006	N/A	4103.3	51.2	83.7
22c	**1**	1092	7.21	0.55	6.22	6.52	0.4	0.054	N/A	12988.3	2345.5	1226.7
22c	**2**	99	5.22	0.04	5.3	5.17	0.11	0.009	N/A	15773.3	2083.0	350.0
22c	**3**	62	7.24	0.03	5.57	5.72	0.12	0.003	N/A	19176.7	596.7	429.3
22c	**4**	844	8.16	0.25	7.76	6.96	0.38	0.19	N/A	5558.3	389.2	165.7
22c	**5**	193	8.47	0.09	9.02	7.16	0.21	0.001	N/A	3416.7	54.3	64.5
23	**1**	378	7.05	0.16	6	6.01	0.31	0.041	N/A	11211.7	2228.7	1241.0
23	**2**	54	5.69	0.02	5.01	5	0.11	0.0084	N/A	19673.3	2337.0	316.3
23	**4**	30	6.37	0.01	5.99	6.2	0.11	0.001	N/A	6916.7	273.7	129.8
23	**5**	36	5.93	0.01	5.79	5.6	0.15	0.003	N/A	18263.3	1574.8	171.0
23	**6**	154	8.03	0.07	8.11	7.55	0.18	0.002	N/A	2078.3	43.2	46.7
23	**7**	677	8.14	0.3	7.42	7.4	0.42	0.047	N/A	506.7	577.5	10.8
24	**1**	307	8.28	0.15	7.79	7.55	0.3	0.032	N/A	15515.0	2020.7	1700.0

Site	ID	Paste SC (µS cm^{-1})	Paste pH	1:1 SC (dS m^{-1})	1:1 pH	1:1 Peroxide pH	1:1 Peroxide SC (dS m^{-1})	Total S (%)	CCE (%)	CD - Fe (mg kg^{-1})	CD - Al (mg kg^{-1})	CD - Mn (mg kg^{-1})
24	**2**	98	5.44	0.05	5.16	6.12	0.21	0.007	N/A	22016.7	2244.8	416.7
24	**3**	23	6.59	0.01	5.22	5.8	0.01	0.009	N/A	8270.0	1662.5	6.8
24	**4**	466	6.58	0.24	4.21	4.15	0.35	0.85	N/A	823.3	253.2	10.7
24	**5**	1000	7.52	0.55	6.95	6.85	0.67	0.49	N/A	8750.0	202.2	327.2
24	**6**	203	7.77	0.1	7.05	7.05	0.25	0.008	N/A	1208.3	569.5	38.5
25	**2**	34	6.77	0.001	5.27	5.2	0.1	0.004	N/A	8103.3	1961.8	234.8
25	**3**	217	5.95	0.12	5.04	5.11	0.25	0.001	N/A	5495.0	617.5	368.7
25	**4**	101	7.11	0.04	5.56	5.5	0.15	0.008	N/A	835.0	46.3	31.0
25	**5**	195	7.98	0.09	8	7.5	0.2	0.003	N/A	16391.7	1714.2	138.8